

1-1-2012

Investigation Of A 16s Rna Central Domain Pseudoknot

Jenna Marie Jasinski-Bolak
Wayne State University,

Follow this and additional works at: http://digitalcommons.wayne.edu/oa_theses

Recommended Citation

Jasinski-Bolak, Jenna Marie, "Investigation Of A 16s Rna Central Domain Pseudoknot" (2012). *Wayne State University Theses*. Paper 210.

This Open Access Thesis is brought to you for free and open access by DigitalCommons@WayneState. It has been accepted for inclusion in Wayne State University Theses by an authorized administrator of DigitalCommons@WayneState.

INVESTIGATION OF A 16S RNA CENTRAL DOMAIN PSEUDOKNOT

by

JENNA JASINSKI-BOLAK

THESIS

Submitted to the Graduate School

of Wayne State University,

Detroit, Michigan

in partial fulfillment of the requirements

for the degree of

MASTER OF SCIENCE

2012

MAJOR: BIOLOGICAL SCIENCES

Approved by:

Advisor

Date

ACKNOWLEDGMENTS

I would like to thank my advisor, Dr. Phil Cunningham for his patience with me throughout my time in the lab, both during undergrad and grad school. I'd like to think of my mischief and curiosity as assets, but in all reality, I owe him a big thanks for not kicking me out every time I did something stupid, which was a lot of times. I hope I become a big name that he can tell his future students, "we still stay in contact".

A special thanks to Dr. Wes Colangelo, who hoodwinked Phil into letting me join the lab as an undergrad. He is really one of the smartest people I'll ever know, and always willing to help...after I badger him long enough. Here's to listening to Alex Jones 8 hours a day, arguing about the temperature of the lab, the "istab" phenomenon, the 4XL Moses lab coat, and the unanswered question, "where the heck is John!?!"

I would also like to thank all the past and present Cunningham Lab members for helping me troubleshoot experiments and making the lab a fun place; Kris Ann, Tek, Marny, Ami, Vidisha, Kumar, Sathya, Thilakam, Rania, Chandani, and Jun. Dr. Jun Jiang was instrumental in helping with the homology modeling software (DNA-123) while working in Dr. Santalucia's lab, and also provided tons of information and ideas related to my research.

Finally, my friends and family deserve a shout-out. Though most of you don't quite understand what I'm still doing in school, I appreciate the support, or at least hiding your apprehension. I promise I will make money one day.

TABLE OF CONTENTS

Acknowledgements	ii
List of Tables	iv
List of Figures	vii
CHAPTER 1 – Introduction	1
1.1 RNA.....	1
1.2 Ribosome.....	1
1.3 Subunits.....	2
1.4 Assembly.....	4
1.5 Protein Synthesis.....	6
1.6 Initiation.....	9
1.7 Elongation.....	11
1.8 Termination.....	15
1.9 16S ribosomal RNA Structures and Regions.....	15
1.10 Pseudoknots.....	23
1.11 Genetic System.....	28
CHAPTER 2- MATERIALS AND METHODS	30
2.1 Reagents.....	30
2.2 Bacterial Strains.....	30
2.3 Media.....	30
2.4 Plasmids.....	31
2.5 Construction of Site-Directed Mutations.....	32

2.6 DNA Purification.....	34
2.7 Ligations.....	38
2.8 Transformation.....	38
2.9 Sequencing.....	39
2.10 Freezer Storage of Bacterial Strains.....	40
2.11 Green Fluorescent Protein Assay.....	40
2.12 Ribosome Preparation.....	41
2.13 Sucrose Gradient Separation.....	42
CHAPTER 3- RESULTS.....	46
3.1 Functional Analysis of Pseudoknot Mutations.....	46
3.2 Analysis of Single Mutations within the Pseudoknot	48
3.3 Analysis of Double Mutations within the Pseudoknot.....	50
3.4 Saturation Mutagenesis of the Pseudoknot.....	52
3.5 Ribosomal Protein Complementation.....	56
3.6 Thermodynamic Influence on the Pseudoknot.....	56
3.7 Effects of Pseudoknot Mutations on Ribosome Structure.....	59
3.8 Mutant Structure-Function Analysis.....	66
CHAPTER 4- DISCUSSION.....	72
4.1 Analysis of Single Mutations within the Pseudoknot.....	72
4.2 Analysis of Double Mutations within the Pseudoknot.....	73
4.3 Analysis of Saturation Mutagenesis.....	75
4.4 Ribosomal Protein Complementation.....	76
4.5 Thermodynamic Influence on the Pseudoknot	78

4.6 Effects of Pseudoknot Mutations on Ribosome Structure.....	79
4.7 Mutant Structure-Function Analysis	81
4.8 Pseudoknot Base Conservation.....	83
4.9 Future Directions.....	83
References.....	86
Abstract.....	104
Autobiographical Statement.....	106

LIST OF TABLES

Table 2.1: Primers Used to Create Pseudoknot Mutations in 16S RNA	43
Table 2.2: List of Specialized PCR Primers Used for Sequencing	44
Table 2.3: List of Infra Red Dye (IRD) Sequencing Primers.....	45
Table 3.1: Functional Analysis of Single Mutations.....	48
Table 3.2: Double Mutation Analysis	53
Table 3.3: Double Mutant Statistical Analysis.....	53
Table 3.4: Saturation Mutagenesis Table of Functionality.....	54
Table 3.5: Functional Mutant Temperature Analysis	63
Table 4.1: 16S rRNA Base Pair Frequencies for Helical Element 570	84

LIST OF FIGURES

Figure 1.1:	Composition of the Prokaryotic Ribosome.....	3
Figure 1.2:	Assembly Diagram for the 30 S Subunit.....	5
Figure 1.3:	Processing of Ribosomal RNA Operon	7
Figure 1.4:	Assembly Landscape for the 30S Ribosomal Subunit.....	8
Figure 1.5:	Translation Initiation.....	10
Figure 1.6:	Translation Elongation.....	12
Figure 1.7:	Hybrid-State Model.....	14
Figure 1.8:	Translation Termination.....	16
Figure 1.9:	<i>E.coli</i> 16S Ribosomal RNA Secondary Structure.....	17
Figure 1.10:	<i>E. coli</i> 16S Ribosomal RNA Tertiary Structure.....	18
Figure 1.11:	Morphological Features of the 30S rRNA.....	19
Figure 1.12:	RNA A-Form Helix.....	21
Figure 1.13:	Common Secondary Structural Motifs.....	22
Figure 1.14:	Common Tertiary Structural Motifs.....	24
Figure 1.15:	Folding of an RNA Pseudoknot.....	26
Figure 1.16:	Pseudoknots of Other Types.....	26
Figure 1.17:	Genetic System for Analysis of Ribosome Function	29
Figure 2.1:	Commonly Used Plasmids.....	33
Figure 2.2:	pKan5 T1T2	33
Figure 2.3:	Experimental Approach for Construction of 570N, 571N Mutants.....	35
Figure 2.4:	Experimental Approach for Construction of 865N, 866N Mutants.....	36
Figure 2.5:	Experimental Approach for Saturation Mutagenesis.....	37

Figure 3.1:	Secondary Structure of Nucleotides 570,571 and 865, 866.....	47
Figure 3.2:	Tertiary Structure of Nucleotides 570, 571 and 865, 866.....	47
Figure 3.3:	Crystal structure of Nucleotides 570,571 and 865,866.....	49
Figure 3.4:	Crystal Structure of Nucleotides 570-866 Watson-Crick Bond.....	50
Figure 3.5:	Crystal Structure of Nucleotides 571-865 Watson-Crick Bond.....	51
Figure 3.6:	Watson Crick Base-Pairs.....	55
Figure 3.7:	Ribosomal Proteins Near Pseudoknot.....	57
Figure 3.8:	Ribosomal Protein Complementation.....	58
Figure 3.9:	Single Mutation Temperature Analysis	60
Figure 3.10:	Double Mutation Temperature Analysis.....	61
Figure 3.11:	Functional Mutant Temperature Analysis.....	62
Figure 3.12a:	Ribosome Profile of Select Pseudoknot Mutations.....	64
Figure 3.12b:	Ribosome Profile of Select Pseudoknot Mutations.....	65
Figure 3.13:	Homology Model of U571A	68
Figure 3.14:	Homology Model of U571G	68
Figure 3.15:	Homology Model of U571C.....	69
Figure 3.16:	Homology Model of A865C	69
Figure 3.17:	Homology Model of G570U-C866A, U571G-A865C.....	70
Figure 3.18:	Homology Model of G570A-G866U, U571G-A865C.....	70
Figure 3.19:	Homology Model of U571G-A865C	71
Figure 4.1:	Potential Alternate Binding Partners.....	85

CHAPTER 1

Introduction

1.1 RNA

For many years, ribosomal RNA (rRNA) was only considered a scaffold molecule that bound and organized the ribosomal proteins, which were assumed to be the catalytic components of ribosomes. It wasn't until 1967 that Carl Woese suggested that RNA itself could be catalytic, leading to the RNA world hypothesis.¹ In 1982, Thomas Cech was the first to show that RNA was catalytic and could participate in cellular functions.² Sidney Altman also showed how RNA was essential for enzymatic activity.¹³⁷ Together, Cech and Altman were awarded the Nobel prize in chemistry in 1989 for their discoveries of catalytic properties of RNA.^{74; 75} Since then, many catalytic RNAs or ribozymes and a large array of functionally important non-coding RNA's have been identified,^{3; 4; 5; 6; 7; 8} demonstrating the importance and complexity of RNA in cellular functions. Fittingly, even simple linear RNA strings of adenine, cytosine, guanine and uracil are known to form a myriad of elaborate secondary and tertiary structures that rival the complexity of proteins.^{9; 10} The ability to form complex three-dimensional structures is one characteristic that allows RNA to play multiple roles in biological systems. As our ideas of the limitations of RNA dissolve, we watch the growing clout of this structurally and functionally dynamic molecule stretch from interfering RNAs to riboswitches and various essential ribozymes.^{76; 77; 78; 79}

1.2 RIBOSOME

Many genes are required to build and maintain replicating cells. In all cells, genetic information is stored as DNA and transcribed to RNA, and in many cases, translated into

proteins. Three types of RNA are directly involved in protein synthesis (translation); messenger RNA (mRNA) contains the genetic information, transfer RNA (tRNA) is an adaptor molecule that carries the amino acids that will be assembled into proteins, and ribosomal RNA (rRNA) is the functional core of ribosomes, which are the ribozymes responsible for assembling amino acids into proteins by reading the genetic message in mRNA.

Ribosomes are composed of ribosomal RNA (rRNA), the catalytically active component, and ribosomal proteins (rproteins), which serve primarily to optimize the tertiary structure by folding the rRNA into its active three-dimensional conformation. Though there are differences in the size and complexity of prokaryotic and eukaryotic ribosomes, they all follow the same general composition and structure, and contain the same phylogenetically conserved regions. In fact, portions of ribosomal RNAs are among the most highly evolutionarily conserved sequences known, which is why rRNA is often used in molecular phylogeny studies. *Escherichia coli* (*E. coli*) is a commonly used model organism for ribosome research, because the mechanism of protein synthesis is similar in all organisms.

1.3 SUBUNITS

The ribosome is one of the largest and most complex structures in the cell, composed of three different RNA's and 55 different proteins in bacteria (figure 1.1). Ribosomes are abundant in the cell, about 70,000 per actively growing *E. coli* cell, and use 85%-95% of the cells available energy.^{17; 29; 80} *E. coli*'s 70S ribosome is 20 nm in diameter, 2.6-2.8 mDa, and approximately 65% rRNA and 35% rproteins.^{12; 13} The 70S ribosome is composed of a 30S subunit and a 50S subunit.¹⁴ Formation of mature 70S ribosomes depends on correct subunit

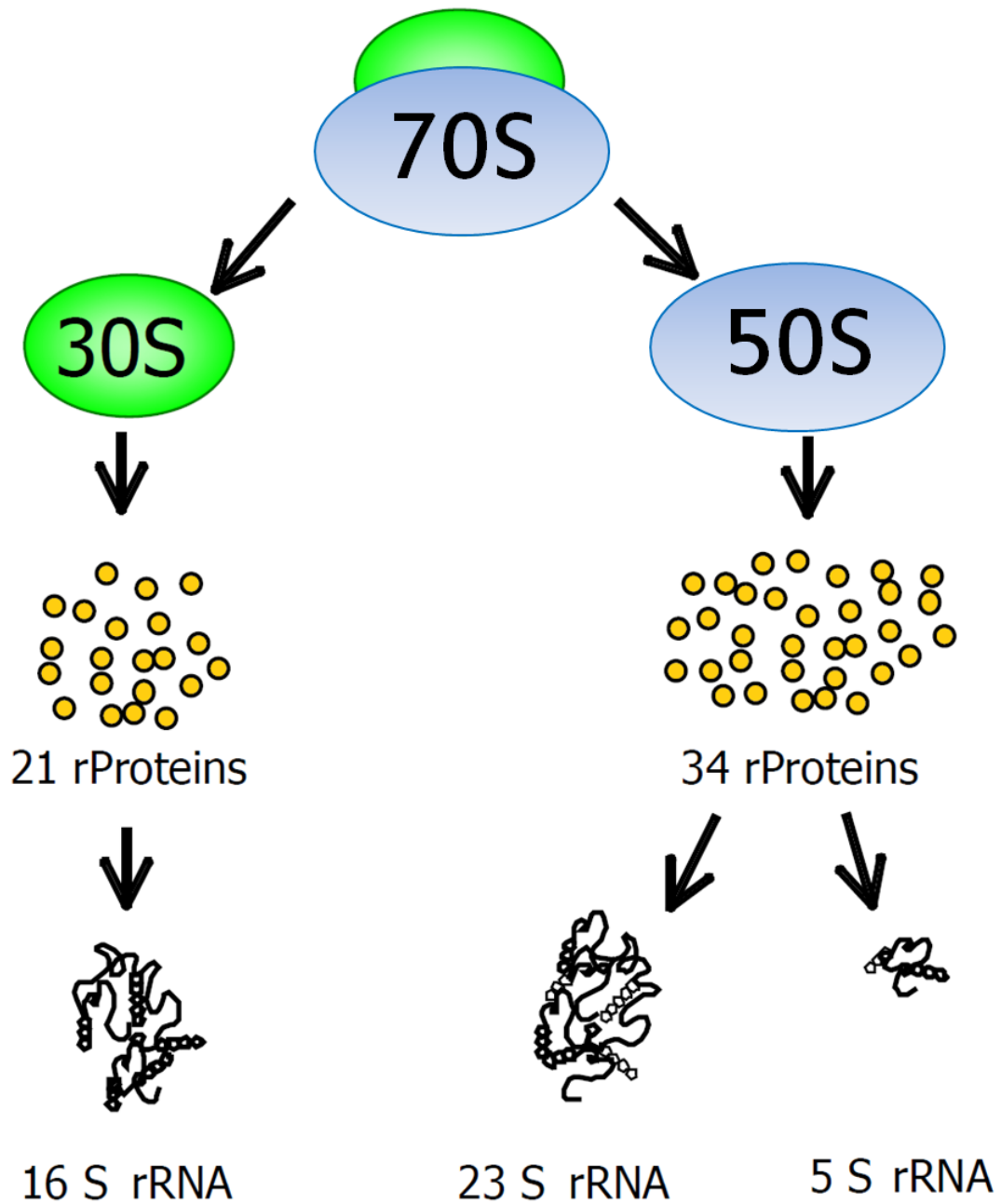


Figure 1.1: Composition of the Prokaryotic 70S Ribosome

The prokaryotic ribosome is composed of 30S and 50S subunits. The 30S is composed of 16S rRNA and 21 ribosomal proteins. The 50S is composed of 23S rRNA, 5S rRNA and 34 ribosomal proteins.

assembly and association. The 30S subunit is composed of the 16S rRNA (1542 nucleotides long) and 21 rproteins (figure 1.1).¹⁶ These proteins may be classified by the order in which they bind during the assembly process as primary, secondary, tertiary, and quaternary proteins (figure 1.2). Primary rproteins (S4, S7, S8, S15, S17, and S20) bind to naked 16S rRNA to form a pre-RNP complex. Only after the pre-RNP complex is formed and conformational changes have taken place can the secondary rproteins (S6, S9, S12, S13, S16, S18, and S19) bind. Next, the tertiary rproteins (S5, S6, S10, S11 and S14) bind, and finally the quaternary rproteins (S2, S3 and S21) bind to form the fully assembled 30S subunit.¹¹

The 50S subunit is composed of RNA and proteins as well, though the assembly process is more complex because of its size. It begins as naked 23S and 5S rRNA and combines with 34 rproteins. The 23S rRNA is 2923 nucleotides and the 5S rRNA is just 122 nucleotides. Just as the 30S goes through a highly ordered pathway to maturation, the 50S rproteins are highly dependent on each other for binding.³² It has been difficult to study the rRNA intermediates during 50S assembly, mostly due to the lack of an appropriate experimental strategy. Crystal structures of the 50S show placement of the rproteins, and some studies have solved a few intermediate steps.^{18; 19}

1.4 ASSEMBLY

There are seven ribosomal RNA operons in the genome of *E. coli* and each one contains all three of the rRNAs (23S, 16S and 5S).¹²³ As the RNA polymerase transcribes the operon, one long strand of RNA is made. As it is being transcribed, the rRNA transcript folds into a series of secondary structures that form site specific cut sites for RNases that process the RNA into the 16S, 23S and 5S, as seen in figure 1.3.⁴³ Following formation of the individual rRNA molecules, little processing occurs. As the rRNAs for each subunit are being transcribed, rproteins also bind

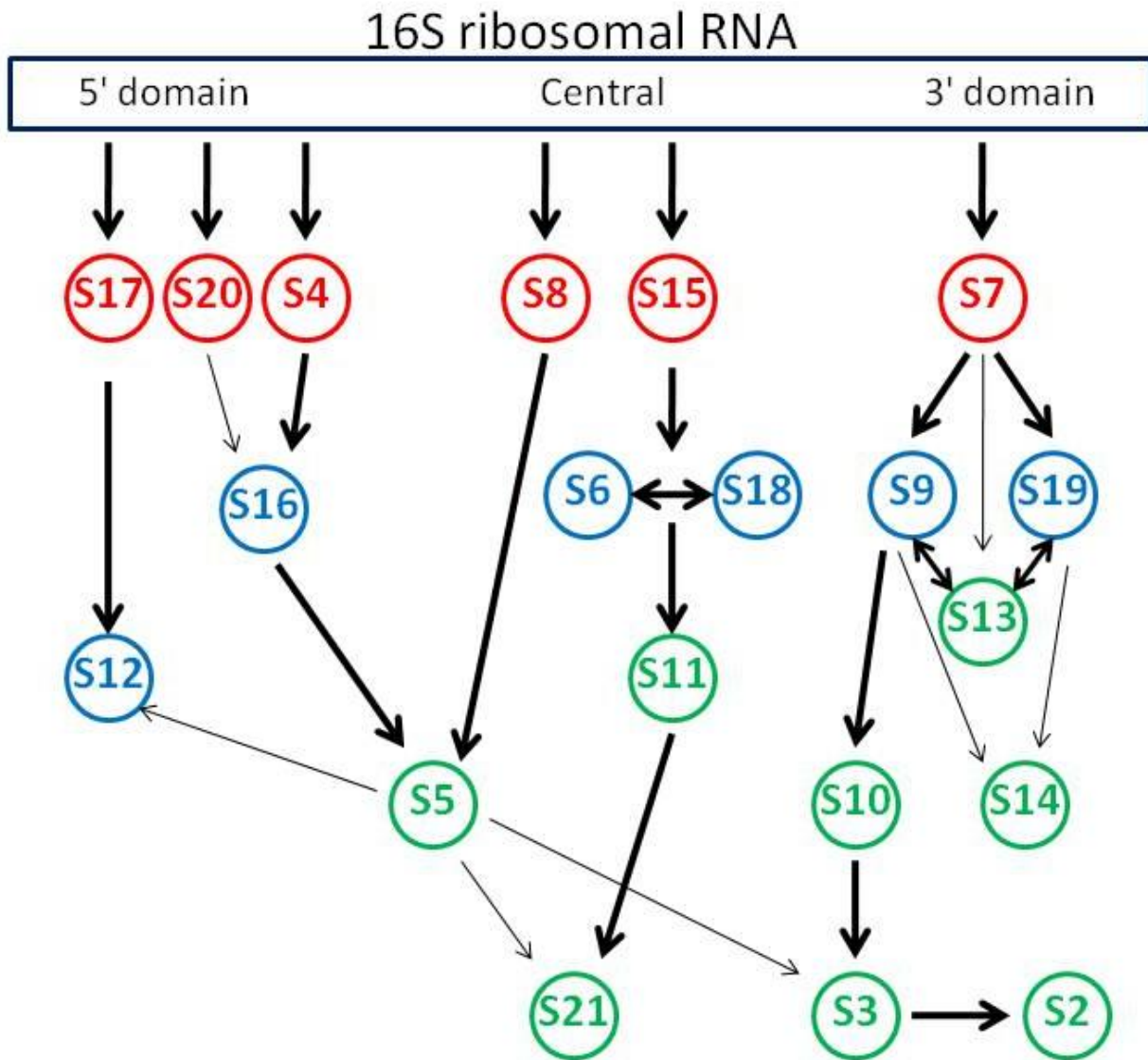


Figure 1.2: The Assembly Diagram for the 30 S Subunit.

Primary binding proteins are in blue, secondary binding proteins are in red, and tertiary binding proteins are in green. Primary binding proteins bind directly to the 16S ribosomal RNA. Secondary binding proteins bind to structures formed by binding of primary proteins while tertiary proteins bind to structures formed by the binding of both primary and secondary proteins. Adapted from Talkington, Megan W. et al, 2005.³⁸

into individual components, which may be reconstituted into active subunits and fold them sequentially, into mature subunits.²³ Both ribosomal subunits can be broken down *in vitro*.²⁴ Reconstitution experiments have been used to explain the hierarchy of protein binding leading to cooperative assembly of the subunits.^{26;27;28} Assembly of the 30S occurs in steps with the sequential association of specific rproteins that induce conformational changes in the rRNA, allowing for the next set of rproteins to bind (see figures 1.2 and 1.4). Binding of one of these proteins, S16, causes a conformational switch that stabilizes pseudoknots in the 30S and helps to prevent formation of incorrect conformations.³⁵

Ribosomal proteins generally do not make base-specific contacts with rRNA, but instead bind to specific structures in the rRNA or make specific charge interactions.³⁴ rProteins generally have two domains; a globular domain that is found on the surface of the ribosome, and an extended domain that penetrates into the rRNA core of the subunits.³¹ The majority of the rprotein extended regions stabilize the interaction between the protein and the rRNA as well as reducing the electrostatic clash between the phosphate backbones. Fine morphological features are resolved with late protein-protein interactions.²⁵ As many rproteins can be deleted without affecting translation, it has been concluded that the role of rproteins is to stabilize and assist ribosomal RNA folding. No rproteins are found in the peptidyl transferase center or the decoding region of the ribosome and this has been cited as further evidence that rproteins play mostly a structural role.⁸⁵

1.5 PROTEIN SYNTHESIS

Protein synthesis is a process where mRNA is recognized and moved through the decoding region of the ribosome along with tRNA, catalyzing the formation of a peptide. rRNA's form the structural core of the ribosome, with the proteins as secondary elements. There

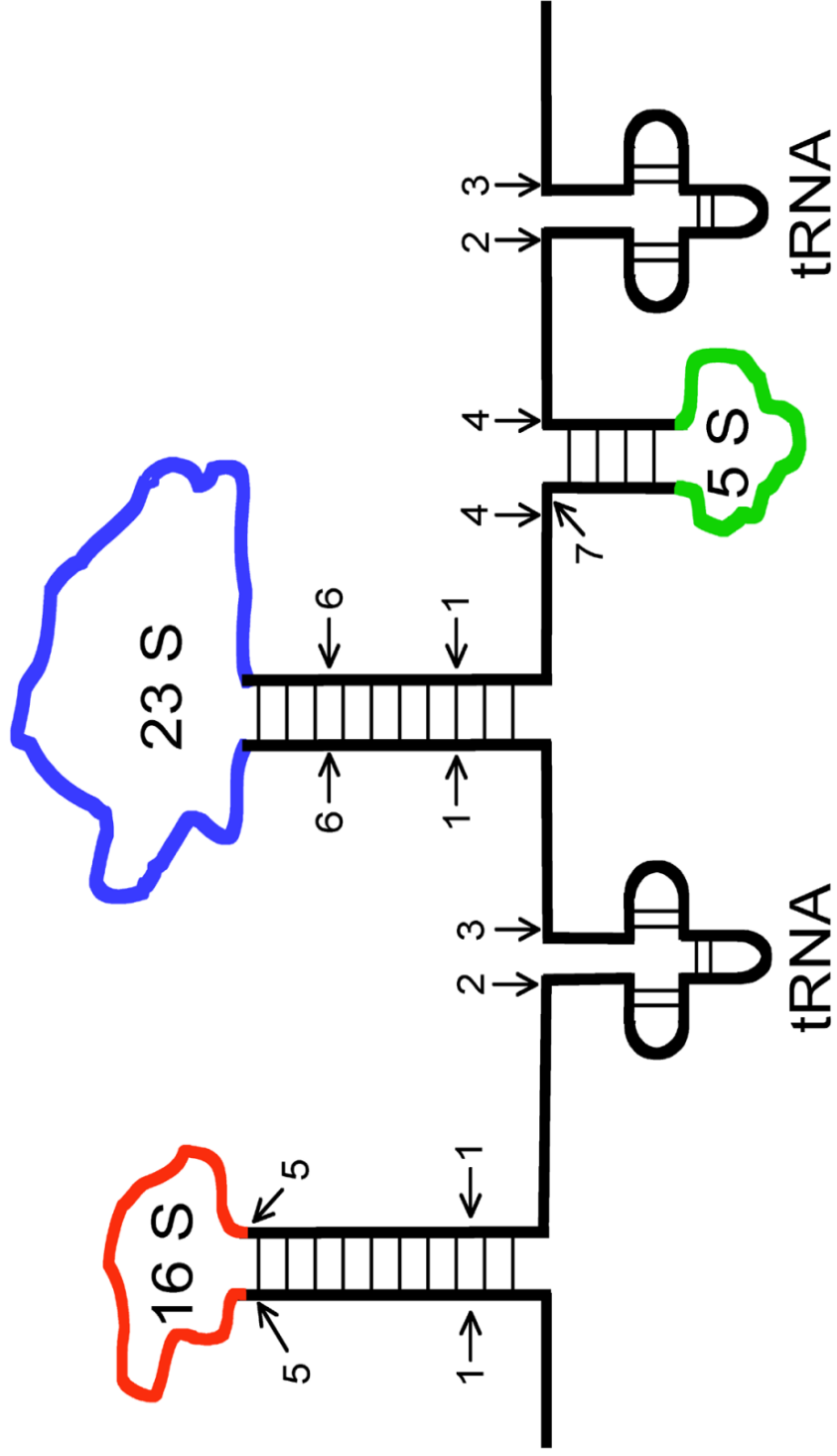


Figure 1.3: Processing of Ribosomal RNA Operon

Colored lines indicate mature rRNA. RNases shown; 1. RNase III, 2. RNase P, 3. RNase F, 4. RNase E, 5. RNase M16, 6. RNase "M23", 7. RNase "M5". Adapted from Gegenheimer and Apirion, 1981.

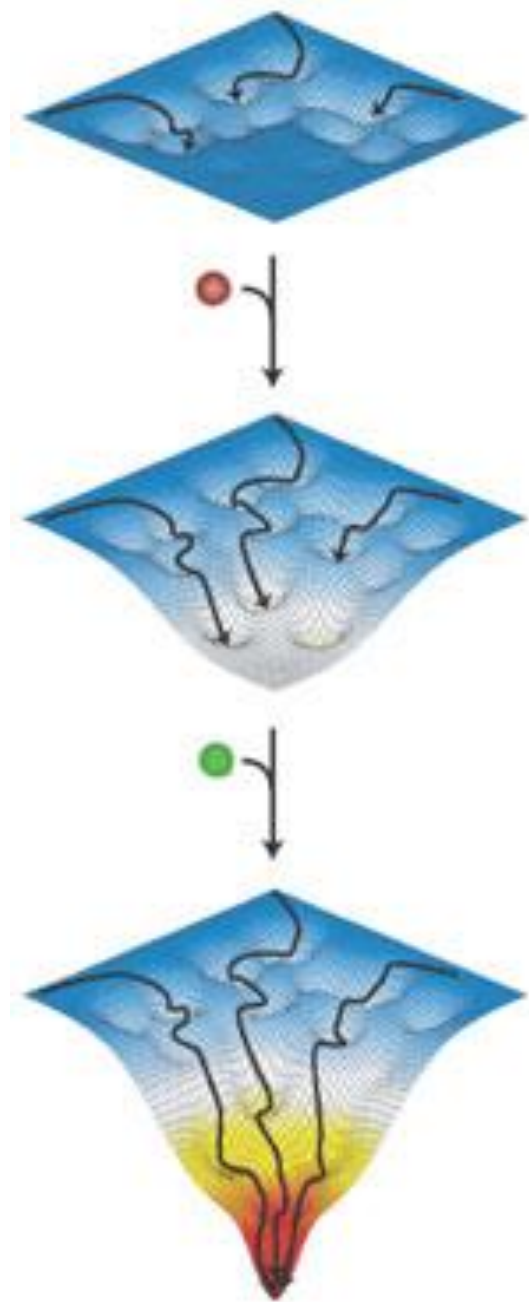


Figure 1.4: An Assembly Landscape for the 30S Ribosomal Subunit

This diagram illustrates the relationship between folding pathways, ribosomal proteins and free energy. The horizontal axes of the surface correspond to 16S rRNA conformational space, and the vertical axis is free energy. In the absence of proteins, the RNA cannot reach its lowest-energy conformation. Local folding creates binding sites for proteins (colored spheres), which, upon binding, create large changes in the assembly landscape. Though various folding pathways exist, sequential protein binding eventually stabilizes the native 30S conformation in the most energetically favorable conformation. Image taken from Talkington et al, Nature 2005. ³⁸

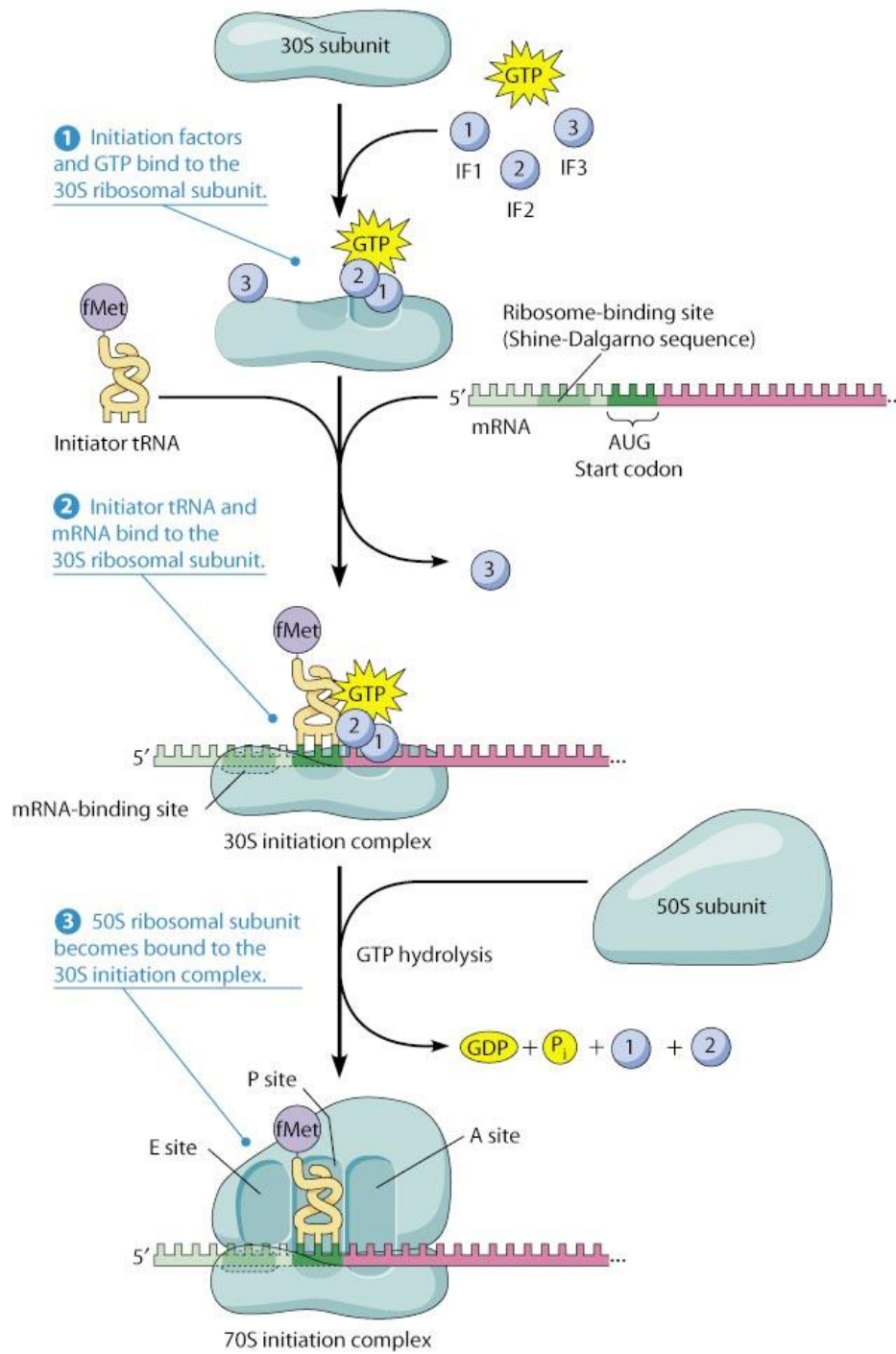
are no proteins within 18Å of the peptidyl transferase region, and it has been shown that upon deletion of most rproteins, the depleted rRNA can still catalyze peptide bond formation.^{84; 85}

These findings clearly show that the ribosome is a ribozyme.

Each subunit is responsible for specific functions, such as decoding by the 30S and peptidyl transferase activity within the 50S.³³ Though the individual subunits are capable of performing parts of protein synthesis alone (*in vitro*)^{141; 142}, a mature 70S is required to transcribe an entire protein. Usually, the 30S and the 50S subunits exist separately in the cell unless they are actively translating mRNA. There are three recognized stages of protein synthesis; initiation, elongation, and termination.

1.6 INITIATION

In bacteria, the initiation complex forms in three steps with the help of three initiation factors and a single GTP (figure 1.5). Initiation factor 1 (IF1) binds the free 30S subunit at the A-site to block incoming aminoacyl-tRNA's while IF3 binds the 30S to prevent the 50S from binding.^{81; 82} At the 3' end of the 16S RNA is a feature of the primary structure called the anti-Shine-Dalgarno (ASD) sequence. During initiation, the ASD forms Watson-Crick (WC) base pairs with a complementary sequence called the Shine-Dalgarno (SD) sequence which is located upstream of the start codon in most bacterial mRNAs.¹⁵ The SD-ASD interaction places the mRNA AUG start codon in the ribosomal P-site. The SD sequence in *E. coli* is characterized by a pyrimidine rich sequence, though some SD regions are difficult to recognize because there is no distinct sequence. Some mRNAs have been shown to lack a SD sequence all together and can still be translated *in vivo*, albeit with an affinity for the 30S at an order of magnitude lower than mRNAs with the SD sequence.²² The degree of complementarity between the SD and the ASD



Copyright © 2009 Pearson Education, Inc.

Figure 1.5: Translation Initiation

See text for details. Image copyright of Pearson Education, Inc. 2009.

influences the efficiency of translation of mRNAs and mutations in the SD sequence have been shown to reduce translation due to weakened mRNA-ribosome complementarity.²¹

In bacteria, the start codon of most mRNAs is AUG, which encodes formyl methionine bound to the initiator tRNA that binds specifically to the ribosomal P-site. Step two of initiation occurs once the start codon is positioned properly at the P-site. IF2, a GTPase⁸³, is bound to GTP and fmet-tRNA^{fmet}, and joins the complex in such a way that the tRNA anticodon is correctly paired with the initiation codon in the mRNA. In the final step of initiation, the 50S joins this complex. As simple and straight forward as this sounds, the interaction between the two subunits is actually mediated through a series of at least 12 RNA-RNA, RNA-protein, or protein-protein intersubunit bridges.³⁰

Most of the RNA-RNA bridges are found close to the functional sites of the ribosome, while the others are found mainly towards the margins.⁸⁷ Some intersubunit bridges are dynamic and must be disrupted during each translocation event during elongation and may interact with associated tRNA's.^{40; 86} When the 30S and 50S are properly positioned, the GTP bound to IF2 is hydrolyzed and all three initiation factors are released. When the two subunits assemble, a cleft or channel forms that allows the mRNA and tRNA's to pass through during elongation.^{138; 139}

1.7 ELONGATION

In the elongation stage seen in figure 1.6, three principle steps occur during each cycle: the mRNA codon is recognized by the correct tRNA, a peptide bond is formed between the incoming amino acid (bound to tRNA) and the nascent peptide, and finally the tRNAs bound to the ribosome are translocated to the next position to create an available tRNA binding site for the next cycle.

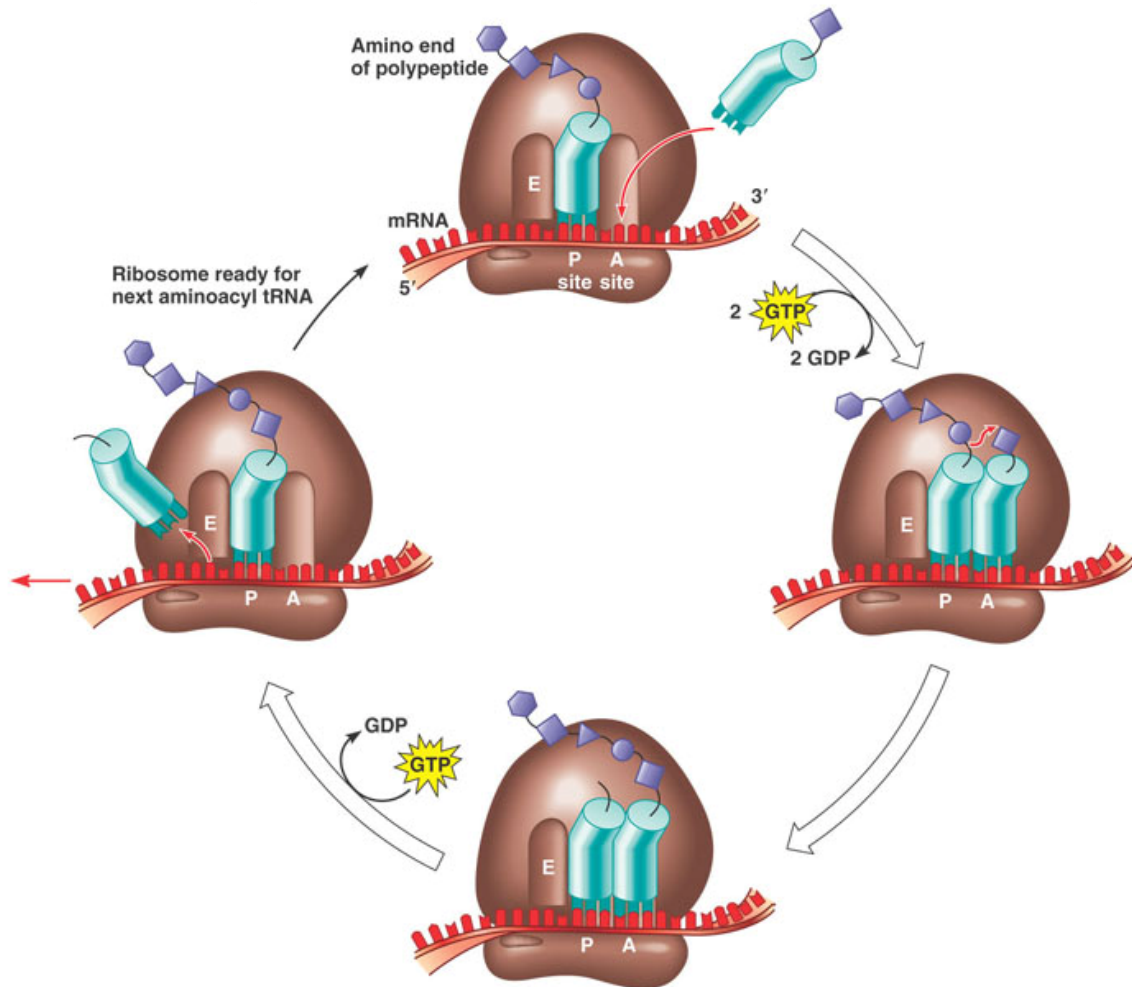


Figure 1.6: Translation Elongation

See text for detailed description.

Image taken from <http://kvhs.nbed.nb.ca/gallant/biology/translation_elongation.html>

The process of elongation begins with the formation of a ternary complex between elongation factor-Tu (Ef-Tu), GTP, aminoacylated tRNA (aatRNA) and the ribosome. Once the complex of EF-Tu, GTP and aatRNA binds, the anticodon-stem loop (ASL) of the tRNA moves into the A-site of the 30S subunit, base pairing with the mRNA codon.⁸⁹ If the tRNA in position is the cognate tRNA, the 30S subunit undergoes a conformational change.^{90; 91} This conformational change leads to the hydrolysis of GTP by EF-Tu and the release of EF-Tu from the complex.^{91; 92}

With the correctly coded charged tRNA in place, a peptide bond can be formed. The actual formation of the peptide bond is catalyzed by the peptidyl transferase center, which is formed by folded portions of the 23S rRNA within the 50S subunit. The initiating formyl methionine is transferred from its tRNA to the amino acid group on the tRNA in the A-site, a process called transpeptidation. The amine from the new amino acid on the tRNA bound at the A site attacks a carbonyl at the end of the growing peptide chain in the P site. Formation of this peptide bond creates a dipeptidyl-tRNA in the A-site, which shifts position in the 50S to form a hybrid binding state between the A-site and P-site of the ribosome (figure 1.7).⁹⁴ The uncharged tRNA in the P-site tilts to one side so that its 5' and 3' ends are in the E-site.⁹⁶ Similarly, the charged tRNA in the A-site tilts so that its 5' and 3' ends (and the growing peptide chain) are in the P-site. The anticodons, however, of the uncharged and charged tRNA's still remain in P-site and A-site, respectively. Ribosomal translocation is catalyzed by elongation factor G (EF-G), which is released from the ribosome after hydrolysis of GTP.⁹³ These tRNA's need to be moved in order to allow new aminoacylated tRNA's to enter. This process, called translocation, results in the movement of tRNA's from the A-site to the P-site, or from the P-site to the E-site via P/E and A/P hybrid states.⁹⁴

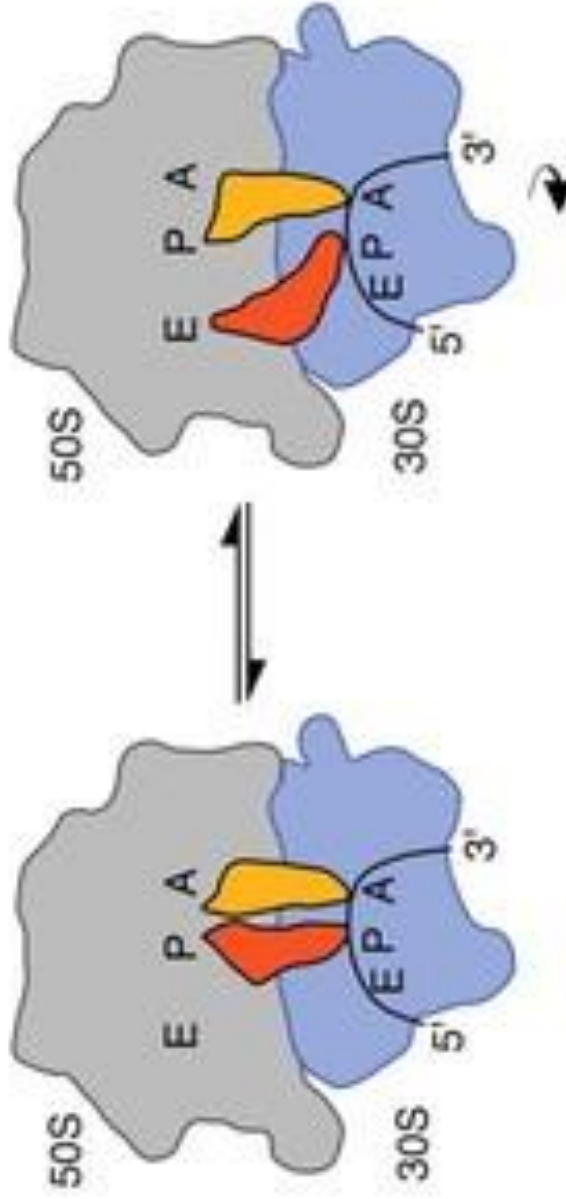


Figure 1.7: Hybrid-State Model

Schematic of tRNA-binding states on the ribosome. In the transition of tRNA binding in the A/A and P/P sites (30S subunit and 50S subunit, respectively) to occupy hybrid binding sites (A/P and P/E for 30S/50S sites). Letters indicate the locations of the aminoacyl (A), peptidyl (P) and exit (E) tRNA binding sites. Image modified from Zhang et al., 2009 Science.⁹⁶

In the process of translocation, tRNAs cycle through three sites of the ribosome, A (aminoacyl)-site, P (peptidyl)-site and the E (exit)-site.⁸⁸ GTP dependant EF-G, also known as translocase, enhances this movement by stabilizing the hybrid-state conformation of the 70S ribosome, causing framshifting.⁹⁵ Because the structure of EF-G mimics the structure of EF-Tu-tRNA, it presumably binds the A-site and displaces the peptidyl-tRNA in a ratchet-like movement. Translocation and transpeptidation continue as the peptide chain grows. The newly uncharged tRNA is displaced from the P-site to the E-site, and is then released into the cytosol.

1.8 TERMINATION

The translation of a polypeptide chain terminates when one of three stop codons (UAA, UAG, UGA) enters the A-site (figure 1.8). Stop codons have no cognate tRNA's. When a termination codon occupies the A-site of the ribosome, one of two release factors (RF) will recognize it and bind to the A site, signaling the termination of peptide elongation. RF1 recognizes UAG and UAA stop codons, and RF2 recognizes UGA and UAA stop codons.^{124; 125} Binding of a RF results in the peptidyl transferase center hydrolyzing the ester bond between the tRNA and polypeptide from the P-site tRNA, releasing the nacent protein.^{127; 140} . Another release factor, RF 3, is thought to release the ribosomal subunits, but is not essential for cell survival.¹²⁶

1.9 16S RIBOSOMAL RNA STRUCTURES AND REGIONS

All ribosomal RNAs form similar secondary structures. To analyze these structures, ribosomes are separated into domains and secondary structures or regions. The secondary structure of 16S RNA is divided into four domains; the 5' domain, the central domain, the 3' major domain and the 3' minor domain (figure 1.9 and 1.10). These domains form the

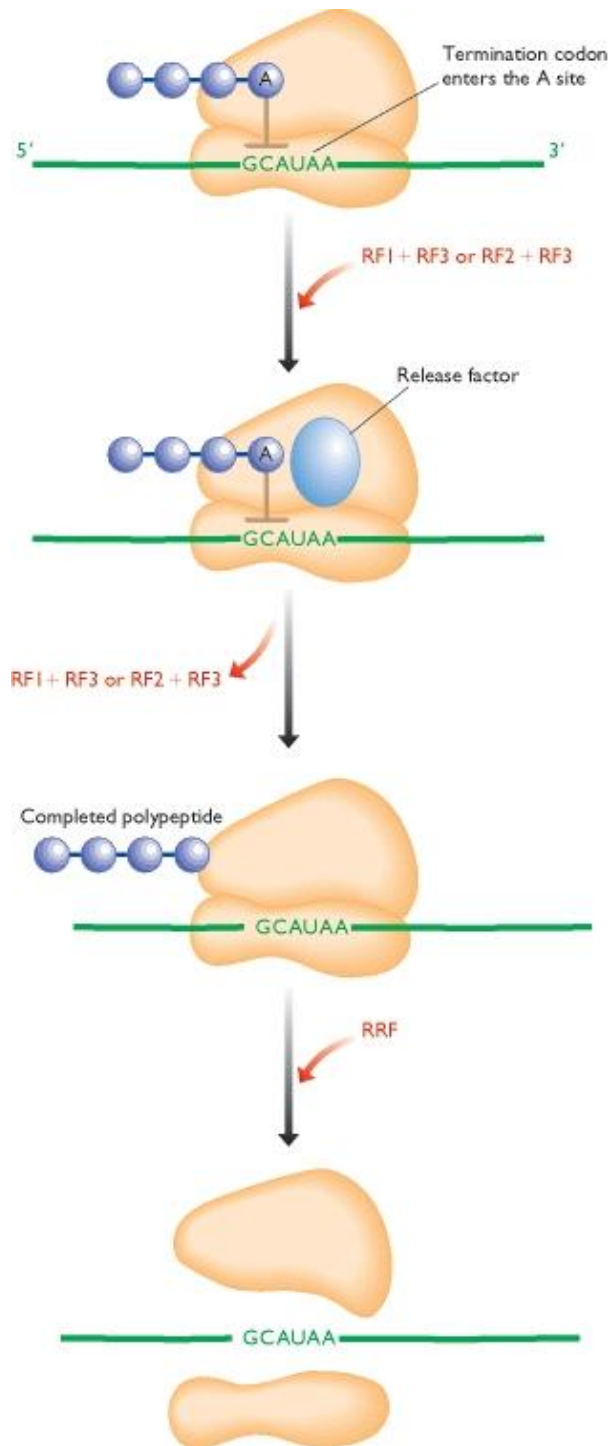
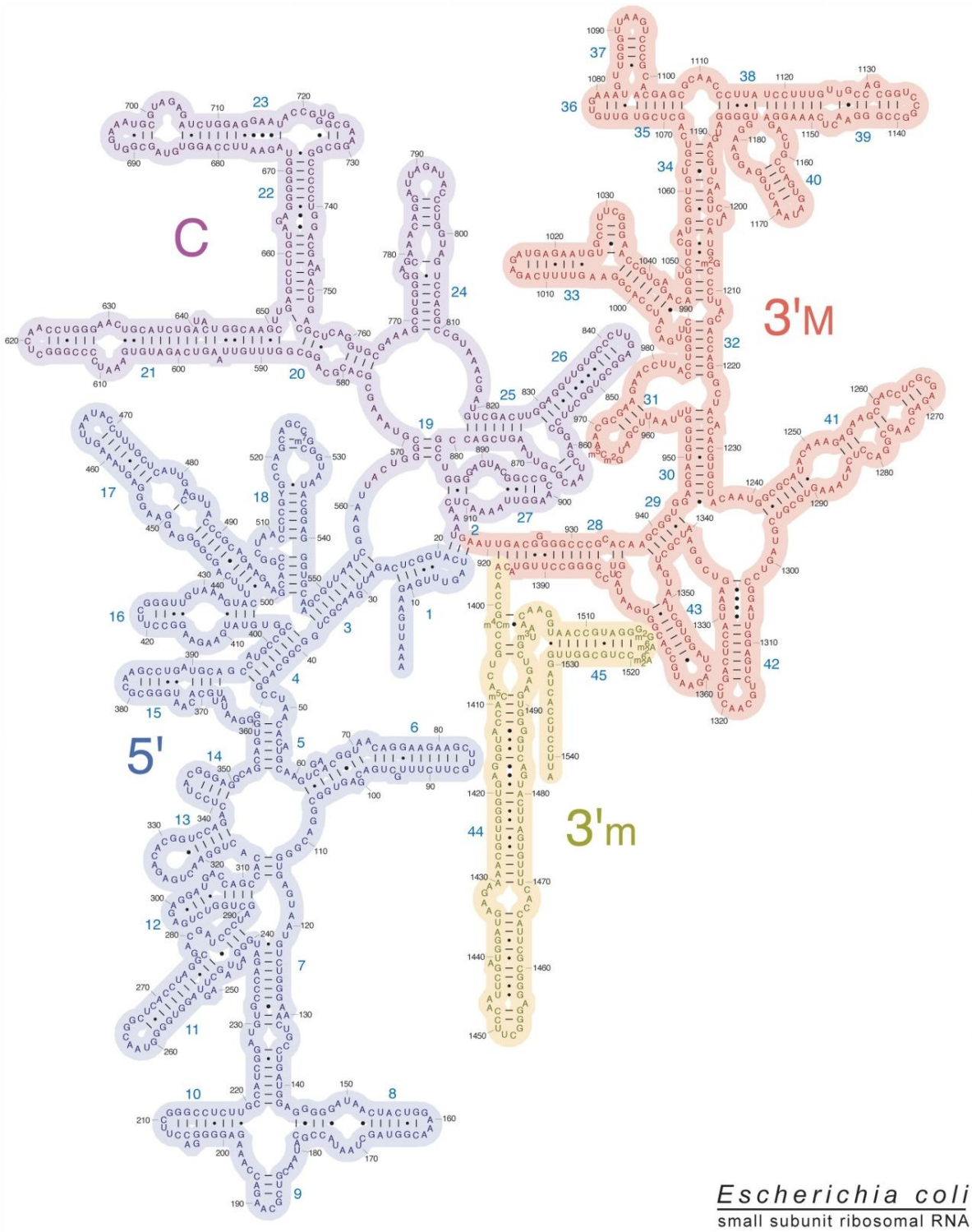


Figure 1.8: Translation Termination

See text for detailed information. Image taken from Garland Science, Copyright © 2002
<http://www.ncbi.nlm.nih.gov/bookshelf/br.fcgi?book=genomes&part=A7712>



Escherichia coli
small subunit ribosomal RNA

Figure 1.9: *E.coli* 16S Ribosomal RNA Secondary Structure
Image taken from Noller, H.F. <rna.ucsc.edu/rnacenter/ribosome_images.html>

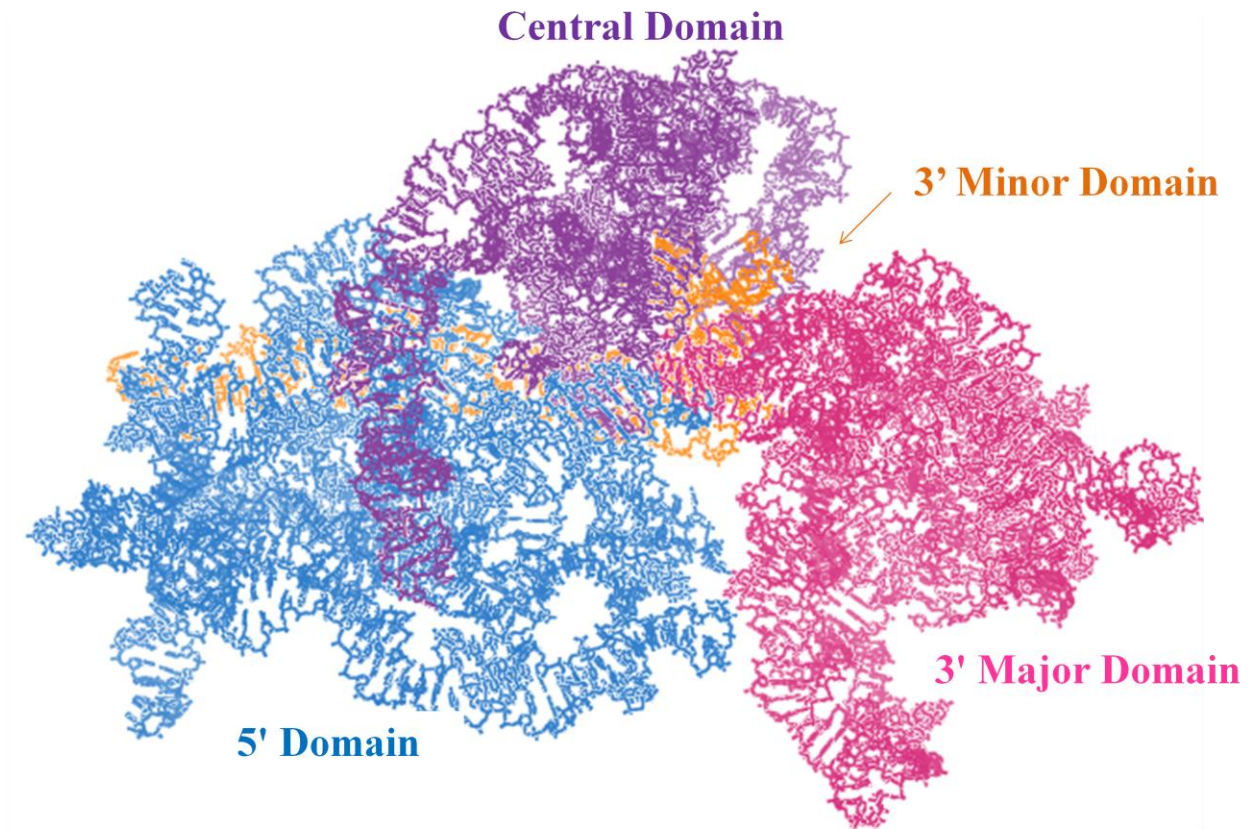


Figure 1.10: *E. coli* 16S Ribosomal RNA
Image modified from PDB 2I2P

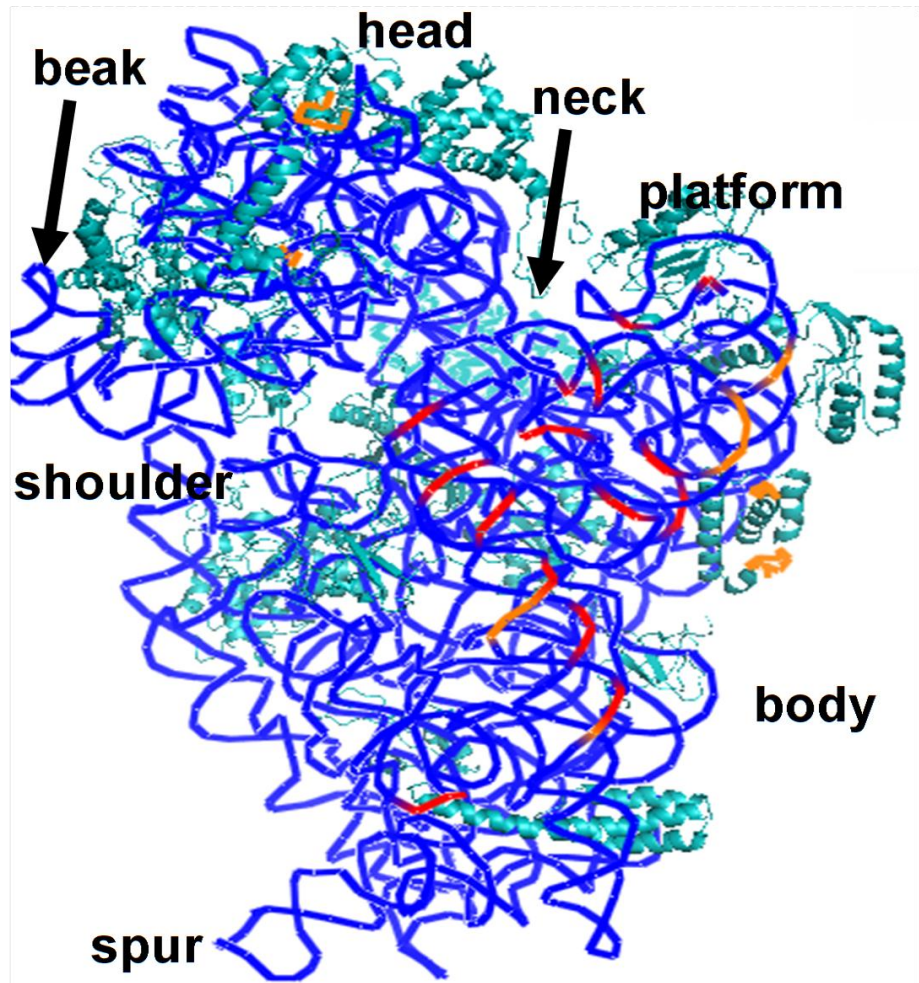


Figure 1.11: Morphological Features of the 30S rRNA

16S rRNA is in blue; 30S rproteins are in cyan; Red (RNA-RNA) and orange (RNA-protein and protein-protein) regions are involved in subunit association contacts.¹⁴

body, platform and head of the 30S subunit (figure 1.11). The 5' domain (nucleotides 1-559) makes up the bulk of the 30S body and consists of 19 helices. The central domain (nucleotides 560-918) is composed of nine helices that forms the 30S platform. The 3' major domain (nucleotides 919-1396) contains 15 helices that form the head, and the 3' minor domain (nucleotides 1397-1542) is just two helices that extend from the subunit to interact with the 50S subunit.

Within each of these domains are several secondary structure motifs that include single-stranded regions, double-stranded regions (helices), internal loops, internal bulges, and stem loops. Single-stranded regions are unpaired nucleotides that often interact with other structural elements. Double-stranded regions, or helices, take on the basic A-form helix structure from anti-parallel single stranded regions of rRNA. The A-form helix generates a deep but narrow major groove (4-5Å width and 13.5Å depth) which makes protein interactions difficult (see figure 1.12). The minor groove, is broader and shallower than the major groove (10-11Å width and 2.8Å depth) it is for this reason that, unlike DNA, many RNA interactions occur in the minor groove.^{12; 45} Unpaired bases within these helices may form internal loops or bulges. In bulges, one strand has uninterrupted base pairing, but the other strand has unpaired bases that bulge out. Internal loops are similar, but both strands have unpaired bases. These unpaired bases have the ability to interact with other ribosomal elements. Finally, stem-loops or hairpin-loops are composed of a single continuous strand of RNA that folds over on itself with an inverted complementary sequence, leaving only a small region of unpaired nucleotides (usually four or more) at the end of the helix. The most common type of loop is the tetraloop, making up nearly 55% of all stem loops in the 16S rRNA.³⁶

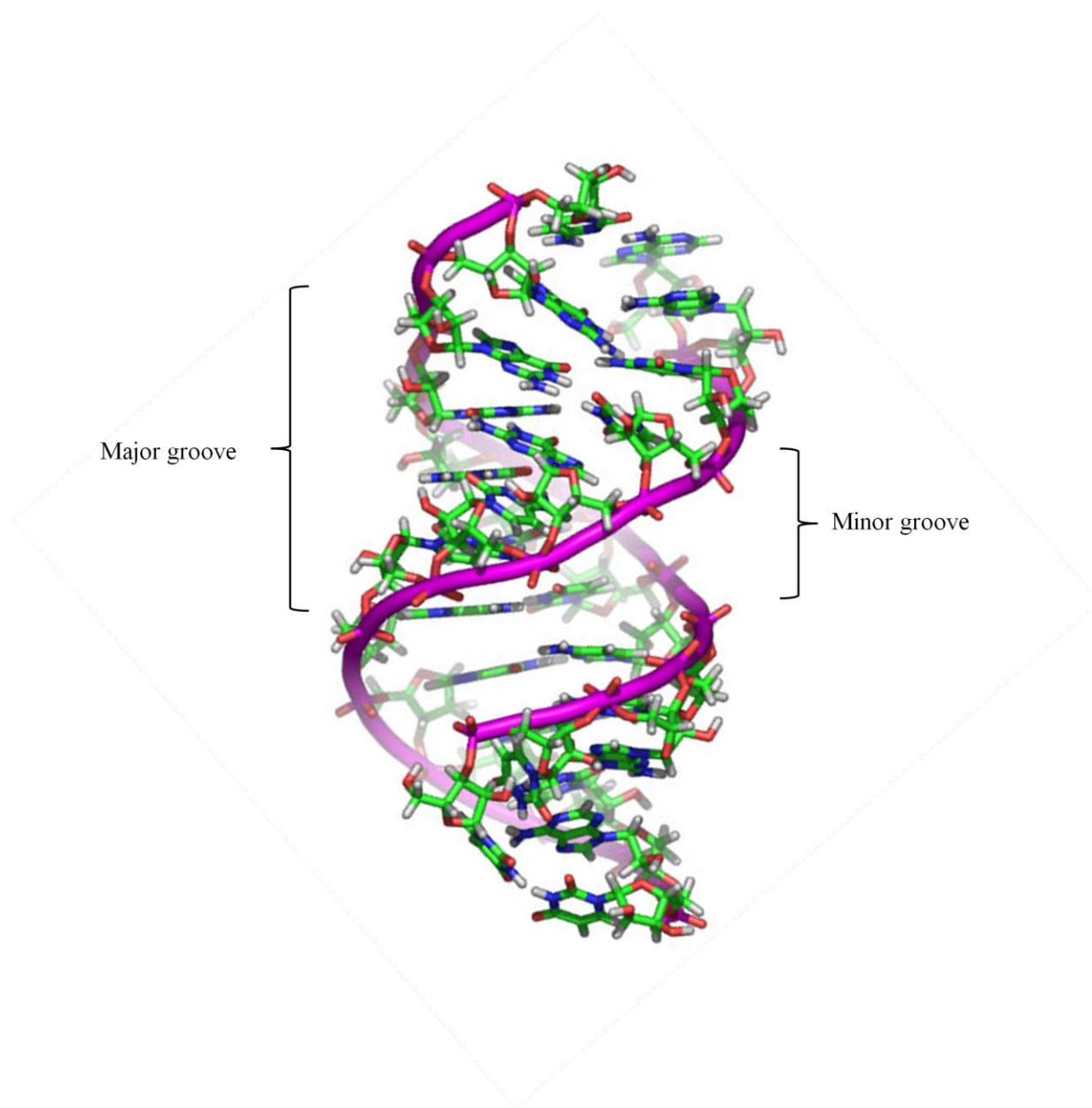


Figure 1.12: RNA A-form Helix

A-form RNA helix, showing major and minor grooves. Refer to text for detailed description.
Adapted from White, et al (2002)⁴⁵

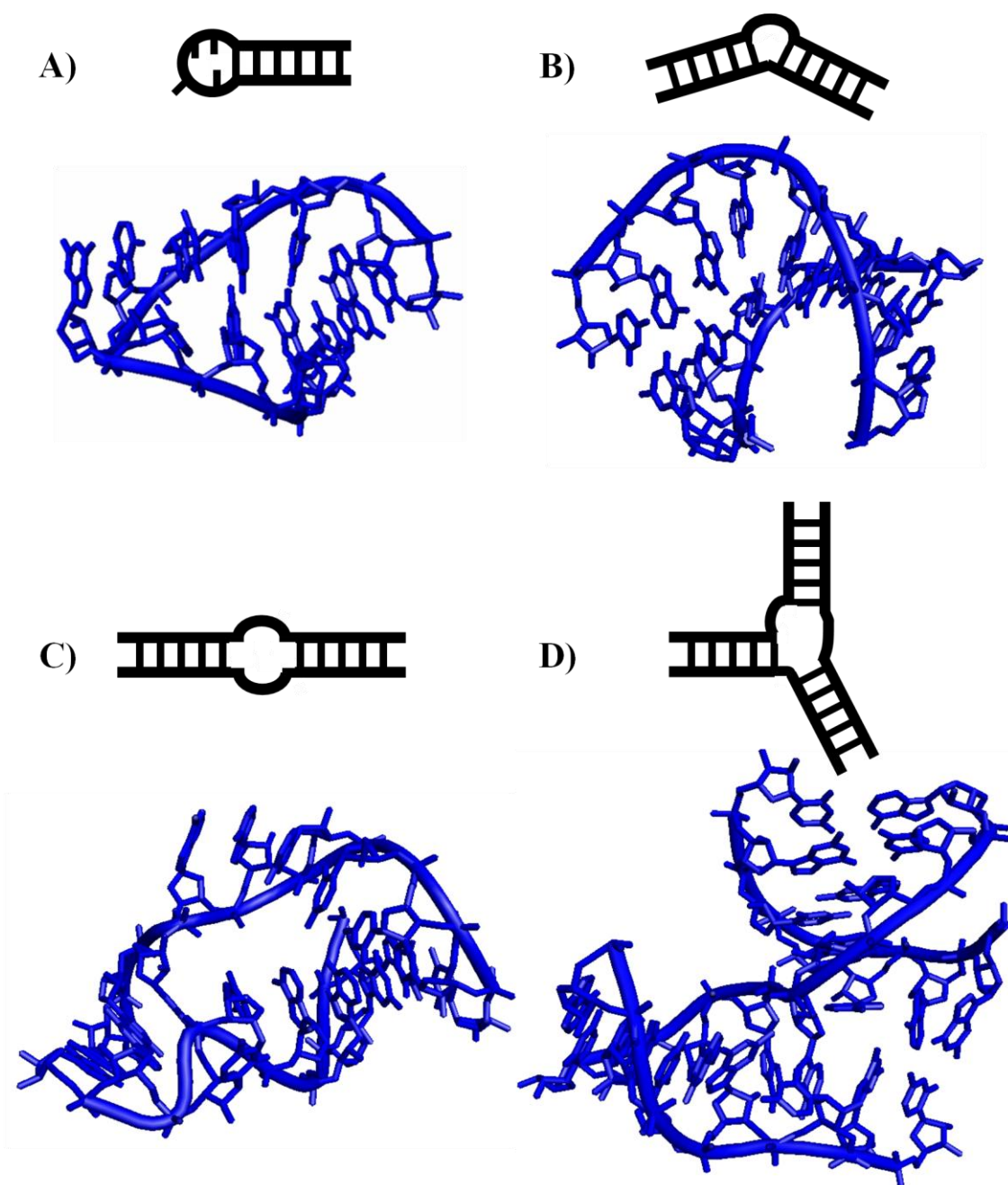


Figure 1.13: Common Secondary Structural Motifs

A) stem/hairpin loop ; B) internal bulge; C) internal loop; D) junction loop. (Schuwirth *et al.*, 2005)⁴⁴

Tertiary structural motifs are formed by interactions between secondary structures (Figure 1.13). RNA tertiary structures may involve (a) two helices, (b) two unpaired regions, or (c) one unpaired region and a double-stranded helix.³⁷ Under appropriate conditions, structured RNA molecules undergo further modeling to occupy specific 3-D structures. It is this level of organization that provides the complexity in RNA that is indispensable for its catalytic activity. These precise three dimensional structures allow the refined function of the finely tuned ribosome. There are several common tertiary structures; co-axial stacking, adenosine platforms (A-platforms), base triples, loop-loop interactions, tetraloop-tetraloop receptors, ribose zippers, and pseudoknots (figure 1.14). Co-axial stacking is an energetically favorable motif in which helices are stacked to form a semi-continuous helix.¹⁴⁴ The A-platform is an interaction between two adjacent adenosines stacking onto a non-canonical base pair.^{143; 166} A base triple is the interaction of an unpaired nucleotide with a Watson-Crick base pair in either the major or minor groove.¹⁴⁵ Loop – loop interactions involve the formation of Watson-Crick base pairs between existing complementary hairpin loops.¹⁴³ Tetraloop receptors are among the most prevalent motifs observed in natural RNAs, which is the interaction of nucleotides between four nucleotide loop sequences.^{143; 145; 146} The ribose zipper is distinguished by consecutive hydrogen-bonding between the ribose 2'-hydroxyls from different regions of an RNA chain or between different RNA chains.¹⁴⁷ Pseudoknots, though more of a folding topology than a specific structure, are characterized by two stem-loops, of which the loop regions form short double helices by interacting with upstream or downstream sequences.¹⁴⁸

1.10 PSEUDOKNOTS

Pseudoknots are among the most prevalent motifs in RNA structures. Originally recognized in the yellow turnip virus⁴², their complex tertiary interactions made them difficult to

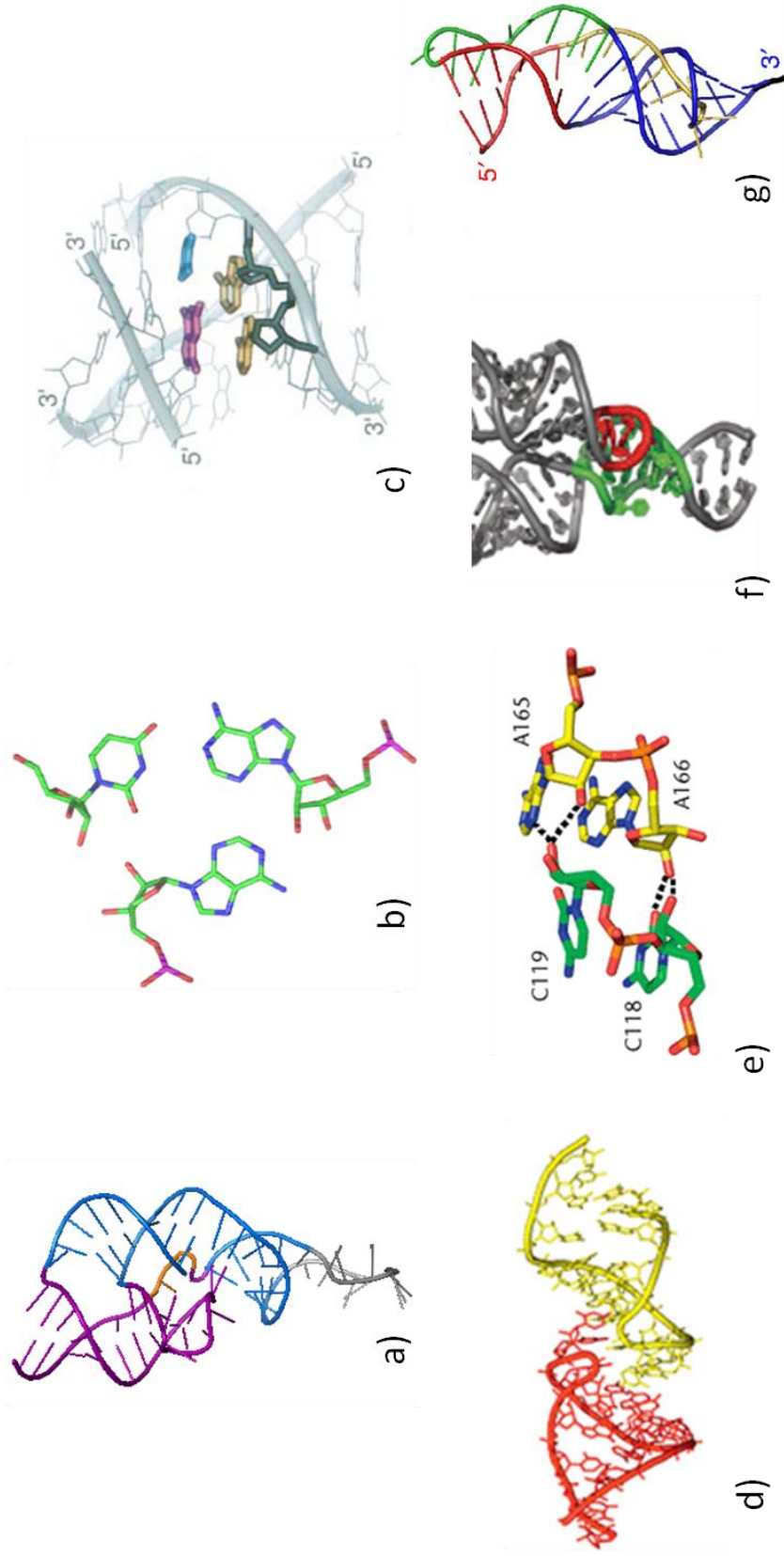


Figure 1.14: Common Tertiary Structural Motifs

(a) Coaxial stacking: Two coaxially stacked helices (blue and violet) along with the single-stranded region (orange). PDB 1DRZ. (b) Base triplets: from 30S crystal structure. PDB 1IBM. (c) Adenosine platform: Adenosine shown in yellow.¹⁶⁶ (d) Loop loop interaction: Red and yellow correspond to different external (hairpin) loops. (e) Ribose zipper: Hydrogen-bonding in the A-minor motif and ribose zipper tertiary interactions are illustrated with dotted lines. PDB 1CXO. (f) Tetraloop-tetraloop receptor. Tetraloop shown in red and the receptor is shown in green. PDB 1HR2. (g) Pseudoknot: See text for details.¹⁶⁷

recognize and predict. Though several pseudoknot topologies exist, they are generally recognized as two helical segments connected by single-stranded regions or loops (figure 1.15).⁴¹ Based on the length of the helix or loop, or surrounding interactions, the pseudoknot can take on various structural conformations. Accordingly, this structure has been at the core of diverse functional hotspots.^{50-57; 70-71}

The best characterized and most commonly occurring pseudoknot topology is the H-type, where H stands for hairpin loop.⁴⁶ In this type of fold, the unpaired bases of the loop in a stem loop form pairs with bases outside of the stem. These new base interactions cause the formation of a second stem and loop, which can stack on top of each other due to hydrogen bonds stabilizing the structure. This coaxial stacking of the stems means the pseudoknot mimics a single stem, making the pseudoknot a difficult structure to identify. In most cases, the second loop is very short, or completely absent.⁴⁹ Figure 1.16 shows other types of pseudoknots that have longer loops than the traditional H type and can take on secondary structures of their own; LL type, HL_{OUT} type, HL_{IN} type, HH type, and the HHH type (H: hairpin loop, L:bulge loop, internal loop or multiple loop).⁴⁷ Although various conformations have been identified, for many of these pseudoknots, much of their primary sequence is unimportant to the function of the structure as long as the conformation and overall stability is maintained.⁴⁸

RNA pseudoknots are seemingly “everywhere” and are essential for many important biological processes. They have been found in various ribozymes^{51; 52}, self splicing introns⁵³, telomerase⁵⁰, riboswitches^{70; 71}, frame shifting viral RNAs^{54; 55; 56; 57}, and other active sites. These pseudoknots are not simply RNA architecture, they are often catalytically active in biological systems. Two of the fastest-known ribozymes, the hepatitis delta virus⁶⁷ and one capable of forming Diels-Alder reactions⁶⁶, both harbor nested pseudoknot structures^{128; 129} which is when

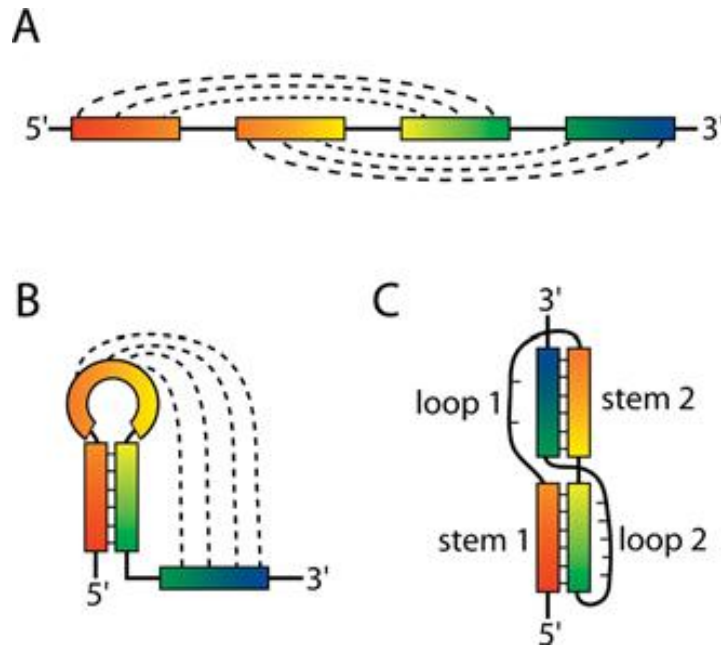


Figure 1.15: Folding of an RNA Pseudoknot

(A) Linear arrangement of base-pairing elements within an H-type RNA pseudoknot. Base pairing is indicated with dashed lines. (B) Formation of initial hairpin within pseudoknot sequence. Base pairings from loop to bases outside the hairpin are indicated with dashed lines. (C) Classic H-type pseudoknot fold. (Staple and Butcher 2005)⁴¹

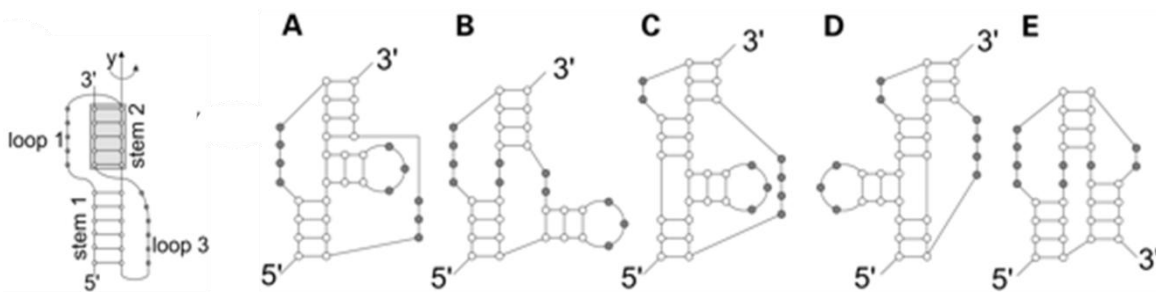


Figure 1.16: Pseudoknots of Other Types

First image: H type (A) LL type; (B) HL_{OUT} type; (C) HL_{IN} type; (D) HH type; (E) HHH type. H: hairpin loop, L: bulge loop, internal loop, or multiple loop.

Taken from Kyungsook Han and Yanga Byun (2003)⁴⁷

two pseudoknots stack on top of each other. Some well studied (group I) spliceosomes include pseudoknot structures, in *Tetrahymena*, for example, that hold the molecule together and establish the catalytic core.⁵⁸ Human telomerase has a highly conserved classic H type pseudoknot at its 5' end that is essential for function.^{59; 60} Loss of this pseudoknot has been directly linked to the diseases aplastic anaemia^{61; 63}, bone marrow failure^{62; 64}, Cri du chat Syndrome¹³⁰, and autosomal dyskeratosis congenita^{131; 63}. Pseudoknots are also commonly responsible for the induction of ribosomal frameshifting, and are therefore a critical component of this type of regulation of gene expression. At a slippery sequence in the mRNA, the pseudoknot causes the ribosome to stall and the codon frame is disrupted and realigned at a -1 position for a new reading frame.⁶⁵ A number of viruses use this mechanism for proliferation of retroviruses and it is therefore an attractive target for antiviral drugs.

In *E.coli*, four pseudoknots have been identified in the 16S subunit, and another 15 are predicted to be in the 50S subunit. In the 16S, the central pseudoknot exists between nucleotides 9-13/21-25, and between 17-19/ 916-918. Powers and Noller showed another pseudoknot in the 530 hairpin region exists between 505-507/524-526, and that this pseudoknot is essential for ribosome function.⁷² A third pseudoknot, also found in the central domain is between 570-571/865-866, is also essential for ribosome function.⁷³ Pseudoknots can play many different roles; stable pseudoknots can offer binding sites for proteins or other RNA's, assist in overall folding and/or fitness of a molecule (as unfolding a pseudoknot can be difficult)⁶⁹, or take on different conformations in response to environmental changes,⁶⁸ can be a dynamic structure needing to break and re-form.

1.11 GENETIC SYSTEM

Early biochemical studies have contributed to our basic general knowledge about ribosomal assembly and translation. However, more detailed information was concealed because of three problematic features of using *E. coli* as the model system; the presence of multiple ribosomal operons, not being able to study dominant lethal rRNA mutations, and the difficulty of separating plasmid derived and chromosomally derived ribosomes. Prokaryotic ribosomes use the SD-ASD interaction to bind mRNAs and initiate translation.

Lee et al.⁹⁸ took advantage of this critical interaction to develop an *in vivo* genetic system for the analysis of the role of ribosomal RNA in protein synthesis. (Figure 1.17). In this system, the complete *rrnB* operon (including the 16S, 23S and 5S), is under control of a *lacUV5* promoter which can be induced by IPTG (Isopropyl β -D-1- thiogalactopyranoside).^{97; 98; 99} This plasmid also contains a *lacI^q* gene encoding the *lac* repressor¹³² to facilitate regulation of *rrnB* transcription. An ampicillin resistance marker is included under a constitutive promoter to maintain the plasmid in the cell. Two reporter genes, green fluorescent protein (GFP)^{133; 134} and chloramphenicol acetyltransferase (CAT)¹³⁶, are under a constitutive *trp* promoter¹³⁵. The SD sequences of the reporter genes as well as the ASD sequence of the 16 S rRNA were mutated from 5'-CCUCC to 5'-GGGAU.^{97; 100}

This modified sequence allows only ribosomes with the specialized ASD sequence can translate the reporter genes and nothing else. Consequently, cells expressing this system are chloramphenicol-resistant and the level of this resistance and the amount of GFP fluorescence produced is directly dependent upon the amount of functional CAT protein and GFP produced by the plasmid-derived ribosomes. Thus, deleterious rRNA mutations in plasmid-encoded ribosomes inhibit translation of only the CAT and GFP messages, resulting in lower

chloramphenicol resistance and fluorescence without affecting translation of other cellular messages. Minimum inhibitory concentration (MIC) of chloramphenicol and/or GFP fluorescence can be assayed directly from an induced culture, allowing the coveted feature of *in vivo* analysis with minimal preparation.

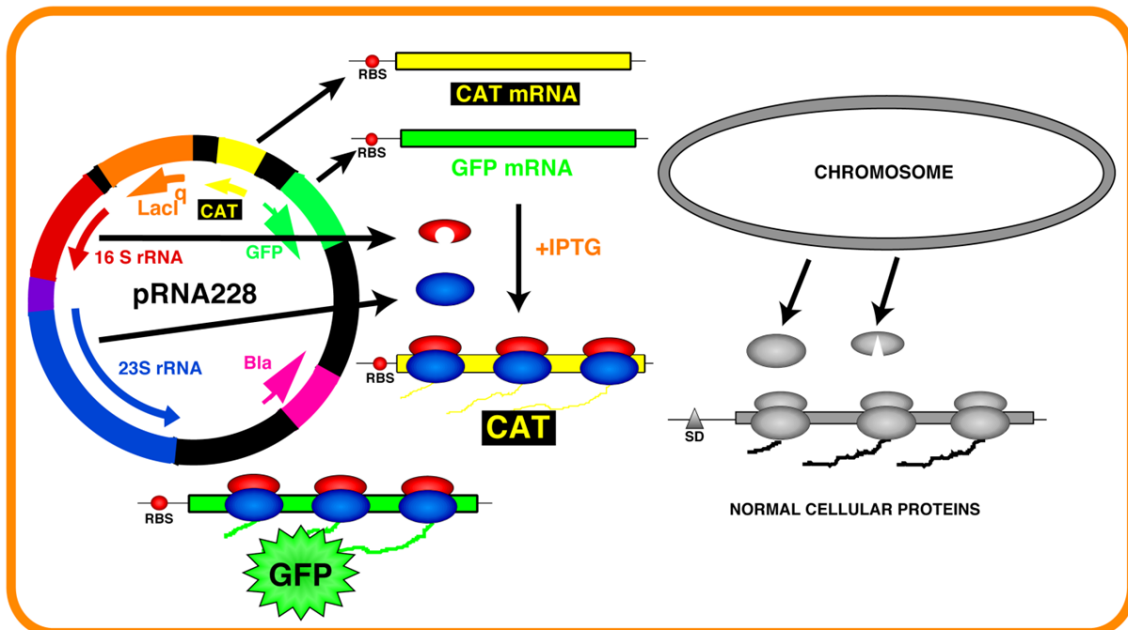


Figure 1.17: Genetic System for Analysis of Ribosome Function

Plasmid pRNA228 contains the *rrnB* operon under transcriptional regulation by the *lacUV5* promoter. The anti-Shine Dalgarno sequence in the 16S rRNA has been altered, as well as the Shine Dalgarno sequence in both reporter genes CAT and GFP. Red and blue oval represent plasmid derived 30S and 50S subunits, respectively. Gray ovals represent host chromosomally derived 30S and 50S subunits. As the reporter genes cannot be translated by host ribosomes, this system allows for the analysis of plasmid derived ribosomes exclusively without affecting the viability of the cell.³⁹

Chapter 2

Materials and Methods

2.1 REAGENTS

Restriction enzymes and buffers were purchased from New England Biolabs. Sequencing DNA polymerase, nucleotides, and buffer were purchased from Epicentre Biotechnologies. PCR primers and IRD labeled sequencing primers were ordered from IDT DNA. Silica for DNA purification was purchased from Sigma-Aldrich. DNase I was purchased from Worthington Biochemical Corporation. Other chemicals were purchased from either Sigma-Aldrich or Thermo-Fisher Scientific.

2.2 BACTERIAL STRAINS

All plasmids for rRNA mutagenesis and analysis were maintained and expressed in *E. coli* DH5 (*supE44*, *hsdR17*, *recA1*, *endA1*, *gyrA96*, *thi-1*, *relA1*).¹⁰⁹ If methylation sensitive enzymes such as *BcII* restriction endonuclease were employed, the plasmid was cultured from either *E. coli* GM2929¹⁰² (*dam-13::Tn 9*, *dcm-6*, *hsdR2*, *recF143*, *mcrA0*, *mcrB9999*, *galK2*, *galT22*, *ara-14*, *lacY1*, *xyl-5 thi-1*, *tonA31*, *rpsL136*, *hisG4*, *tsx-78*, *mtl-1*, *supE44*, *leuB6*, *rfbD*, *fhuA13*) or *E. coli* ER2925¹⁰³ (*ara-14*, *leuB6*, *fhuA31*, *lacy1*, *tsx78*, *glnV44*, *galK2*, *galT22*, *mcrA*, *dcm-6*, *hisG4*, *rfbD1*, *R(zgb210::Tn10)*, *TetS*, *endA1*, *rpsL136*, *dam13::Tn9*, *xylA-5*, *mtl-1*, *thi-1*, *mcrB1*, *hsdR2*). Strains were transformed by electroporation¹⁰⁶ using a Gibco-BRL Cell Electroporator or chemically transformed using TSB competent cells.¹⁰⁹

2.3 MEDIA

All cultures were grown in Luria-Bertani (LB)^{104; 105} medium or LB medium containing 100µg/mL ampicillin (LB-Amp 100), and/or 35µg/mL kanamycin (LB-Km 35). Solid media

were made by adding Bacto Agar (1.8% W/V). To induce synthesis of plasmid-derived rRNA from the *lacUV5* promoter in pRNA plasmids, IPTG (isopropyl-beta-D-thiogalactopyranoside) was added to a final concentration of 1 mM. To induce synthesis of cloned ribosomal proteins under the P_{BAD} promoter in pKan5 plasmids, L-Arabinose was added to a final concentration of 0.2%. A solution of Medium E + 21% DMSO was used for freezer storage of bacterial strains. Medium E is composed of K₂HPO₄ (2% W/V), NaNH₄HPO₄•4H₂O (0.7% W/V), citric acid (0.4% W/V), MgSO₄•7H₂O (0.04% W/V), and DMSO (21% V/V). SOB medium¹⁰⁶ used for preparation of DH5 electrocompetent cells was made by addition of bacto-tryptone (2% W/V), bacto-yeast (0.5% W/V), NaCl (0.05% W/V), and KCl (2.5mM final concentration). SOC medium¹⁰⁹ was prepared as directed for Difco™ SOB Medium and used for the recovery of transformed cells; Per liter; 20g tryptone, 5g yeast extract, .5g NaCl, 2.4g anhydrous magnesium sulfate, 186mg KCl. No glucose was added.

2.4 PLASMIDS

The pWK122 plasmid is a derivative of pWK1.¹¹⁰ In pWK122, however, the 3' terminus of the *rrsB* gene has been modified such that the Shine-Dalgarno sequence and the sequence downstream from the *rrsB* gene are identical to the corresponding sequence in pRNA plasmids.^{39; 110} The *rrsB* genes in the pWK plasmids are under the transcriptional regulation of a Class III T7 promoter¹¹⁶ and were used only as a cloning intermediate for site directed mutagenesis because they have more unique restriction sites than the larger pRNA vectors (figure 2.1). The pRNA228 and pRNA272 plasmids are derivatives of the original pRNA123 vector⁶³ and contain the same *rrnB* operon with an altered Shine Dalgarno sequence under a transcriptional *lacUV5* promoter, a *lacI^q* repressor, GFP and CAT reporter genes, a copy of the 23S and 5S. These plasmids are all derivatives of pRNA123³⁹ which was constructed from

pBR322¹⁵⁰. GFP assays were performed using the pRNA228 plasmid with mutations in the 16S gene at sites corresponding to positions 570, 571, 865, 866 of *E. coli* 16S rRNA.

The pKan5 plasmids are derivatives of pACYC177¹⁵¹ and therefore have a low-copy number (10-12 copies per cell) and are compatible with ColE1-derived plasmids such as the pRNA series plasmids.¹⁰⁷ The pKan5 T1T2 expression vector (figure 2.2) was used to over-express certain ribosomal proteins in the presence of the plasmid-encoded ribosomes. pKan5 confers kanamycin resistance. Ribosomal protein genes cloned into the *HindIII* and *NotI* restriction sites are placed under the transcriptional regulation of the P_{BAD} promoter.¹⁵³

2.5 CONSTRUCTION OF SITE-DIRECTED MUTATIONS

Mutations were introduced into the 16S rRNA gene using recombinant PCR.¹⁵³ pWK122 was used as a template during PCR with primers 570N571N and 16S-H796 for mutations at positions 570 and 571 and primers 865N866N and AVR11 for mutations at positions 865 and 866 (table 2.1). PCR reactions contained 1 μM of each primer, 50 ng template, 200 μM dNTPs, 4 units Pfu polymerase and 1X Pfu Buffer (200mM Tris-HCl pH 8.8, 20mM MgSO₄, 100mM KCl, 100mM (NH₄)₂SO₄, 1% Triton X-100, 1mg/mL BSA) in a 50 μL reaction. The PCR products were gel purified and recovered using silica beads. The products were then digested with *BglII* and *SacII*, and *ApaI* and *BglII*, respectively. The 570, 571 mutations were first subcloned into pWK122 and verified by sequencing (figure 2.3). Each mutation was then transformed into either GM2929 or ER2925, both of which are recombination and dam methylase deficient strains. The mutations were then transferred from pWK122 to pRNA228 using the *BclI* and *BstEII* restriction sites and confirmed by sequence analysis. The 865, 866 mutations were cloned directly into pRNA272 and verified by sequencing (figure 2.4). Finally, 865, 866 mutations were digested with *BglII* and *BstEII* and ligated into both wild-type pRNA228 and pRNA228

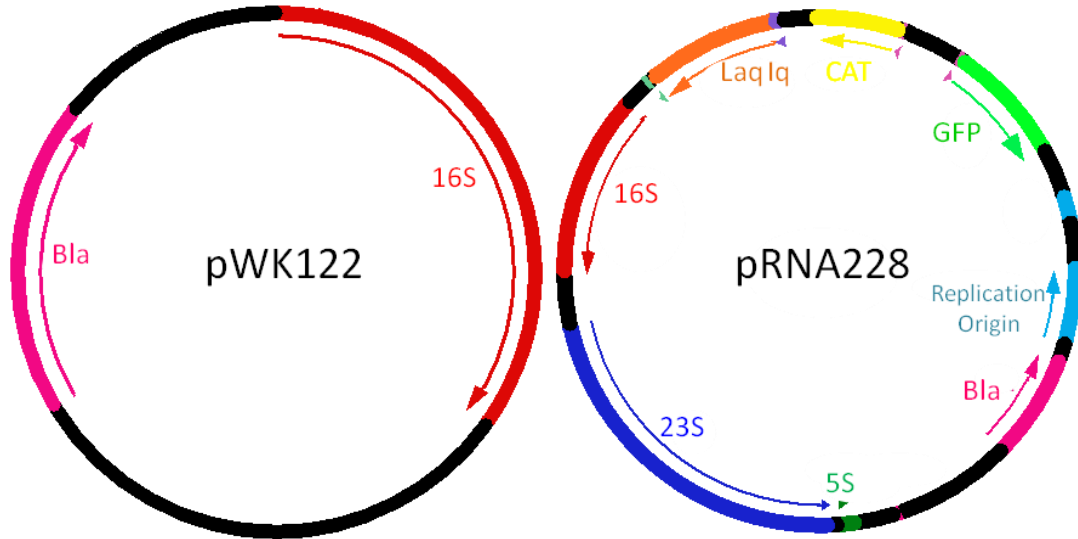


Figure 2.1: Commonly used plasmids.
pWK122 on the left and pRNA228 on the right. See text for details.

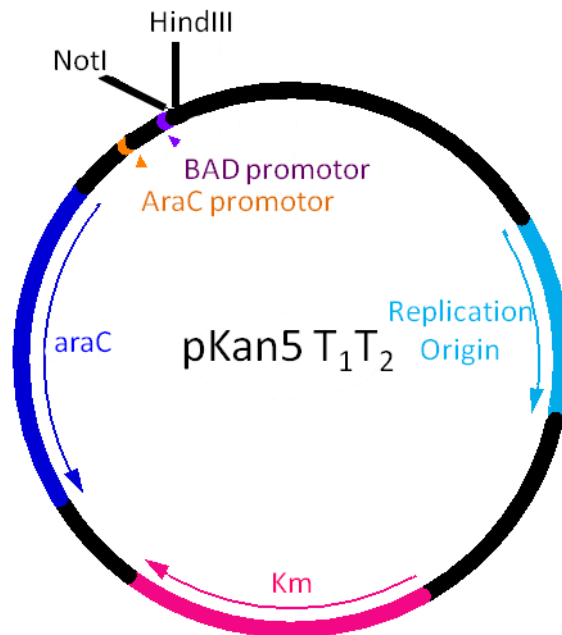


Figure 2.2: pKan5 T1T2

This plasmid is the empty version of the vector. Ribosomal protein genes were cloned between the *NotI* and *HindIII* restriction sites. See text for details.

with each 570, 571 mutation sets (figure 2.4 and 2.5). Once each of the 255 combinations of mutations were identified and confirmed by sequencing, the mutants were stored at -80 °C.

2.6 DNA PURIFICATION

PCR products and digested DNA fragments were purified by electrophoresis in 0.8-1.2% SeaKem® GTG® agarose gels and excising the correct sized band and gene cleaning.¹¹¹ The agarose and DNA was melted in three volumes of a NaI solution (6M NaI, 1X TAE, 10mM Na₂S₂O₃) and incubated at 55°C. Approximately 5µl (100ng) of silica was added, and an extra 1µ of silica was added for each 0.5µg of DNA exceeding 5µg. The silica was mixed with the sample for 15 minutes by gentle inversion and pelleted by centrifugation for 1 minute at 12,000 x g. The silica pellet bound to the DNA was washed three times with a high-salt New Wash solution (50mM NaCl, 10mM Tris-HCl pH 7.5, 2.5mM EDTA, in 50% ethanol in autoclaved deionized water). The pellet was dried under vacuum for 5 minutes at 55°C to remove trace amounts of ethanol. Purified DNA was eluted from the pellet with sterile de-ionized water. Plasmid DNA was isolated using the alkaline lysis miniprep method.¹¹² For overnight cultures, 3 mL of LB medium containing 100µg/mL ampicillin were inoculated with a single colony and incubated at 37°C with shaking overnight (16 hrs). The cells were pelleted by centrifugation for 1min at 4,000 x g, and resuspended in 300µL of resuspension solution (50mM Tris-HCl pH 7.5, 10mM EDTA, 100µg/mL RNase A) vortexing. The cells were lysed by the addition of 300µL fresh lysis solution (200mM NaOH, 1% SDS, sterile water by gentle inversion 3-5 times, and neutralized by adding 300µL neutralization solution (1.32M KOAc pH4.8. Bring to pH with acetic acid) and inverting gently 3-5 times. Cellular debris and chromosomal DNA were removed by centrifuging for 10 minutes at 12,000 x g. Plasmid DNA was precipitated by adding 6 volumes of isopropanol and centrifugation for 15 minutes at 12,000 x g. The DNA pellet was

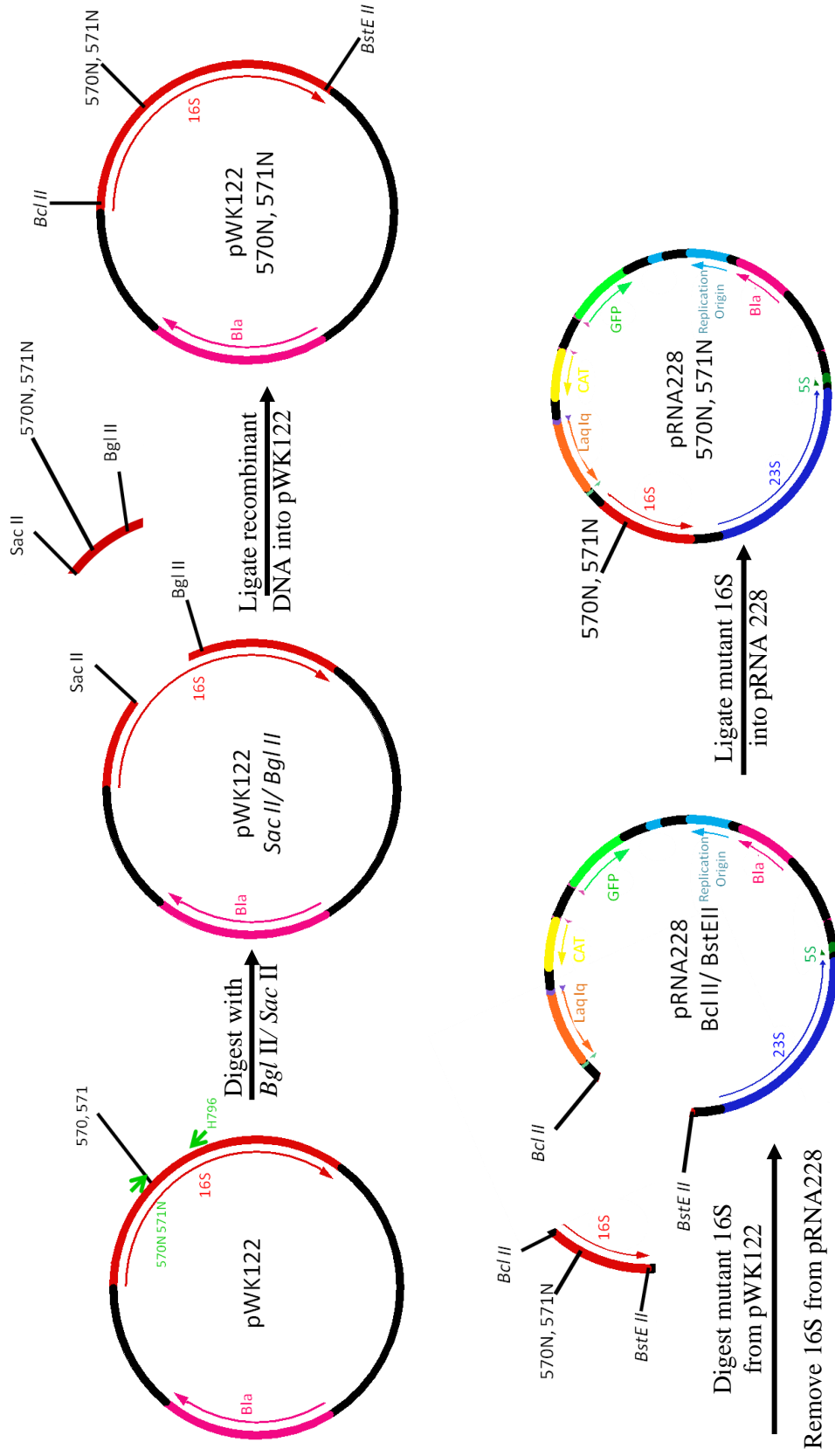


Figure 2.3: Experimental approach for construction of 570N, 571N mutants.
See text for details.

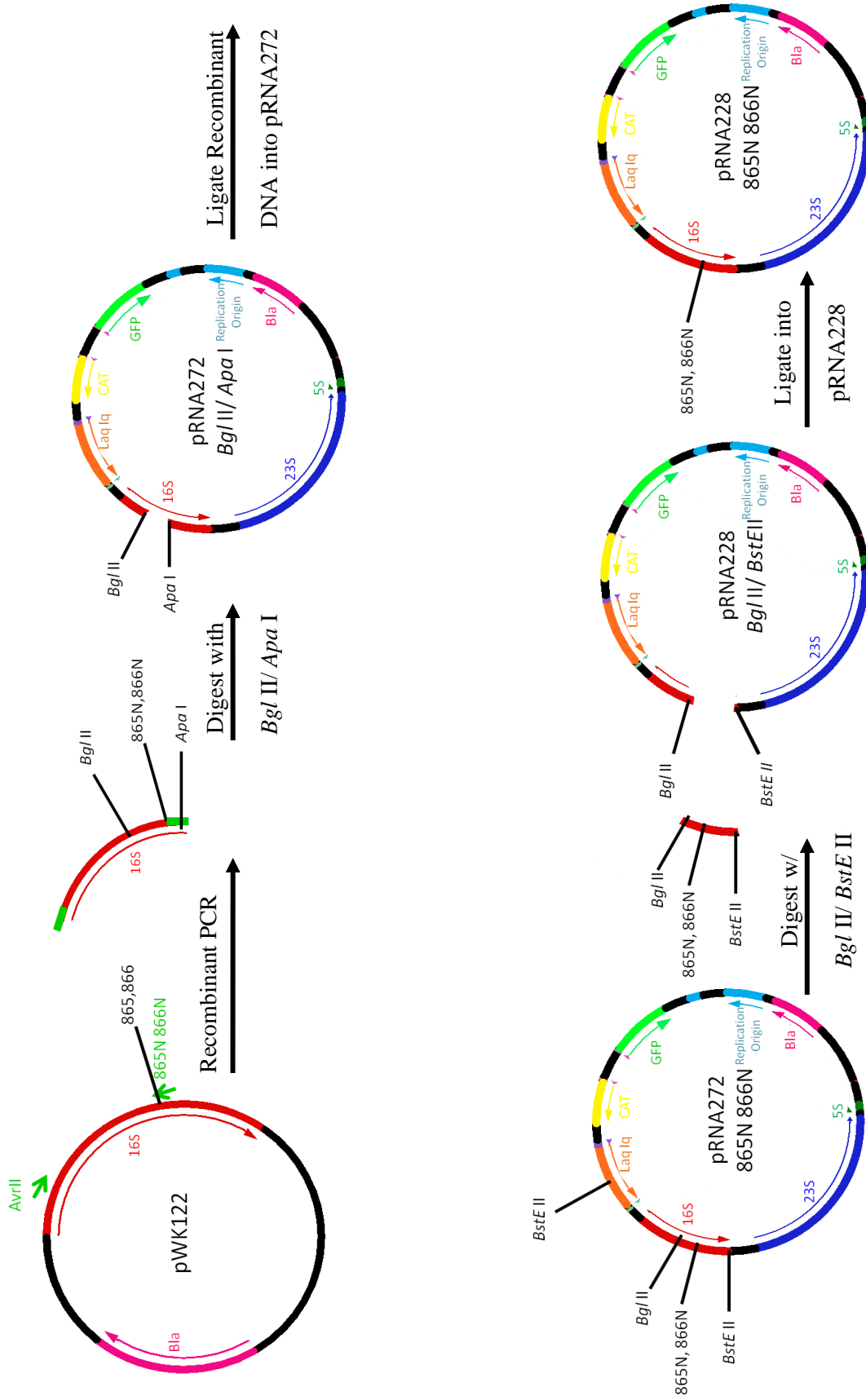


Figure 2.4: Experimental approach for construction of 865N, 866N mutants.
See text for details.

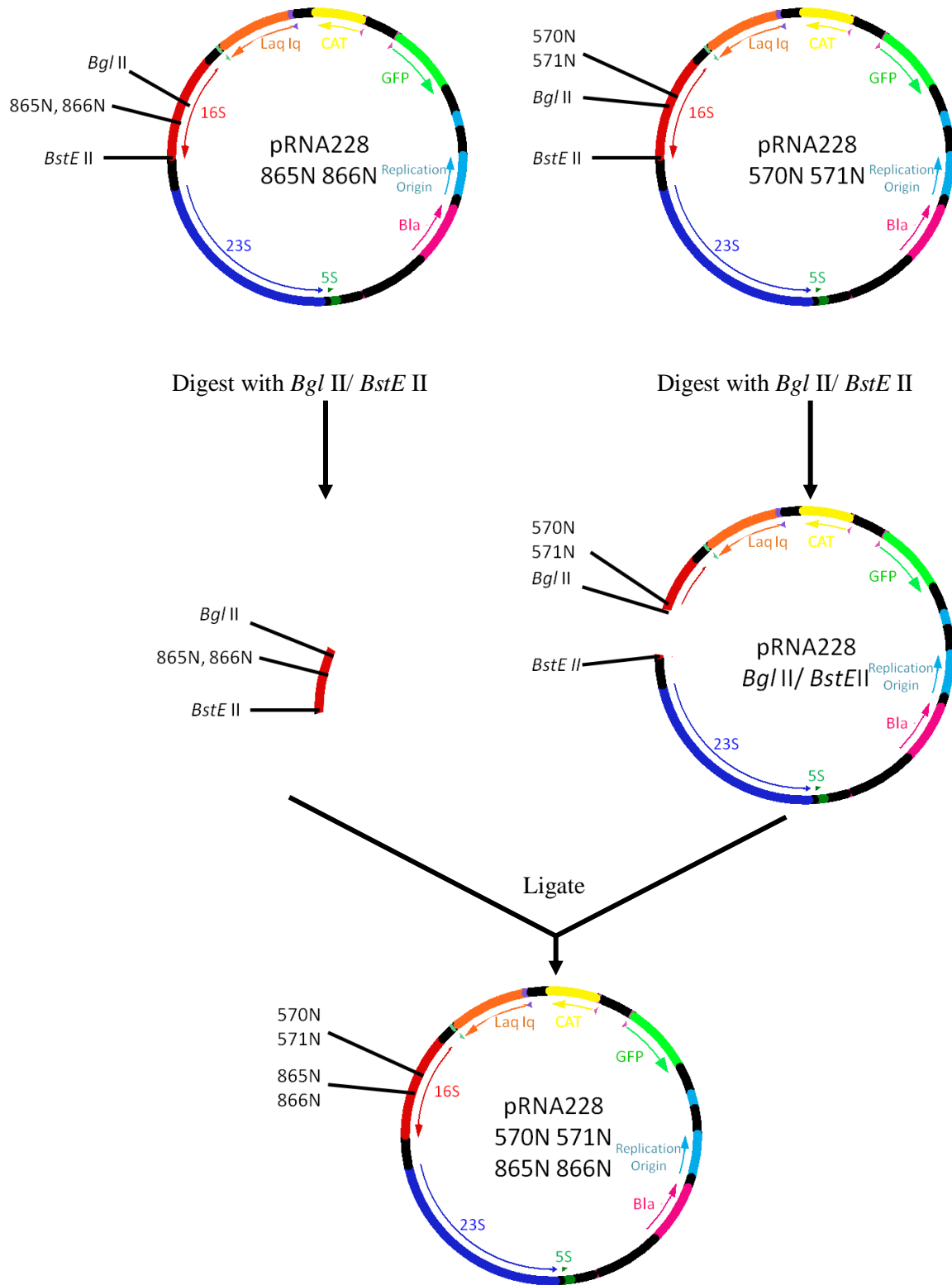


Figure 2.5: Experimental approach for saturation mutagenesis

Approach to clone 570,571,865, and 866 mutations into pRNA 228. See text for details.

washed with 500 μ L of 70% ethanol and pelleted again for 5 minutes at 12,000 x g. The pellet was dried under vacuum at 55 $^{\circ}$ C for 5 minutes, and resuspended in 30 μ L sterile diH₂O.

2.7 LIGATION

Ligation reactions were carried out by the method of Dugaiczky et al.^{113; 114} Typical ligation reactions contained 15ng vector, 8ng insert, 2 units of T4 DNA ligase, 1X ligase buffer and diH₂O in a final volume of 10 μ L. Ligations contained either 1:3 or 1:6 molar ratios of vector to insert and for either one hour at room temperature or overnight at 16 $^{\circ}$ C.

2.8 TRANSFORMATION

Electrocompetent cells were prepared by a method modified by Dower et al.¹⁰⁶ A 3mL overnight culture of *E. coli* DH5 cells was grown in LB medium containing 15 μ g/mL of nalidixic acid (LB-Nal15), and 1 mL of the overnight was used to inoculate 500 mL of SOB medium. The SOB culture was incubated at 37 $^{\circ}$ C with vigorous shaking until the A₆₀₀ was between 0.6-0.8. The cultures were then cooled on ice and pelleted at 4 $^{\circ}$ C, 4,000 x g for 15 minutes. The cells were washed twice in 100 mL of 10% sterile glycerol, and pelleted at 4 $^{\circ}$ C for 4000 x g for 20 minutes. The cells were resuspended in 700 μ L of sterile 10% glycerol, distributed in 150 μ L aliquots and stored at -80 $^{\circ}$ C.

For transformations, 1 μ L of DNA solution was mixed with 25 μ L of electrocompetent cells and the mixture was electroporated at 2.44 kV using an *E. coli* cell Porator (Gibco-BRL). The transformed cells were diluted in 1mL SOC and incubated for 30-60 minutes at 37 $^{\circ}$ C with gentle agitation to allow expression of the antibiotic resistance markers. The transformants were then pelleted at 4,000 x g for one minute and resuspended in 100 μ L of the supernatant and plated on antibiotic selection medium and incubated at 37 $^{\circ}$ C overnight. If two plasmids were being

transformed simultaneously (pRNA228 and pKan5) then 15 ng of each plasmid was added to the 25 μ L of *E. coli* DH5 competent cells and recovery time was between one and 1.5 hours.

E. coli strains ER2925 and GM2929 were stored as TSB competent cells.¹¹⁵ Chemically competent cells were prepared as described by Chung et al.¹⁵⁵ Cultures were grown in LB broth to 0.3-0.6 A_{600} and pelleted by centrifugation at 1,000 x g for 10 minutes at 4°C, resuspended in 0.1 volume of TSB buffer (10% W/V PEG, 10mM MgCl₂, 10mM MgSO₄, 5% DMSO) on ice, aliquoted, and stored at -80°C. For chemical transformation into TSB competent cells, 2 μ L of plasmid DNA was mixed with 50 μ L of competent cells and incubated on ice for 30 minutes. After incubation, 150 μ L of SOC (without glucose) was added, incubated at 37°C for one hour, and then plated on LB agar plates with the appropriate antibiotic.

2.9 SEQUENCING

Two methods were used for sequencing plasmids; a direct method and an indirect method. In the direct method, fluorescent primers that bind directly to the DNA template to be sequenced were used in the sequencing reaction.¹⁵⁴ In the indirect method, the region of the template DNA to be sequenced was first amplified by PCR using primers with unique 5' extensions (table 2.2). The amplicons were then diluted and combined with fluorescently labeled sequencing primers that anneal to the unique 5' sequences of the PCR primers in the sequencing reaction. Sequencing reactions utilized dideoxy chain-termination using SequiTherm EXCEL II sequencing kits from Epicenter according to the manufacturers recommendations.⁹⁷ Sequencing products were resolved and analyzed using the LICOR Global IR² automated sequencer (LICOR Inc).

Typical sequencing PCR reactions contained 150 ng template, 200 nM dNTP, 1X Pfu Buffer, 0.5 μ M of each primer, and 2 units of Pfu polymerase in a 10 μ L volume. The PCR

product was then diluted with 170 μL dH_2O and used as a template in the subsequent sequencing reaction.

Sequencing reactions were assembled in 96 well thin-walled PCR plates (MJ research Inc.). Each reaction contained a 1 μL aliquot of template and a 1.1 μL aliquot of master mix into the appropriate well. A master mix was prepared with 1 pmol/ μL primers (see Table 2.3), 3.54X sequencing buffer (final concentration of 80 mM Tris-HCl and 2mM MgCl_2), dNTP's and 5U/ μL DNA polymerase according to the manufacture protocol. 1 μL of stop solution (Epicentre) was added to each well when the reaction was finished. Samples were then denatured at 94°C for 3 minutes, quenched on ice for 5-10 minutes, and loaded on a 6% denaturing polyacrylamide gel. The sequences were aligned using ALIGN-IR software by LICOR biosciences to confirm mutations.

2.10 FREEZER STORAGE OF BACTERIAL STRAINS

For long-term storage of bacterial cultures, stationary phase cells in Medium E¹⁰⁸ with 7% dimethylsulfoxide (DMSO) were dispensed into 2 mL Nalgene cryogenic vials (Thermo-Fisher 5012-0012) and stored at -80°C. For storage of multiple stocks, 96 well microtiter plates were used instead of individual vials. Each well of a 96 well microtiter plate (Thermo-Fisher 14-230-232) containing 200 μL of LB-Amp100 was inoculated with a single bacterial colony. The plates were incubated with shaking in a HiGro Microplate Cell Incubator (DigiLab) at 37°C overnight (16hrs). Following incubation, sterile glycerol was added to a final concentration of 10% w/v, the plates were covered with sterile aluminum adhesive and stored at -80°C.

2.11 GREEN FLOURESCENT PROTEIN ASSAY

Bacteria were cultured in a 96 well plate in LB with the appropriate antibiotic overnight at 37°C in a HiGro Microplate Cell Incubator (DigiLab) and shaken at 500 rpm with positive

aeration. When the cultures reached stationary phase, they were diluted in LB-IPTG and the appropriate antibiotic and incubated for 24 hours at 500 rpm in the HiGro. At the end of the incubation, the cultures were pelleted in a Sorvall® Legend T centrifuge at 1000 x g for 3 minutes. The supernatant was discarded, the pellets were washed twice in 200µl of HN buffer (20mM Hepes pH 7.4, 0.85% NaCl) and resuspended in 200 µL of HN buffer and a 150 µL aliquot was transferred a microtiter plate (Costar clear-bottom assay plate #3631) and the A_{600} and fluorescence were measured in a SPECTRAMax® 190 absorbance microplate reader and a SPECTRAMax Gemini™ XPS Fluorescence Microplate Reader (Molecular Devices). The A_{600} and fluorescence measurements (excitation 395 nM, emission 509 nM) were performed in triplicate, and the mean fluorescence per A_{600} was calculated for each of the mutants and presented as a percentage of the wild-type control cells. Measurements of cells containing the plasmid pWK122 were used as a blank for all samples. The final GFP activity data are the average of three analyses conducted from three separate overnight cultures on three separate days. Standard errors were calculated and presented.

2.12 RIBOSOME PREPARATION

Ribosomes were prepared essentially by the method of Jelenc and edited Spedding.^{117; 118} Cells containing pRNA plasmids were grown to $A_{600} = 1.0$ and the *rrnB* operons of the plasmids were induced with 1 mM IPTG. Induced cultures were incubated at 37 °C to mid log phase ($A_{600} = 0.6-0.8$) and immediately cooled on ice. The cells were pelleted in Sorvall tubes using the SLA 1500 rotor at 4°C, 10min at 5,000 x g and then resuspended in 4 mL Buffer A (50mM Tris-HCl, pH 7.6, 10mM MgCl₂, 100mM NH₄Cl, 500mM EDTA) and lysed in a French Pressure Cell once at 18000 psi. DNaseI was added to the lysate to a final concentration of 5µg/mL and incubated on ice for five minutes. The cells were pelleted at 7,000 x g at 4 °C using a Sorval SS-

34 rotor, for 15 minutes. The supernatant was collected and NH_4Cl was added to a final concentration of 500 mM. Ribosomes were pelleted by ultracentrifugation at $100,000 \times g$ for 4 hrs at 4°C in a T-1270 rotor (Sorvall). The buffy coat on the surface of the pellet was removed by gently swirling the pellet twice with 1mL of Buffer B (50 mM Tris-HCl, pH 7.4, 10mM MgCl_2 , 100mM NH_4Cl). The resulting ribosome pellet was then resuspended in 500 μL Buffer B by 4°C incubation overnight and either used immediately or stored at -80°C .

2.13 SUCROSE GRADIENT SEPARATION

Sucrose gradients were prepared (10% and 30% sucrose, 7.5 mM MgCl_2 , 48 mM Tris pH 7.6, 100mM NH_4Cl) and loaded into a 36 mL polyallomer Beckman centrifuge tube (9/16 x 3.5 in). The gradient was created using a Biocomp® Gradient Master™ at angle 76, speed 25 for 2.5 minutes. Each sucrose gradient had 20 A_{260} units of ribosomes added to it and centrifuged at $21,000 \times g$ for 21 hours at 4°C . 1.0 mL fractions of each gradient were collected and the A_{260} of each fraction was measured and plotted to identify the location of the ribosome peaks in the gradients.

PCR Primers

Primer	Sequence (5' to 3')
570N 571N	GTG CCA GCA GCC GCG GTA ATA CGG AGG GTG CAA GCG TTA ATC GGA ATT ACT GGG CNN AAA GCG CAC GCA GG
16S - H796	CAT CGT TTA CGG CGT GGA CTA CCA GHG TAT CTA ATC CTG TTT GCT
865N 866N	CCA CCG CTT GTG CGG GCC CCC GTC AAT TCA TTT GAG TTT TAA CCT TGC GGC CGT ACT CCC CAG GCG GTC GAC TTA ACG CNN TAGACTC CGG AAG CC
AVR II	ACG TCG CAA GAC CAA AGA GG

Table 2.1: Primers used to create pseudoknot mutations in 16S rRNA

Specialized PCR Primers

Set	Primer	Sequence (5' to 3')
Set 1	16Set 1A JSL2	5' GCG TCC ACC AGT CCT AGC AAC TCT CAG ACC AGC TAG GGA T 3'
	16Set 1B JSL	5' GCC GTC GCA CTC GTT AGG AAG TCA AAC TTT TAA ATT GAA GAG 3'
Set 2	16Set 2A JSL2	5' GCG TCC ACC AGT CCT AGC AAT ACC GCG GCT GCT GGC ACG G 3'
	16Set 2B JSL	5' GCC GTC GCA CTC GTT AGG AAC GCA TAA CGT CGC AAG ACC AAA G 3'
Set 3	16Set 3A JSL2	5' GCG TCC ACC AGT CCT AGC AAG GTA TTC CTC CAG ATC TC 3'
	16Set 3B JSL	5' GCC GTC GCA CTC GTT AGG AAG GCC TTC GGG TTG TAA AGT AC 3'
Set 4	16Set 4.1A JSL2	5' GCG TCC ACC AGT CCT AGC AAT TGT GCG GGC CCC CGT CAA TT 3'
	16Set 4B JSL	5' GCC GTC GCA CTC GTT AGG AAA TCC CCG GGC TCA ACC TTG G 3'
Set 5	16Set 5A JSL2	5' GCG TCC ACC AGT CCT AGC AAA GTT TAT CAC TGG CAG TCT C 3'
	16Set 5.1B JSL	5' GCC GTC GCA CTC GTT AGG AAT GGA GGT TGT GCC CTT GAG 3'
Set 6	16Set 6A JSL2	5' GCG TCC ACC AGT CCT AGC AAT AAT CCC ATG ATC CAA CCG CAG GTT 3'
	16Set 6B JSL	5' GCC GTC GCA CTC GTT AGG AAG CGC AAC CCT TAT CCT TTG TTG 3'

Table 2.2: List of specialized PCR primers used for sequencing.

Nucleotides shown in bold are regions that pair with IRD labeled sequencing primers.

IRD labeled Sequencing Primers

Primer	Sequence	Annealing Temp
16S seq2 R (700)	5' IRD700/ CAA AGG ATA AGG GTT GCG GT 3'	65°C
16S seq2 R (800)	5' IRD800/ GTT ACC CGC AGA AGA AGC AC 3'	65°C
JSL-UniF (700)	5' IRD700/ GCC GTC GCA CTC GTT AGG AA 3'	68°C
JSL-UniR (800)	5' IRD800/ GCC GTC GCA CTC GTT AGG AA 3'	68°C
JSL2- 800F	5' IRD800/ GCG TCC ACC AGT CCT AGC AA 3'	68°C

Table 2.3: List of Infra Red Dye (IRD) sequencing primers.
Nucleotides shown in **bold** bind to specialized PCR primers in table 2.2.

Chapter 3

Results

3.1 FUNCTIONAL ANALYSIS OF PSEUDOKNOT MUTATIONS

The pseudoknot in the central domain of the 30S subunit is a convoluted structure spanning 313 bases, and is characterized by the formation of Watson-Crick base pairing between G570-C866 and U571-A865 (figure 3.1 and 3.2). A previous study by Vila et al. showed through mutational analysis that Watson-Crick base pairing at these phylogenetically conserved nucleotides is critical for ribosome function.⁷³ Using the rRNA plasmid expression vector, pKK1192U^{119; 120}, single mutations U571A and A865U of the *E. coli* 16S rRNA gene that disrupt Watson-Crick base pairing between these residues were constructed and analyzed.⁷³ When expressed *in vivo*, the U571A mutant was lethal and A865U significantly inhibited growth of the culture. The U571A, A865U double mutant, however, grew normally. Ribosomes with the single mutations were also less stable than ribosomes from the double mutants as measured by sucrose gradient profiles of isolated tight couple ribosomes. These data indicate that a Watson-Crick interaction between nucleotides at positions 571-865 of the 570-571 pseudoknot is a critical component of ribosome function. However, as this study used only three mutations to generate these conclusions (U571A, A865U and U571A•A865U), we wondered if there was more to the observed loss of function besides canonical base pairing. To more thoroughly examine the structural and functional constraints on the central pseudoknot and its role in ribosome function we used the high-throughput combinatorial genetic system developed in the Cunningham Lab^{39, 110} to construct all possible mutations in the residues hypothesized to form the pseudoknot and determined their effects on protein synthesis under a variety of *in vivo* and *in vitro* conditions.

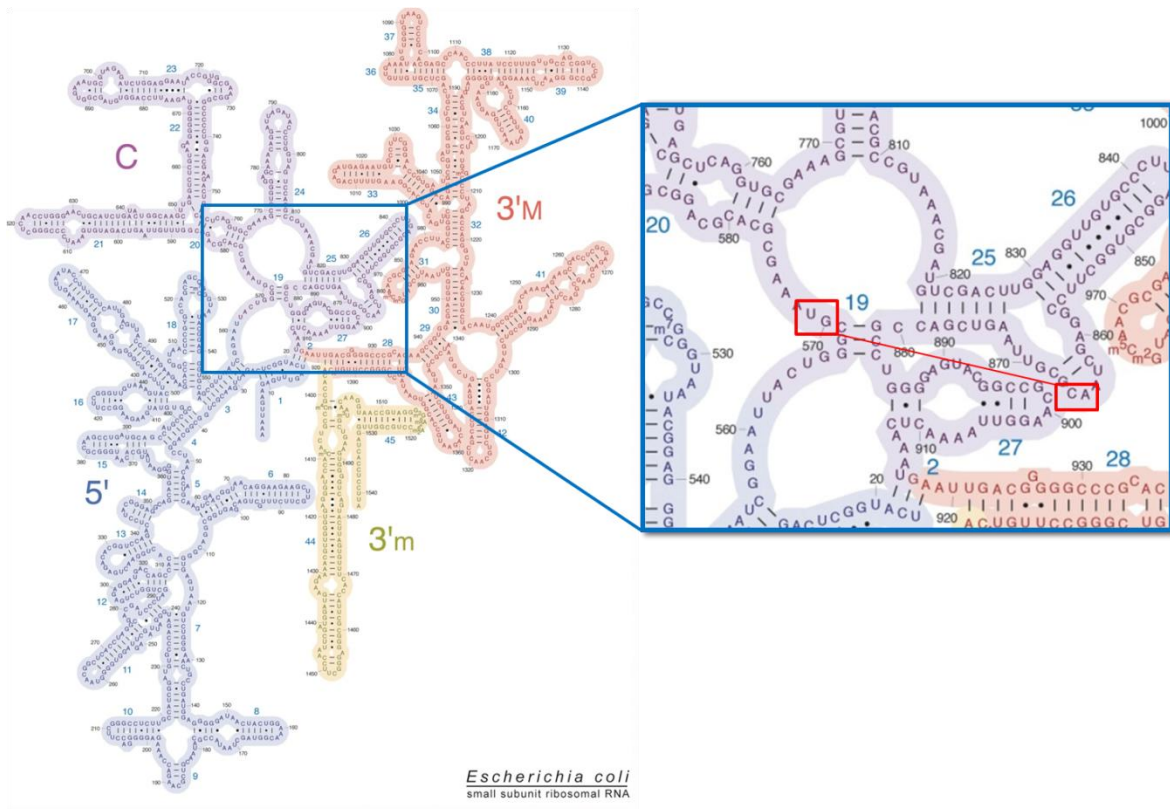


Figure 3.1: Secondary Structure of Nucleotides 570,571 and 865,866
Nucleotides 570, 571 and 865, 866 are shown in *E. coli*'s 16S secondary structure.

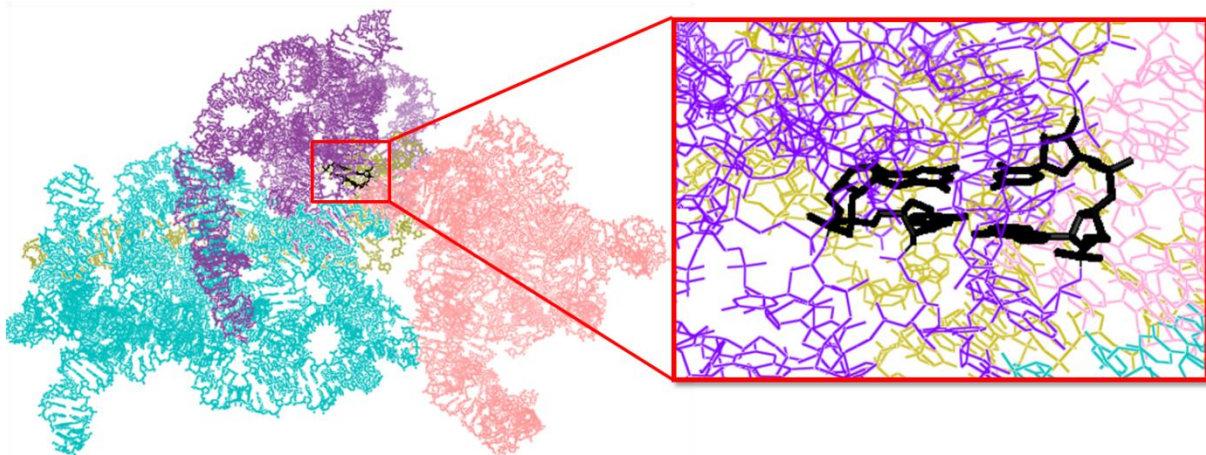


Figure 3.2: Tertiary Structure of Nucleotides 570, 571 and 865, 866
Nucleotides 570, 571, 865, 866 are shown in *E. coli*'s 16S tertiary structure. Image modified from PDB 2i2P

3.2 ANALYSIS OF SINGLE MUTATIONS WITHIN THE PSEUDOKNOT

To begin analyzing the mutant library, we first examined the effects of single mutations at each of the mutated positions on ribosome function. These data are shown in table 3.1.

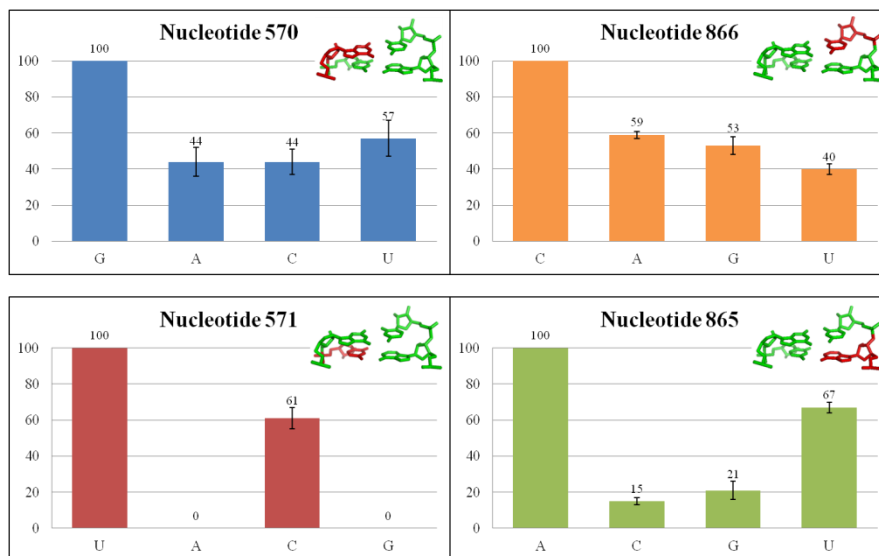


Table 3.1: Functional Analysis of Single Mutations.

Red represents the mutated nucleotide. See text for details

570 mutants: In *E. coli* ribosome crystal structures¹⁴⁹, G570 forms a Watson-Crick base pair with C866, which can be seen in figure 3.3. The transition mutation, G570A (44 ±8%) and the transversion mutations G570C (44±7%) or G570U (57±10%) each reduce ribosome activity by approximately 50% *in vivo*. Mutating G570 to any other nucleotide results in about a 50% loss of function.

866 mutants: The wild type nucleotide at this position is the pyrimidine cytosine that base pairs with the guanosine at position 570. This interaction can be seen in figure 3.3. A transition mutation to uracil leaves the ribosome with 40±3% activity. A transversion mutation to either adenosine or guanosine results in 59±2% or 53±5% activity respectively. Losing approximately

50% activity regardless of the nature of the mutation suggests that this position is not largely influenced by the size of the base.

571 mutants: The wild type nucleotide at this position is the pyrimidine uracil that pairs with adenosine at position 865 (figure 3.3). Mutating this base to another pyrimidine, cytosine, the ribosome maintains $61\pm 6\%$ function. However, a transversion mutation to either purine leaves the ribosome with less than 1% function. These data show that a purine at position 571 is detrimental to the ribosome. As purines are larger than pyrimidines, these data show the damaging steric effect of inserting a large base at 571.

865 mutants: The wild type nucleotide at this position is the purine adenosine and base pairs with the uracil at position 571. Mutation of this base to a uracil results in $67\pm 3\%$ ribosome activity. Mutation to a cytosine results in $15\pm 1\%$ activity, and mutation to guanosine results in $21\pm 1\%$ activity.

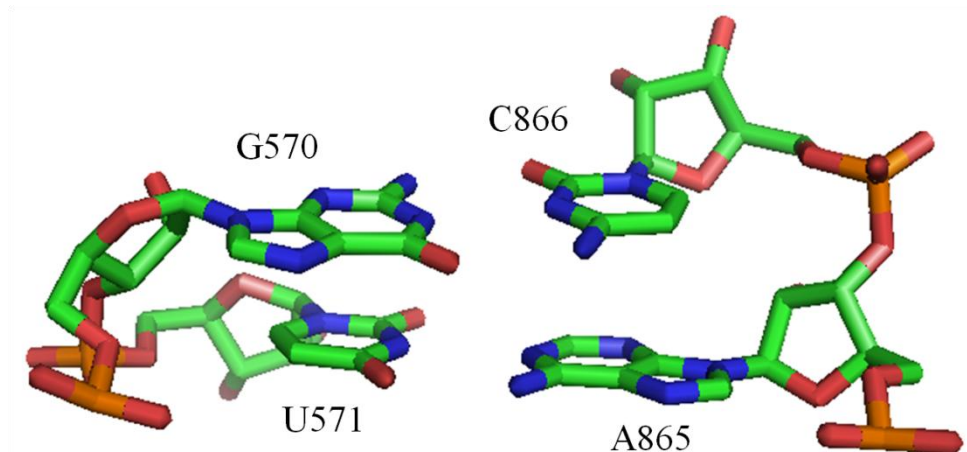


Figure 3.3: Crystal Structure of Nucleotides 570, 571 and 865,866

Crystal structure modified from PDB 2i2p highlighting the G570-C866, A865-U571 Watson-Crick bond.

3.3 ANALYSIS OF DOUBLE MUTATIONS WITHIN THE PSEUDOKNOT

By combining the single mutations at positions 570 and 866, we can expand the amount of information gathered by functional analysis. We can see various canonical and non canonical base pairs at the same position which will give insight to the types of interactions that are important for function at this region.

570-866 Double Mutations: Figure 3.4 highlights the interaction between nucleotides 570 and 866. As seen in table 3.2, any combination of mutations will result in loss of 50% ribosome activity, with the exception of G570U-C866A which is $97\pm 2\%$ active. However, table 3.3 shows the statistical analysis of canonical double mutant functionality and confirms interactions between these nucleotides. We analyze the base interactions by comparing the product of the single mutants to the observed function of the double mutant that combined the two single mutations. All three of the other canonical combinations of C-G, U-A and A-U all show a higher

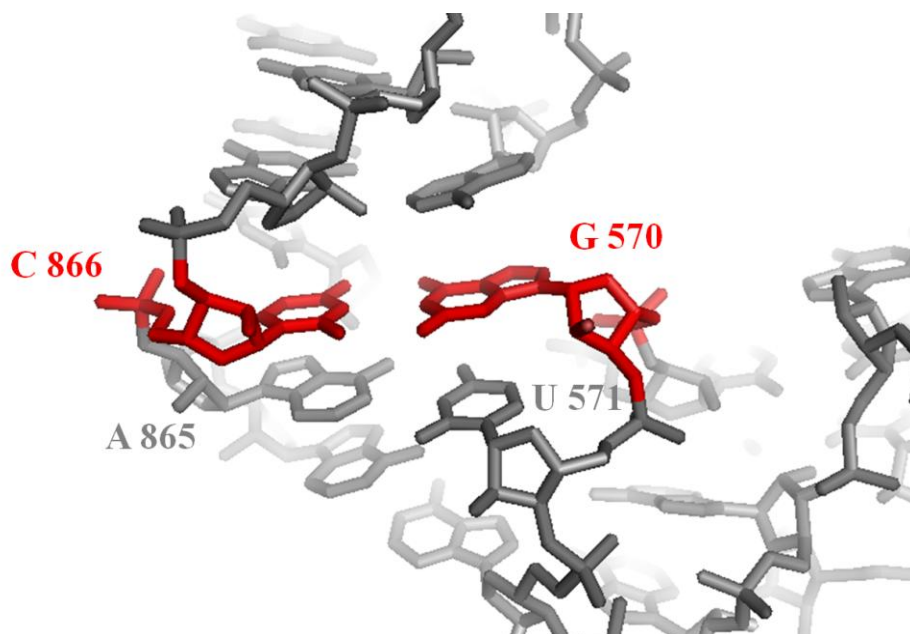


Figure 3.4: Crystal Structure of Nucleotides 570-866 Watson-Crick Bond
Crystal Structure modified from PDB 2i2p highlighting the C866-G570 Watson-Crick bond

observed function than expected by statistical analysis. While these bases are communicating, their interactions are not limited to that of traditional Watson-crick base pairing.

571-865 Double Mutations: A close view of nucleotides 571 and 865 within the 571 pseudoknot can be seen in figure 3.5. Table 3.2 shows the functionality of ribosomes with mutations at both positions 571 and 865. It appears that the interactions between 571 and 865 are more sensitive than at 570 and 866 as many of the double mutants are inactive. The highlighted boxes show wild type and non-wild type canonical base pairs. These data show that Watson-crick base pairing is preferred here, with the exception of U571G-A865C having only $10\pm 1\%$ function. However, all mutants containing 571G are dead, which might indicate a steric problem rather than the inability to form a Watson-crick base pair. Mutants U571C-A865 and U571-A865U both have high functionality of $61\pm 6\%$ and $67\pm 3\%$, respectively, but neither form

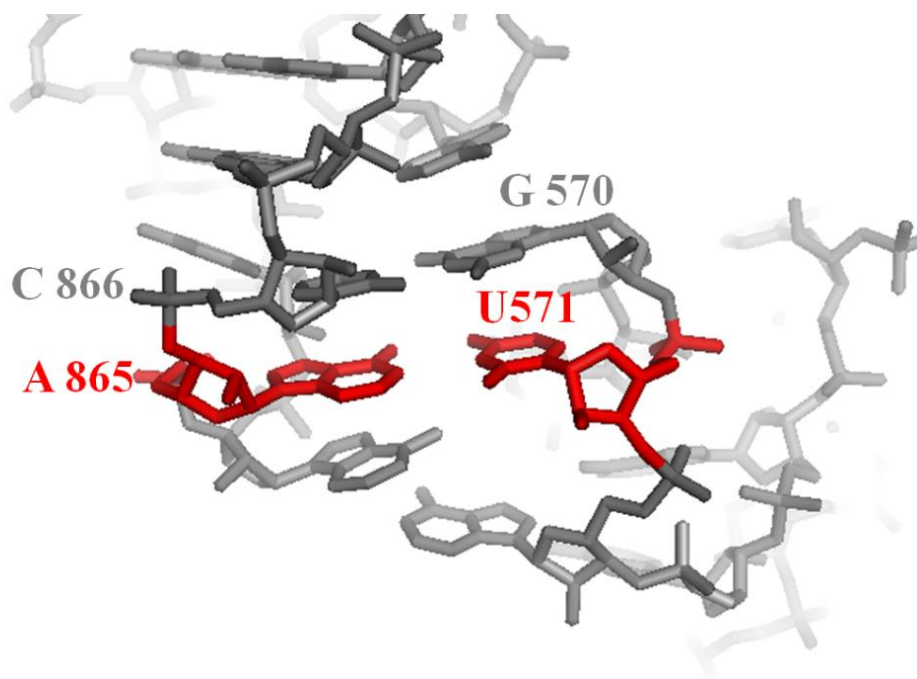


Figure 3.5: Crystal Structure of Nucleotides 571-865 Watson-Crick Bond.

Crystal Structure of modified from PDB 2i2p highlighting the A865-U571 Watson-Crick bond.


Watson-crick base pairs. Both of these mutants do, however, maintain a pyrimidine at position 571 and at least one wild type base in the pair. We expected the U571A-A865U mutations to cause the ribosome to be non-functional based on statistical analysis (Table 3.3) but these ribosomes maintain 75% function. We see a similar effect with mutations U571C-A865G that maintain 70% function when we only expected to see about 12% function. These data show that the bases alone are not responsible for the amount of function these ribosomes maintain.

Statistical analysis of canonical base pairing seen in table 3.3 clearly shows the interaction between the bases at these positions. We see 75% function in U571A A865U when the expected function was zero, and observed 70% function for U571C A865G mutations when only 12% was expected. The only exception is G571-C865, with an expected function of less than 1% and an observed function of only $10 \pm 1\%$.

3.4 SATURATION MUTAGENESIS OF THE PSEUDOKNOT

PCR saturation mutagenesis⁹⁸ was used to construct all possible nucleotide combinations involving 16S rRNA positions 570, 571, 865, and 866 (figure 3.3). The resulting 255 mutants were then assayed for GFP production *in vivo* to determine the effect of each set of mutations on protein synthesis. The resulting mutation database was analyzed to identify key sequence and structural features of the pseudoknot that are important for ribosome function.

Table 3.4 is a comprehensive table of the ribosomal function of all possible mutations between nucleotides 570, 571, 865 and 866. This table reveals the clear need for Watson-Crick base pairing at position 571-865, as without this feature, very few active mutants exist. Interestingly, regardless of the bases at position 570 or 866, U571-A865 is preferred to U571A-A865U and U571C-A865G is preferred to U571G-A865U. Because canonical base-pairs are isosteric, meaning they occupy the same volume, they should be able to substitute for each



		865			
		A	C	G	U
571	A	0	2	0	75 ₊₆
	C	61 ₊₆	0	70 ₊₆	19 ₊₄
	G	0	10 ₊₁	0	0
	U	100	15 ₊₁	21 ₊₁	67 ₊₃

		866			
		A	C	G	U
570	A	46 ₊₁₀	44 ₊₈	56 ₊₅	60 ₊₆
	C	48 ₊₃	44 ₊₇	50 ₊₆	77 ₊₂
	G	59 ₊₂	100	53 ₊₅	40 ₊₃
	U	97 ₊₂	57 ₊₁₀	68 ₊₄	59 ₊₅

Table 3.2: Double Mutation Analysis

Highlighted boxes represent canonical base pairs. Red represents mutated bases.

Base Pairing Double Mutant Statistical Analysis							
570	866	%	expected	571	865	%	expected
G	C	100		U	A	100	
G	G	53		U	U	67	
C	C	44		A	A	<1	
C	G	50	23.32	A	U	75	0
U	C	57		C	A	61	
G	A	59		U	G	21	
U	A	97	33.63	C	G	70	12.81
G	U	40		G	A	<1	
A	C	44		U	C	15	
A	U	60	17.6	G	C	10	0

Table 3.3: Double Mutant Statistical Analysis

Nucleotides in **bold** are wild-type, and those in red are mutant.

Nucleotides 571-865																	
	AA	AC	AG	AU	CA	CC	CG	CU	GA	GC	GG	GU	UA	UC	UG	UU	
Nucleotides 370-866	AA	0	0	0	0	0	14±4	1	0	0	0	0	46±10	0	0	0	
	AC	0	0	0	30±1	0	71±2	0	5	2	0	0	44±8	0	7	0	
	AG	0	0	0	1	0	46±2	0	0	2	0	0	56±5	0	2	0	
	AU	0	0	0	39±1	0	59±4	0	0	28±1	0	0	60±6	1	8±0	10±1	
	CA	0	0	0	13±1	0	18±1	3	11±2	0	0	1	48±3	1	0	1	
	CC	0	0	0	24±3	0	66±2	2	0	0	1	1	44±7	0	2	2	
	CG	0	0	0	25±6	2	53±2	5	0	0	0	0	50±6	3	8±1	14±1	
	CU	0	0	0	8±1	0	4	50±2	0	0	0	2	0	77±2	1	1	1
	GA	0	1	0	11±2	0	1	31±3	0	0	7	0	0	59±2	0	0	0
	GC	0	2	0	75±6	61±6	0	70±6	19±4	0	10±1	0	0	100	15±1	21±1	67±3
	GG	0	0	0	13±1	1	0	61±4	0	1	0	0	0	53±5	0	7	8±2
	GU	0	0	0	6	2	0	61±2	0	1	4	0	1	40±3	0	8±0	0
	UA	4	4	4	53±6	0	7	62±4	20±2	1	64±4	0	0	97±2	35±3	14±2	36±5
	UC	0	0	0	53±4	0	3	49±6	2	0	6	0	0	57±10	4	17±2	10±1
	UG	1	0	0	6	0	0	44±3	1	2	0	0	0	68±4	1	5	11±1
	UU	0	0	2	0	0	1	59±5	3	1	1	0	2	59±5	1	1	7

15-25%
26-40%
41-55%
56-70%
71-85%
86-100%

Table 3.4: Saturation Mutagenesis Table of Functionality

Letters in **bold** represent wild type nucleotides.

other¹²⁰ (figure 3.6). However, site-directed mutagenesis of 570-866 and 571-865 demonstrates that the function of different Watson-crick pairs at this position is not equivalent. Consequently, the individual placement of these particular nucleotides is not arbitrary. Keeping the 570-866 nucleotides constant in a canonical base pair, swapping U571-A865 to U571A-A865U costs the ribosome a minimum of 21% function and up to 44% of its function. Similar analysis of U571C-A865G and U571G-A865C reveals that while 15 of the 16 mutants containing U571C-A865G are active, only two of the 16 mutants containing U571G-A865C maintain any measurable function. If this pseudoknot needs to be dynamic for function, then perhaps the simple act of swapping the orientation of a Watson-Crick bond disrupts a second potential bond somewhere else in the structure.

A more subtle observation can be seen when looking at the few 570-866 mutations that maintained measurable function. Even when canonical base pairing is maintained between 570-866, most of the mutation combinations proved to be deadly. 570A-866U and 570C-866G

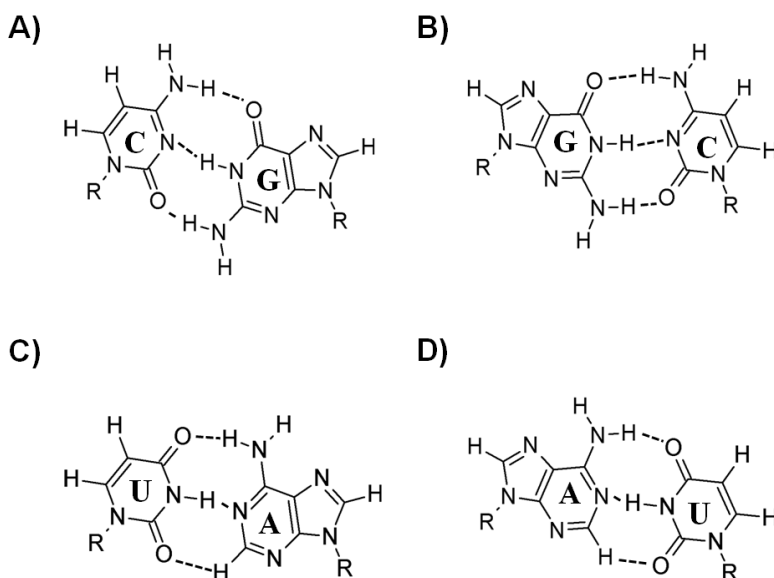


Figure 3.6: Watson Crick Base-Pairs

A) Cytosine-Guanosine; B) Guanosine-Cytosine; C) Uracil-Adenosine; D) Adenosine-Uracil.
Adapted from Leontis *et al.* 2002.¹²⁰

mutations were only active when combined with a 571-865 Watson-Crick pair. 570G-866C and 570U-866A produced only a handful of functional mutants when combined with noncanonical 571-865 pairs, interestingly most occurred in the presence of U571.

3.5 RIBOSOMAL PROTEIN COMPLEMENTATION

Several ribosomal proteins are near the 571 pseudoknot, namely S5, S8 and S11, as seen in figure 3.7. Ribosomal protein S5 is within 6Å to the pseudoknot, S8 is within 20Å, and S11 is within 30Å. To be considered for interaction, a protein should be within 5Å to the nucleotide in question.¹²¹ So while direct interaction of these proteins with the 571 pseudoknot is unlikely, mutations that disrupt the structure of this region may contribute to loss of rprotein binding. To determine if mutations in the pseudoknot affect the binding of these proteins, the genes for S8, S11 and S5 were cloned and co-expressed with representative mutations at each of the sites in the pseudoknot. Figure 3.8 shows the functional analysis of each of the single pseudoknot mutations coexpressed with one of the three rproteins. We were looking for a large difference in the function of the mutant ribosomes that had an empty pKan expression vector (T₁T₂) and the mutant ribosomes that had an abundance of rproteins co-expressed. No complementation was observed in any of the mutants tested, indicating that loss of function in the mutants is not due to reduction in binding of ribosomal proteins.

3.6 THERMODYNAMIC INFLUENCE ON THE PSEUDOKNOT

When Vila et al. were investigating the central domain pseudoknot, they attempted to see a stabilizing effect by monitoring the growth cycle of the three mutants (571A, 865U and 571A-865U) at 30°C and 42°C and found that the deleterious growth phenotype was more pronounced at temperatures lower than 37°C and less pronounced at higher temperatures.⁷³ Similarly, to determine the influence of thermodynamics on the activity of the 571 pseudoknot mutants, each

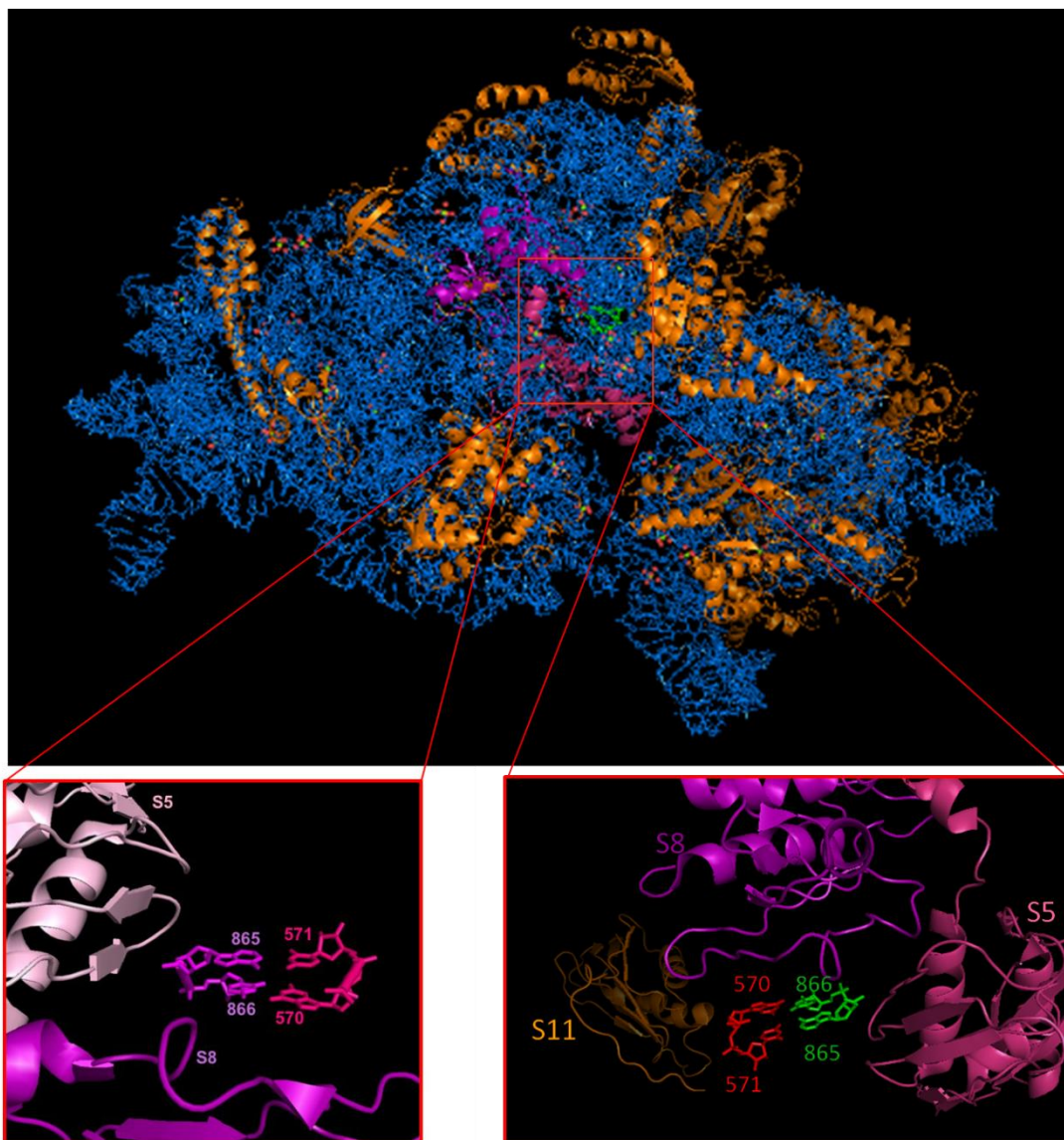


Figure 3.7: Ribosomal Proteins Near Pseudoknot Nucleotides

Image modified from PDB 2i2p. Ribosomal protein S5 is shown in pink, S8 shown in purple, S11 shown in orange. See text for full details.

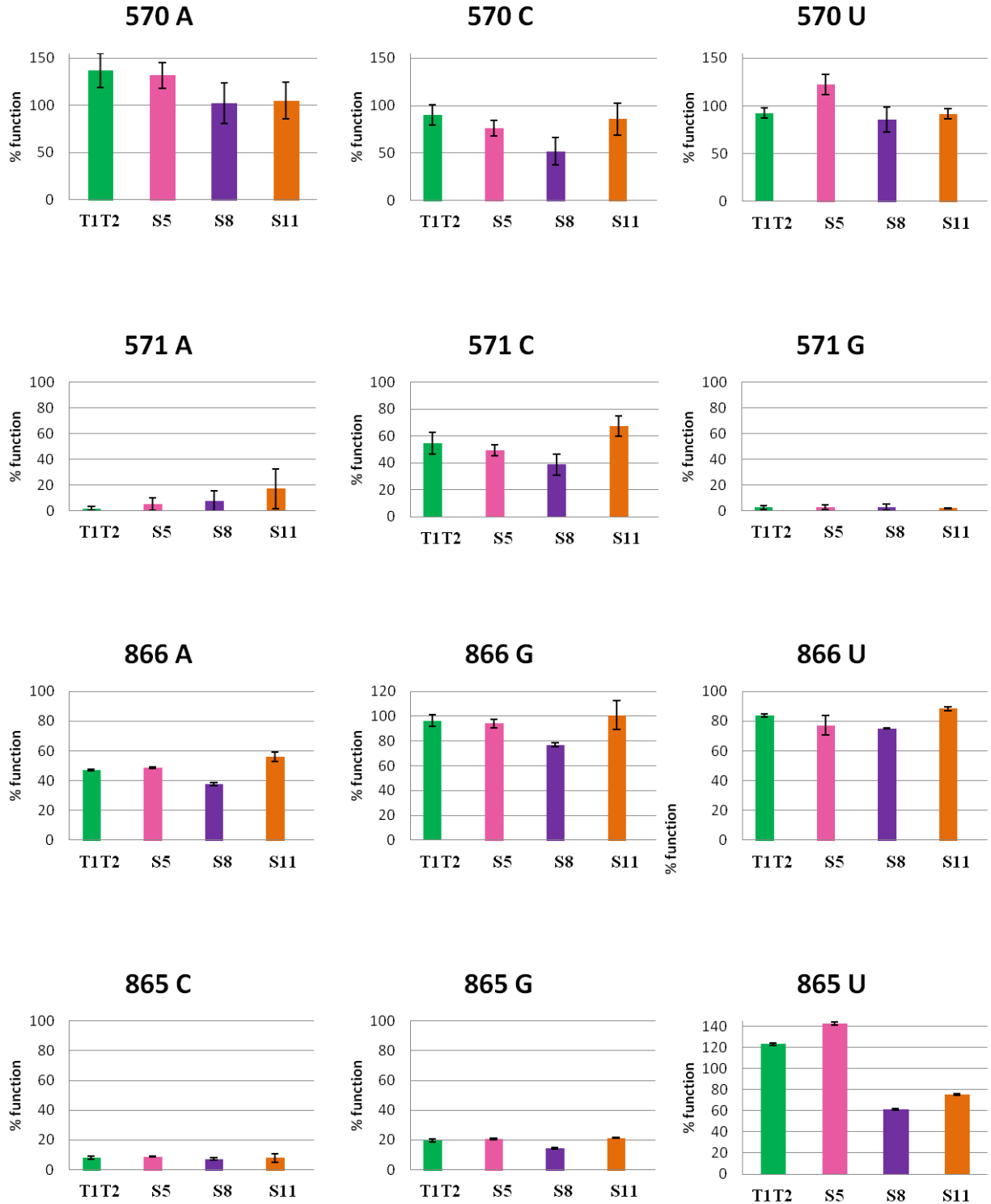


Figure 3.8: Ribosomal Protein Complementation.

Single mutations in the pseudoknot were co-expressed with ribosomal proteins. T₁T₂ is the empty expression vector

mutant was assayed at 25°C, 30°C, 37°C, and 40°C. Mutants with no measurable protein synthesis activity at 37°C were unaffected by changes in incubation temperatures, so these data are not shown. Mutants with partial activity, however, did vary in function at different incubation temperatures, in agreement with Vila et al.

We began by analyzing only the single mutants at the four different temperatures, which can be seen in figure 3.9. These ribosomal mutants were more active at 40°C and were inhibited by incubation temperatures below 37°C. We also looked at double mutants at different temperatures which can be seen in figure 3.10. For a second time, the general trend is a gain of function at higher temperatures and loss of function at lower temperatures. Interestingly, if the 571-865 pair is U-A (the wild type pair), the function of the ribosome at 25°C is not as detrimental as it is for the other mutation combinations. Finally, we looked at all the functional mutants, as seen in figure 3.11 and table 3.5. Again, we see the cold sensitive phenotype and disproportionate increase in function at higher temperatures. While base pairing at this pseudoknot is obviously important to the function of the ribosome, additional factors must also play a role. These data suggest that the central pseudoknot is dynamic and may facilitate the switch between two active conformations of rRNA. Mutations in the pseudoknot may therefore create thermodynamic minima that favor one conformation over the other. Depending on the role of the conformational switch, the mutations may affect ribosome assembly or one of the partial reactions during the protein synthesis process itself.

3.7 EFFECTS OF PSEUDOKNOT MUTATIONS ON RIBOSOME STRUCTURE

Mutant ribosomes were prepared under conditions that maintained 70S particles (7.5mM MgCl₂) as to determine if they are capable of assembling into association competent 30S subunits. Mutations analyzed were selected based on the amount of function they retained and

Single Mutant Temperature Analysis

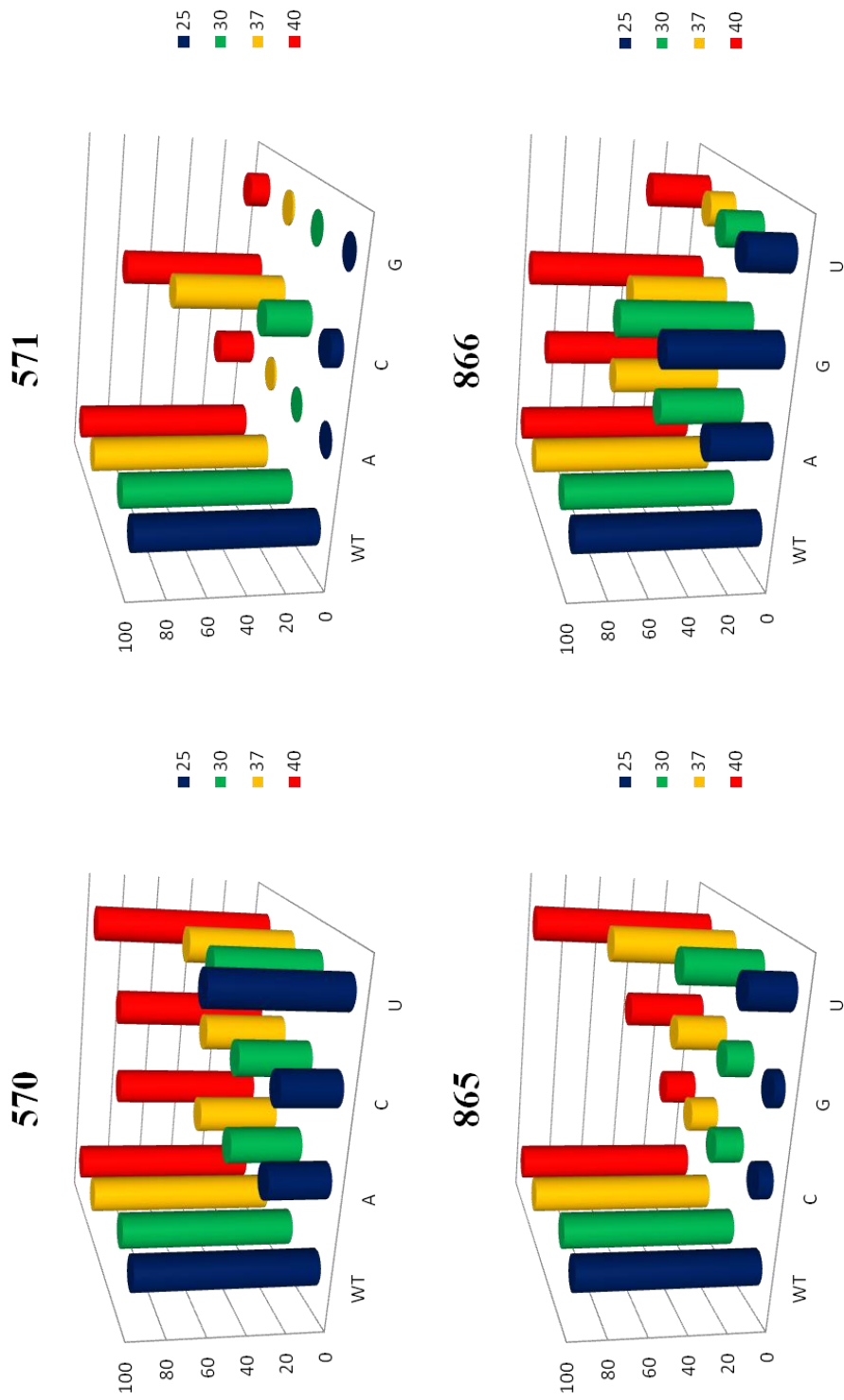


Figure 3.9: Single Mutation Temperature Analysis
 Each single mutation was assayed for function at four different temperatures; 25°C, 30°C, 37°C, and 40°C

Double Mutant Temperature Analysis

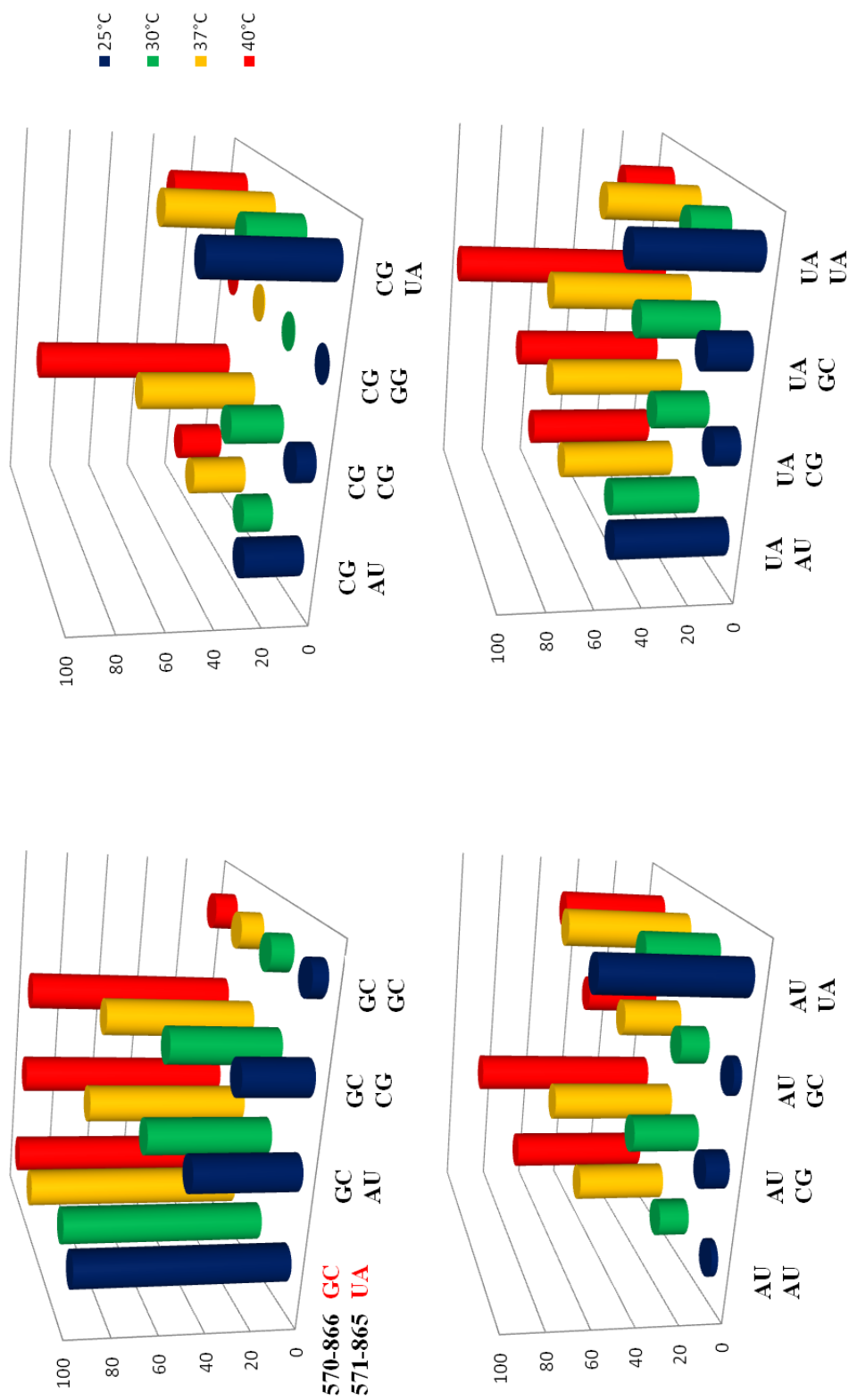


Figure 3.10: Double Mutation Temperature Analysis

Each mutant that maintained Watson-Crick bonds at the pseudoknot was assayed for function at four different temperatures; 25°C, 30°C, 37°C, and 40°C.

Functional Mutant Temperature Analysis

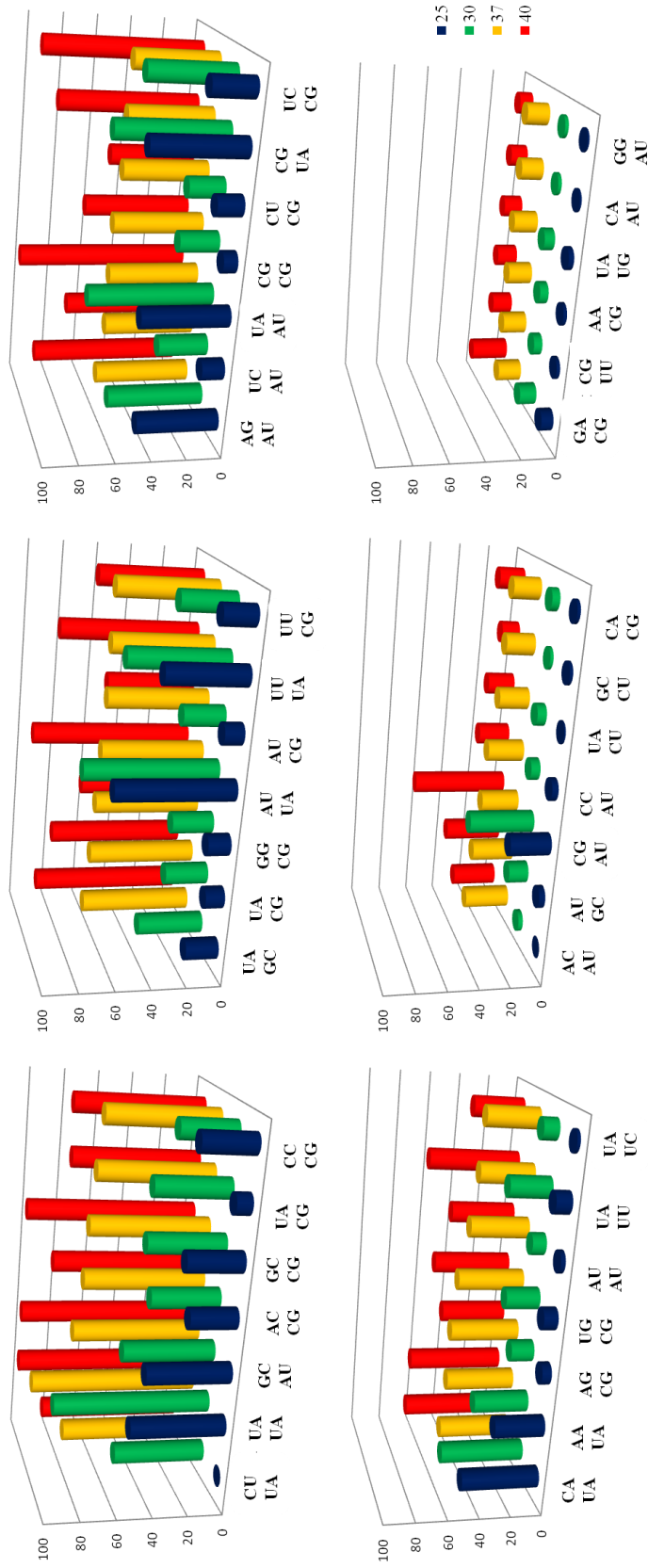


Figure 3.11: Functional Mutant Temperature Analysis

All pseudoknot mutations that displayed measurable function at normal growing temperature (37°C) was assayed for function at 25°C, 30°C, 37°C and 40°C.

Functional Mutant Temperature Analysis

<small>570-866 571-865</small>	25°C	30°C	37°C	40°C	<small>570-866 571-865</small>	25°C	30°C	37°C	40°C
CU UA	0±0	53±2	77±2	84±2	CA UA	50±10	55±2	48±3	65±3
UA UA	54±8	90±4	97±2	108±5	AA UA	32±3	36±1	46±10	64±3
GC AU	48±7	53±3	75±6	103±2	AG CG	6±1	15±1	46±2	44±3
AC CG	27±2	40±2	71±2	83±4	UG CG	9±1	22±1	44±3	52±2
GC CG	32±6	45±1	70±6	106±9	AU AU	3±1	9±2	39±1	43±2
UG UA	9±1	44±1	68±4	76±3	UA UU	10±1	27±1	36±	61±3
CC CG	31±4	33±1	66±2	77±4	UA UC	2±0	10±1	35±	34±4
UA GC	19±3	38±1	64±4	87±8	AC AU	0±0	3±0	30±1	30±3
UA CG	11±3	25±2	62±4	79±9	AU GC	4±1	13±6	28±1	38±15
GG CG	13±3	24±1	61±4	63±1	CG AU	26±5	42±2	25±6	63±4
AU UA	67±6	77±2	60±6	94±1	CC AU	4±2	6±0	24±3	21±1
AU CG	11±2	24±2	59±4	52±4	UA CU	1±0	6±1	20±2	18±2
UU UA	46±3	58±2	59±5	82±3	GC CU	2±1	2±0	19±4	12±5
UU CG	19±1	32±1	59±5	62±5	CA CG	2±1	5±0	18±1	17±2
AG UA	47±6	56±1	56±5	88±2	GA CG	7±2	10±1	14±2	22±2
UC AU	13±1	29±1	53±4	70±5	CG UU	2±0	5±0	14±1	12±1
UA AU	50±5	72±2	53±6	100±6	AA CG	2±1	5±0	14±4	12±1
CG CG	8±2	23±5	53±2	63±8	UA UG	3±0	6±1	14±2	11±1
CU CG	15±4	21±1	50±2	50±1	CA AU	1±1	2±0	13±1	10±1
CG UA	54±6	65±3	50±6	83±15	GG AU	1±0	2±0	13±1	8±1
UC CG	25±2	50±5	49±6	94±5					

Table 3.5: Functional Mutant Temperature Analysis

See text for details.

compared to wild type ribosome sucrose gradient profiles. Figure 3.12a & b shows the ribosome profile of selected mutants; Wild Type (100%), G570C-C866U U571-A865 (77±2%), G570C-C866G U571C-A865G (53±2%), G570G-C866G U571-A865 (53±5%), G570A-C866U U571A-A865U (39±1%), G570U-C865A U571-A865U (36±5%), G570C-C866 U571A-A865U (24±3%), G570-C866 U571G-A865C (10±1%), G570U-C866U U571G-A865U (2%), G570A-C866A U571-A865U (0%).

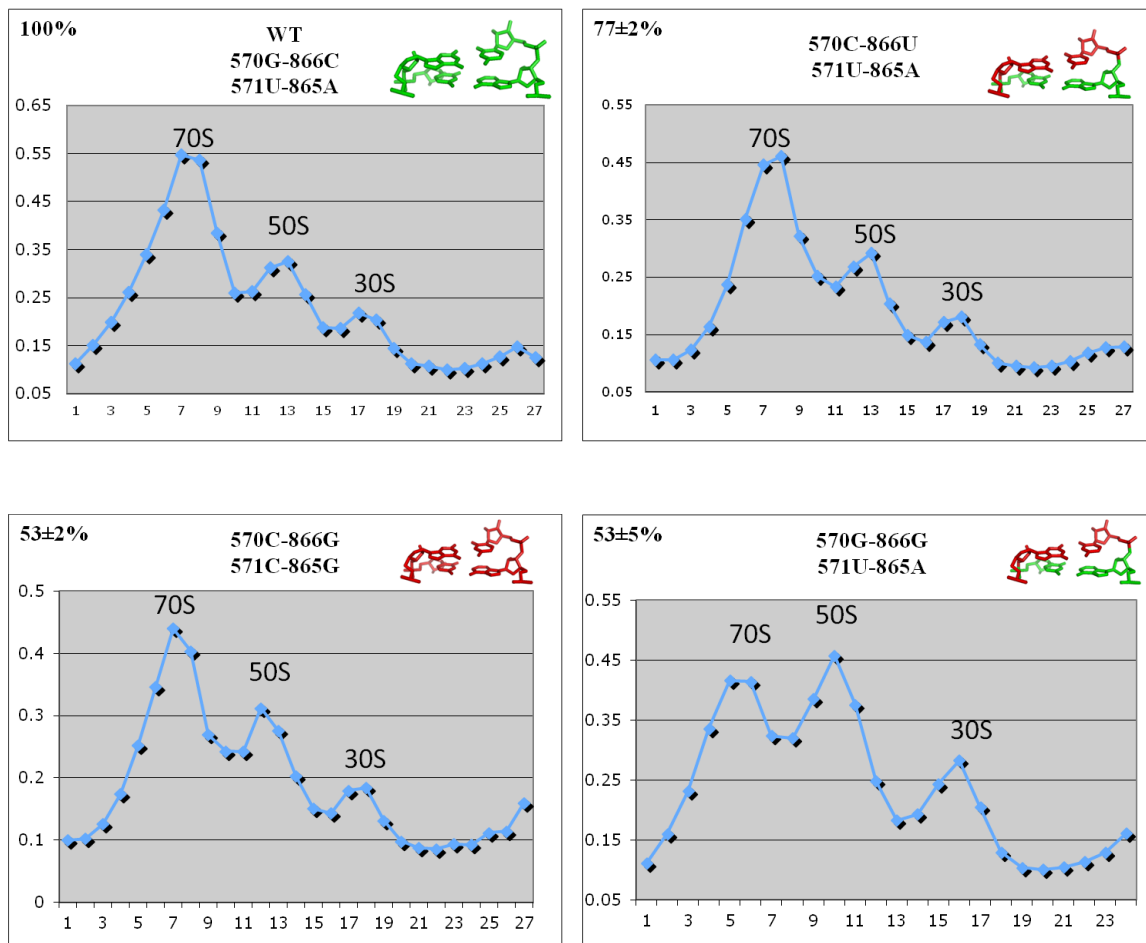


Figure 3.12a: Ribosome Profile of Select Pseudoknot Mutations

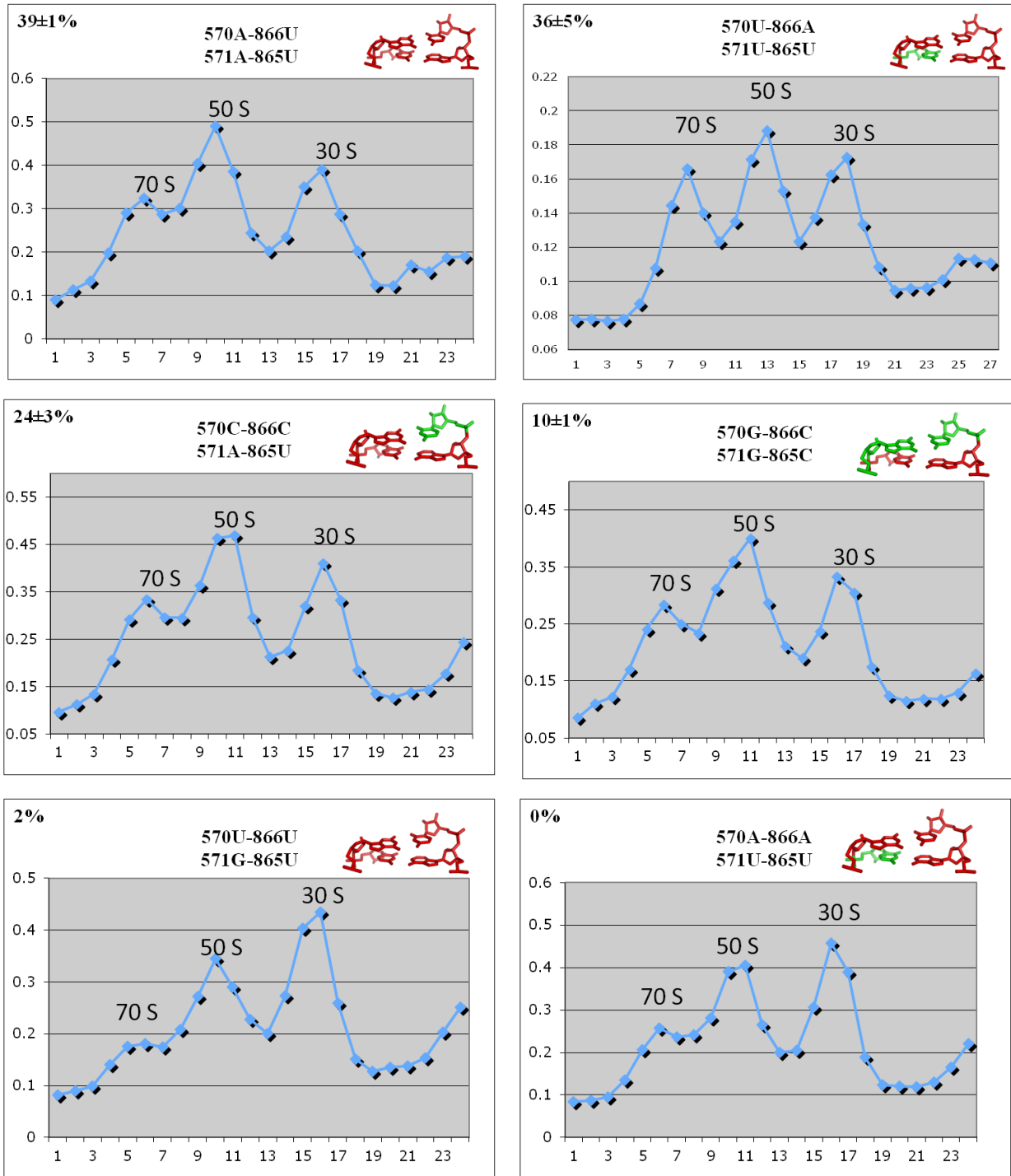


Figure 3.12b: Ribosome Profile of Select Pseudoknot Mutations

As the observed function decreases, we see a smaller 70S peak compared to the unpaired 50S and 30S subunits. See text for details.

The first signs of a decreasing 70S peak and increasing 50S and 30S peaks occur in the ribosome profile of G570-C866G U571-A865. As the ribosome profiles of other mutants with less function are analyzed, it is clear that the 70S peaks never quite reaches the OD of the 50S peaks, though the ratio varies. For example, G570-C866 U571G-A865 (0%) shows a larger 70S to 50S ratio than G570A-C866U U571A-A865U, which has 39% function. These profiles show that some mutations inhibit the long-term formation of 70S tight-couples, but it is unclear if the mutations disrupt association competent 30S subunit.

3.9 MUTANT STRUCTURE-FUNCTION ANALYSIS

Genetic analysis of 571 pseudoknot mutants has revealed a clear relationship between the ability of the pseudoknot to form Watson-Crick base pairs and function of the ribosome. Data also suggest the importance of sterics, and therefore the overall structure of the 571 pseudoknot needs to be analyzed. Due to the difficulty and time requirements of creating crystal structures, we turned to homology modeling software to evaluate the structure of representative mutations.

Homology models of single mutations at position 571 highlight the importance of sterics in this structure. When wild-type U571 undergoes a transversion mutation to U571A (seen in figure 3.13) or U571G (figure 3.14), both the 571 and 865 position become displaced, inhibiting any kind of potential base pairing between nucleotides 571 and 865, while the 570-866 bond seems to be unaffected. This is not surprising because functional analysis by GFP production of these single mutations show these ribosomes are not functional. A transition mutation to U571C (figure 3.15), however, shows little to no displacement of the nucleotides, which is consistent with the 60% activity this mutation retains.

We expected to see some distortion of nucleotide positioning in the homology model of single mutation A865C (figure 3.16) because this transversion mutation reduces the function of

these ribosomes to only $15\pm 1\%$. The distorted Watson-Crick interaction between U571 and A865C seen here is consistent with the loss of function that we observe with most 571-865 mutations. It is worth noting that the distortion is not as prevalent as those observed with position 571 mutations. This suggests that the integrity of the base pairing at the pseudoknot is less important than the ability to form alternate interactions.

We then compared the proposed structures of two mutants that maintained Watson-Crick base pairing, but no positions were kept wild-type; G570U-C866A, U571G-A865C ($64\pm 4\%$) seen in figure 3.17 and G570A-C866U, U571G-A865C ($21\pm 1\%$) seen in figure 3.18. While some very mild adjustments appear to be present, the amount of distortion is not consistent with the loss of function observed. We would expect to see considerably more nucleotide displacement in mutant G570A-C866U, U571G-A865C than that seen in mutant G570U-C866A, U571G-A865C, but because we do not, we have to consider that there is more to this pseudoknot in terms of functionality than simple Watson-Crick base pairing.

In mutant U571G-A865C (figure 3.19) we see ribosomes with low activity functioning at $10\pm 1\%$, yet the proposed structure from homology modeling does not suggest an amount of nucleotide bond distortion proportionate to the amount of function lost. Both G570-C866 and U571G-A865C appear to have the capability of forming a normal Watson-Crick bond with minimal interference. Based on the low function of these ribosomes we would expect to see large bond distortion if Watson-Crick bonding was the driving force for function. However, as these mutations at position 571 and 865 do not appear to cause much structural discrepancy from the original proposed model, these data suggest that there are alternate structural formations needed for the ribosome to be active.

As we see in these collective data, preserving a Watson-Crick bond does not necessarily preserve structure or function of the ribosome. Some mutations caused more bond disruptions than others, but did not correlate with loss of function. From this observation, the data is consistent with our hypothesis that an alternate structure formation is necessary to keep the ribosome active, and to do this, particular bases are needed at either position 571 or 865. Also, if a mutation at position 570 or 866 disrupts the bond formation at 571 and 865, loss of function is observed.

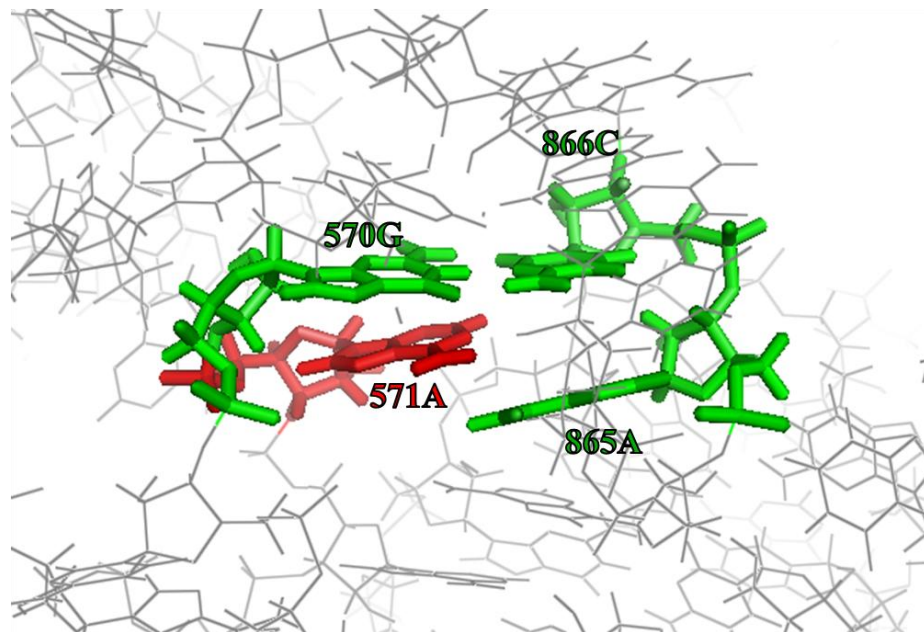


Figure 3.13: Homology Model of U571A

This mutation leaves the ribosome with no measureable activity.

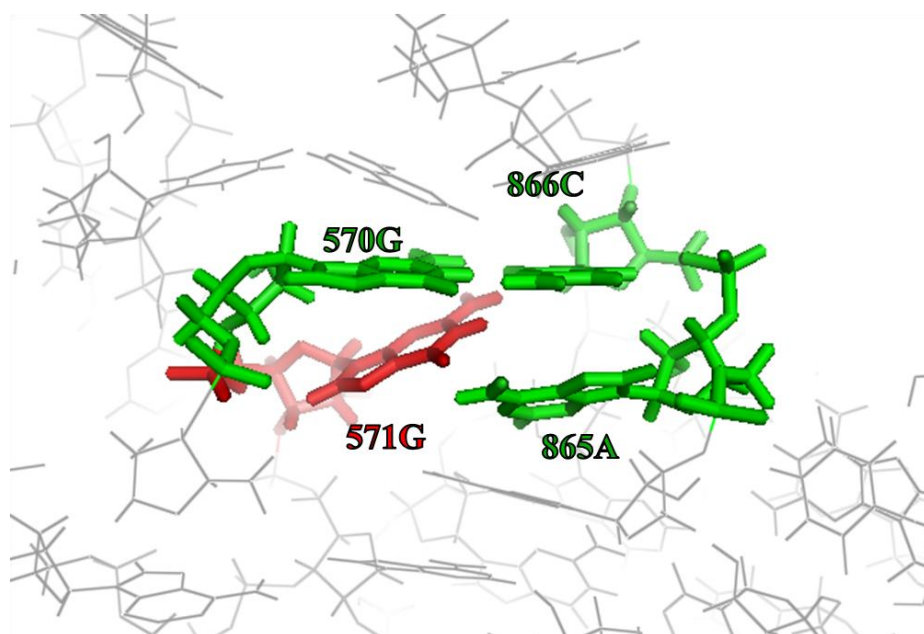


Figure 3.14: Homology Model of U571G

This mutation leaves the ribosome with no measureable activity.

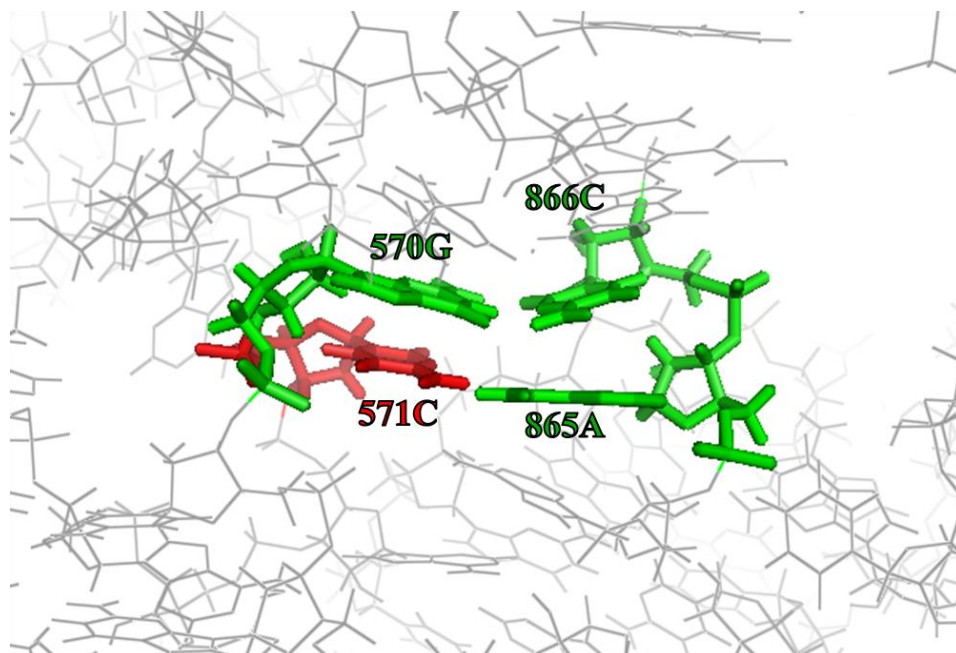


Figure 3.15: Homology Model of U571C

This mutation limits the ribosome to $61 \pm 6\%$ functionality.

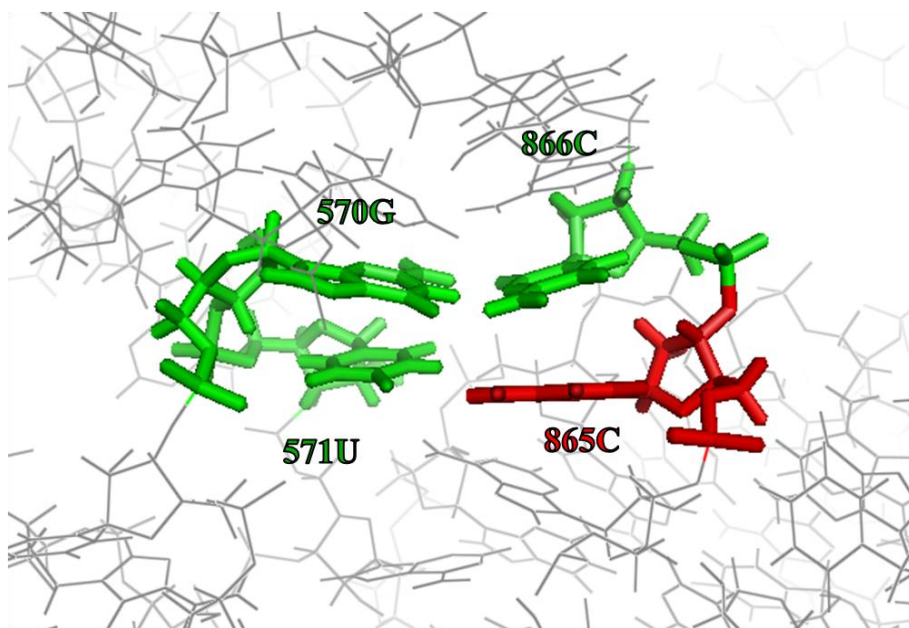


Figure 3.16: Homology Model of A865C
This mutation creates ribosomes that are $15 \pm 1\%$ active.

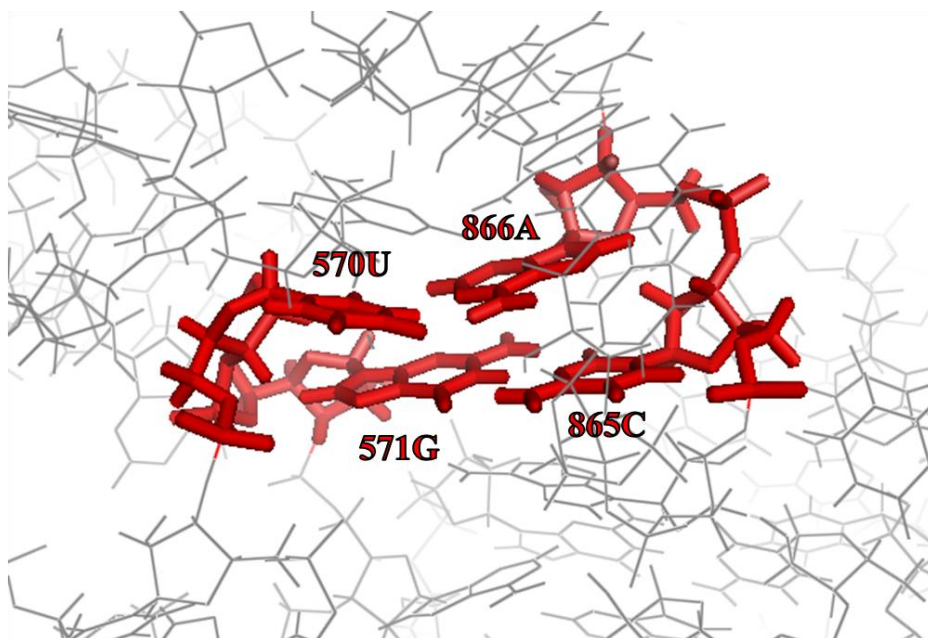


Figure 3.17: Homology Model of G570U-C866A, U571G-A865C
These ribosomes are $64 \pm 4\%$ active.

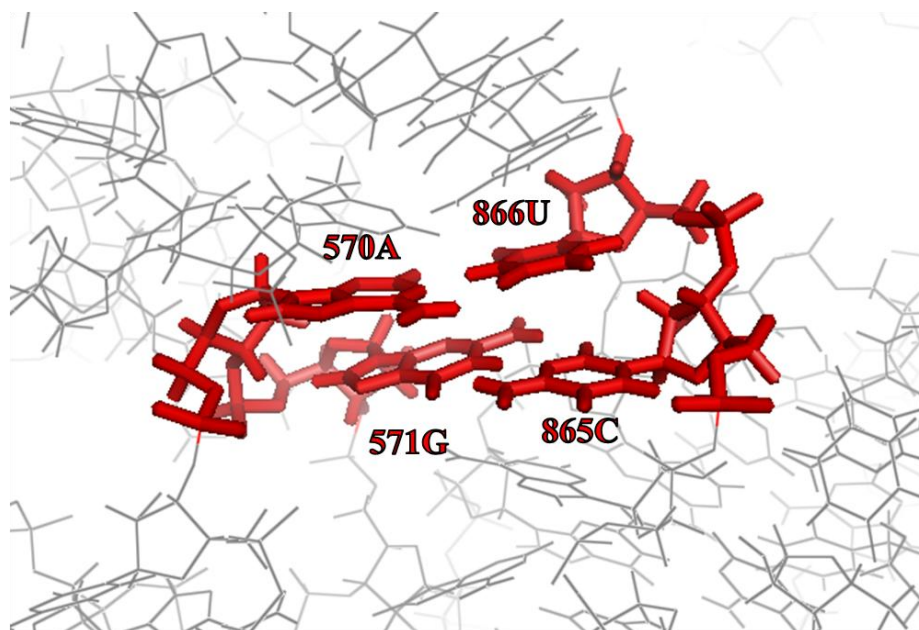


Figure 3.18: Homology Model of G570A-G866U, U571G-A865C
These mutations cause the ribosome to be $21 \pm 1\%$ active.

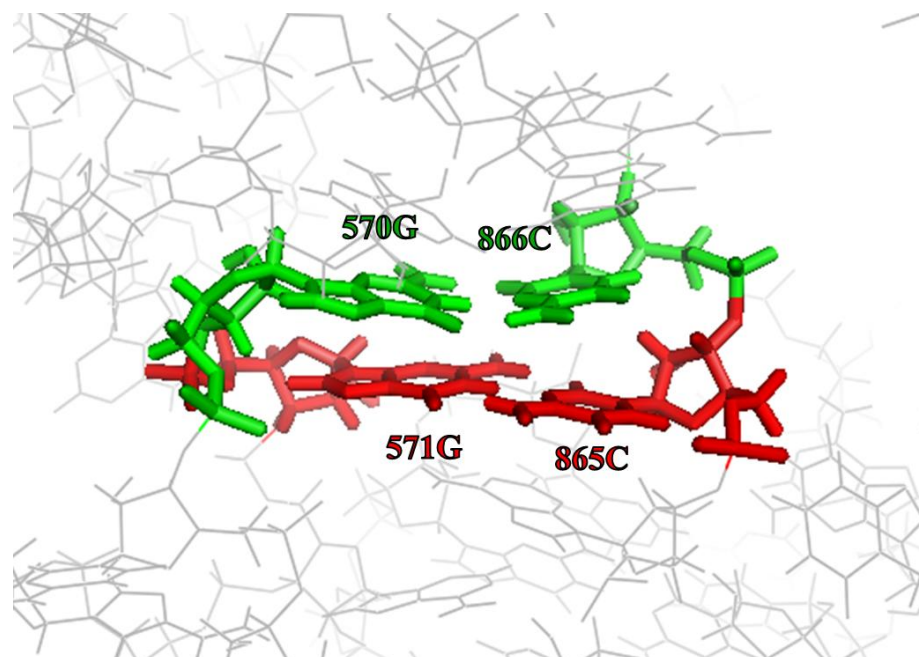


Figure 3.19: Homology Model of U571G-A865C
These mutations cause the ribosome to be $10 \pm 1\%$ active.

Chapter 4

Discussion

4.1 FUNCTIONAL ANALYSIS OF SINGLE MUTATIONS

The results of the functional analysis of single mutations in the central pseudoknot highlight the importance of these nucleotides' ability to interact with their pairing nucleotides. We notice that mutating G570 to any other nucleotide reduces ribosome function by approximately 50% (table 3.1). Since the wild type is a purine, it seems likely that substituting a smaller pyrimidine residue would not make a difference with respect to steric hindrance. No preference for either is seen, suggesting that steric hindrance is not the cause for the loss in function since both transition and transversion mutations yield roughly the same functionality of the ribosome. At position 866, ribosomes with transition mutations have lower activity than transversion mutations. Because the wild type is a pyrimidine, we might expect that adding a purine would cause steric disruption of the local environment and negatively affect ribosome function. In fact, ribosomes carrying the two purine substitutions are more active than the pyrimidine mutants. In the case of positions 570-866, there does not seem to be any indication of a requirement for base pairing preferences. In fact, the pair with the second strongest predicted hydrogen bonding at neutral pH is G570:C866U, which is the single mutant with the lowest activity.

When we look at ribosomes with mutations at the base pair U571-A865, however, we see a more interesting pattern in function. All three mutations of U571A:C:G ribosomes only maintain a significant amount of function in transition mutations, suggesting the need for a small nucleotide in that position. U571A and U571G ribosomes had no function when assayed while U571C maintained more than half of wild type function. The most likely explanation for this

decrease in functionality in transversion mutations is the involvement of steric hindrance. The nucleotide at position 571 could be in an area that is very restricted for space and the substitution of a larger pyrimidine causes the secondary structure to be distorted, possibly disrupting other important interactions leading to an inactive ribosome. Ribosomes with a mutation at position 865 lose quite a bit of function with the exception of A865U. Both A865G and A865C mutations leave the ribosome with very little activity, representing both a transition and transversion mutation. The corresponding transversion mutation, A865U however, allows the ribosome to remain more active ($67\pm 3\%$), with over three times more activity than the guanosine mutation ($21\pm 1\%$). A865U could be forming a U•U wobble pair with U571 which would explain the higher activity ($63\pm 3\%$), but would not explain why A865G has so little activity ($21\pm 1\%$). While there is no clear connection between size of the base and ribosome activity at this position like there is with its opposite base U571, both guanosine and cytosine are rejected here, even though G•U pairs can be relatively stable¹⁵⁷. Therefore, it cannot be concluded that specific bases are responsible for the loss or preservation of function.

4.2 FUNCTIONAL ANALYSIS OF DOUBLE MUTATIONS

When we analyze the function of various canonical and noncanonical base pairs at positions 570-866, we see that any combination of mutants reduces ribosome function by about 50%, with the exception of 570U-866A which maintains $97\pm 2\%$ function (see table 3.2). These data suggest that Watson-Crick base pairing is neither essential, nor preferred. There were no combination of mutations at position 570 and/or 866 that rendered the ribosome unable to make protein or unaffected. Whether the mutation created a strong noncanonical base pair, such as G•U ($40\pm 3\%$), U•G($68\pm 4\%$), G•A($59\pm 2\%$), or A•G($56\pm 5\%$), or a weak noncanonical base pair such as C•C ($44\pm 7\%$), A•A($46\pm 10\%$), A•C($44\pm 8\%$) or U•C($57\pm 10\%$), ribosomal function was

roughly equivalent. However, we do see through statistical analysis presented in table 3.3 that these bases are interacting, as we do not see covariance between mutations and deleterious phenotypes. For example, ribosomes with mutation G570C function at 44%, and mutation C866G functions at 53%. If nucleotides 570 and 866 were not interacting, we would expect the function of G570C-C866G ribosomes to be 23%, but they are in fact 50% active. There is also no definite indication of steric interactions between these two nucleotides, as function seems to remain the same regardless of which base is present at these positions.

Functional analyses of double mutations at base pair 571-865 suggest a relationship between and the steric interactions of bases to activity of the ribosome. As many of the double mutants are inactive, we can evaluate the similarities and differences of the active mutants to determine the important qualities of nucleotides at these positions. Watson-Crick base pairing is clearly preferred, as all of the mutants who maintain a canonical base pair maintain some measureable amount of function; most even maintain a high amount of function. However, it can be seen that a guanosine at position 571 is too detrimental to recover function regardless of its pairing nucleotide, leaving most of these pairs with no function at all; U571G•A866 (0%), U571G•A866C (10±1%), U571G•A866G (0%), U571G•A866U (0%) (see table 3.2). When considering U571G-A865C has only 10% function, even though the potential to Watson-Crick base pair is there, we must consider that perhaps the guanosine is being occupied by some other interaction or twisted out of the pseudoknot completely, withholding its ability to participate in another interaction the wild type U571 usually partakes in. Mutants U571C-A865 (61±6%) and U571-A865U (63±3%) both have high function, but neither form Watson-Crick base pairs. Both of these mutants do, however, maintain a pyrimidine at position 571 and at least one wild type

base in the pair. Obviously, base pairing for nucleotides 571-865 is important, but there must be additional factors besides simple base pairing required for function of the ribosome.

4.3 ANALYSIS OF SATURATION MUTAGENESIS

Functional analyses of ribosomes containing mutations at all four positions clearly demonstrate that Watson-Crick complementarity between nucleotides at position 571 and 865 is critically important, but we also see that in addition to canonical base pairing, pyrimidines are strongly preferred at position 571 and purines are strongly preferred at position 865. We can see in table 3.4 that all the ribosomes with U571-A865 or U571C-A865G maintained function, most maintained a relatively high amount of function. Saturation mutagenesis data shows very few ribosomes with U571A-A865U or U571G-A865C mutations maintained function, even though they still retained canonical base pairing. This trend can be seen when we compare the function of mutants in which the Watson-Crick pairs are reversed; when all possible base pairs at positions 570 and 866 are with U571-A865 are compared to the corresponding mutations at positions 570 and 866 with mutations U571A-A865U, we see a large drop in function. Similarly, if we look at all possible pairs of mutations for base pairs 570 and 866 and compare U571C-A865G to U571G-A865C, most mutants lose all function. These patterns suggest that steric hindrance is a leading factor at position 571; a purine at this position is too large to fit in the available pocket. We also observe a small cluster of mutants that maintain a wild type uracil at position 571 that have preserved a small amount of measureable function. We do not see this phenomenon with A865, indicating that U571 may be involved in some other interaction besides the canonical pair at 865.

Focusing on the 570-866 nucleotide pairs, we see that most of these ribosomes are inactive regardless of their ability to Watson-Crick base pair unless they are combined with a

canonical 571-865 pair. Only twelve of the 60 combinations of Watson-Crick base pairs at 570-866 with noncanonical pairs at 571-866 had function of at least 10%. When we compare this to Watson-Crick base pairs at 571-866 to noncanonical pairs at 570-866, there are 43. When we compare wild type U571-A865 with non-canonical pairs at 570•866, 100% of these mutants maintain some measureable function. However, wild type G570-C866 when combined with any noncanonical 571•866, only five of the twelve combinations maintain function, of which, only three are above 20%. There does not appear to be any preference for one nucleotide over another at either position 570 or 865. When there is a purine at position 570 with its pyrimidine canonical pair at 865, there are eleven active mutants. When there is a pyrimidine at position 570 with its purine canonical pair at 865, there are twelve active mutants. While the G570-C865 pair has been shown to be part of the pseudoknot in crystal structures, it does not seem to be nearly as important as the U571-A865 pair. This is interesting because of the two bonds found in the pseudoknot, the guanosine-cytosine bond shared between nucleotides 570-866 are known to be stronger than uracil-adenosine bonds present in the 571-866 bond.

4.4 RIBOSOMAL PROTEIN COMPLEMENTATION

Because we saw an interesting pattern in function involving the 571-865 pair, we wondered if the bases could be involved in another interaction, potentially with a ribosomal protein. We chose three ribosomal proteins that bind in the central domain of 30S subunit; S5, S8 and S11. We chose tertiary binding protein S5 because of its close proximity (less than 8Å in crystal structures)¹⁴⁹ to the pseudoknot in the 5' and central domains, with known interactions to bases relatively close to the nucleotides involved in the pseudoknot; 559-560, 921-922, and 923 (the full list of interacting bases are as follows; 5-9, 15-16, 18-19, 559-560, 921-923, 1069-1070, 1072-1074, 1077-1081, 1192-1194, and 1396- 1398).³⁴ We also used primary binding protein

S8, though farther away from the pseudoknot (about 20Å in crystal structures), we wondered if the deleterious phenotype was due to early misfolding. S8 is near the center of the back of the body in the 30S and interacts with S5, making base specific interactions with nucleotides A573, G575, G858, A859 and the backbone of nucleotides 860, 861 and 560, all of which are very close to the central domain pseudoknot. Complete nucleotide interactions are as follows: 564, 573, 575, 583, 586-588, 590-591, 593- 600, 629-633, 640-643, 651-654, 810, 820-828, 858-861, and 872-879. Finally, we chose tertiary binding protein S11 for this complementation assay, though very distant from the central domain pseudoknot (about 28Å in crystal structures), it is the closest of the central domain tertiary binding proteins in the 30S. S11 interacts with nucleotides 1235-1236, 1242, 1244, 1267-1269, 1285-1286, 1304-1305, 1324-1329, and 1352-1353.

By increasing the available amount of ribosomal proteins, we could recover function due to poor binding near the distorted pseudoknot. We over-expressed each of the ribosomal proteins along with a single mutation at 570, 571, 865, or 866. Wild type ribosomes were coexpressed with the respective protein and set to 100% for that data set, and compared to mutant ribosomes that had the same rprotein over-expressed. We also compared these data to single mutant ribosomes expressed with an empty ribosomal protein expression vector (pKanT₁T₂). If complementation was occurring, we would have seen a significant difference between the mutant+T₁T₂ activity and mutant+rprotein activity. No such increase in activity was observed, seen in figure 3.8. Some of the single mutant ribosomes activities did not match what was previously seen in the functional analysis assays (table 3.4), but this could be because these cells were treated differently (ampicillin + IPTG + chloramphenicol+ arabinose verses ampicillin + IPTG) and may have been growing slower due to increased cellular stress. The important

comparison is between single mutants with and without over-expression of ribosomal proteins, of which we see no considerable difference. While the results of this experiment were negative, we still gain some insight about this pseudoknot. The loss in function is not due to a reduction in binding of ribosomal proteins. This is not particularly surprising because the rproteins tested were a minimum of 6Å away from the pseudoknot and have not been reported to interact with the nucleotides involved with the pseudoknot.

4.5 THERMODYNAMIC INFLUENCE ON THE PSEUDOKNOT

Raising and lowering optimal growth temperatures of the mutant ribosomes revealed an interesting, albeit complex, cold-sensitive phenotype also seen by Vila et al.⁷³ Double stranded RNA ‘breathes’ at normal temperatures and as heat increases over a small range of temperatures, it can denature completely.^{158; 159; 160;161} Because lower temperatures suppress the separation of strands, convention would tell us that lowering the growth temperature would help to stabilize the pseudoknot and recover some function from mutant ribosomes with low activity. However, when we assayed the central domain pseudoknot mutants at different temperatures (25°C, 30°C, 37°C, 40°C), we saw the opposite effect. Dead mutants did not recover any function (this data is not included) but mutants with activity at 37°C followed a particular growth trend. We first saw the common trend in single mutants (figure 3.9), as temperature decreased, percent function also decreased. We then looked at double mutants (figure 3.10), and saw the same trend with the interesting exception of if wild type U571-A865 was maintained. In this group of mutants where wild type U571-A865 still remained in the pseudoknot, roughly the same amount of function was seen at 40°C as 25°C and cold-sensitivity was less pronounced, though this set of mutants still gained function at 40°C compared to the wild type at the same temperature. When we compared all the functional mutants at this temperature gradient (figure 3.11), it is clear these mutants do

not function well in the cold, as we could describe mutations at lower temperatures ‘extremely deleterious’.

The ribosome is a finely tuned, dynamic machine; any interaction alteration can set off a wave of changes affecting the structure of the ribosome, which causes the formation of several different conformational states during protein synthesis.¹⁶² Because simply stabilizing interactions with colder temperatures does not help to increase ribosomal function, it seems possible that this pseudoknot is not formed at all times. Considering the complex structures surrounding both sides of the pseudoknot, it seems likely that even single mutations could disrupt numerous tertiary structures. Consider position 865; this nucleotide is part of a small hairpin loop (tetra-loop) with nucleotides 863-866.³⁶ If one or two of these four bases is mutated, an alternative conformation might be more favorable than the tetra-loop, which might offer some needed stability in the central domain. The region containing bases 570-571 is even more complex; the strand itself kinds several times and forms a helix involving bases C569-G881, G568-C882, G567-C883, and another helix involving G577-C764, C578-G763, and A579-U762.

A common phenotype associated with changes in regions of RNA that are involved in dynamic structure formation is cold sensitivity. Thus, mutations that stabilize transient structures will be unable to undergo a conformational change and this may result in acute loss of function at low temperatures. To test this hypothesis we examined the activity of the mutants at a variety of temperatures (see section 3.8), and then analyzed the effects of pseudoknot mutations on the structure of the ribosome (see section 3.9).

4.6 EFFECTS OF PSEUDOKNOT MUTATIONS ON RIBOSOME STRUCTURE

While low temperatures would tend to stabilize RNA structures, the mutations made to the pseudoknot were extremely deleterious at lower temperatures. This cold sensitivity suggests

that the pseudoknot is part of a dynamic structure; the involved bases could be engaging in alternate interactions during a conformational change when they are not forming the pseudoknot. Mutations might create folding traps which cause the pseudoknot to become permanently locked in a low energy intermediate or misfolded structure. While the individual domains can assemble independently, folding of the ribosome is not a trivial process; to assemble a given domain within the context of full 16S rRNA, folding follows a hierarchical and ordered pathway. Helix 26 (which includes nucleotides 865 and 866 of the pseudoknot) can only associate with preformed core RNP complex.¹⁶⁴ Association of S15 has been shown to induce a conformational change in a junction between helices 20, 21 and 22 of the 16S rRNA, which facilitates binding to the central domain.¹⁶⁵ Helix 3 has also been shown to be involved in a conformational switch during assembly which is coupled to processing of the pre-rRNA and later steps of 30S subunit assembly.¹⁶³ Our 571 pseudoknot is located in the central domain where the 3'domain, central domain and the 5'major domain meet, so there is a possibility that these interactions are what bring these regions of the 16S rRNA into the same area in the 30S subunit.

We wanted to determine if mutant ribosomes are capable of assembling into association-competent 30S subunits, so we prepared ribosomes under conditions that would maintain 70S particles. The first signs of a decreasing 70S peak and increasing 50S and 30S peaks occur in the ribosome profile of the mutant C866G, which had a function of $53 \pm 5\%$. Among the other low function mutants, the 70S peaks never quite reaches the OD of the 50S peaks, though the ratio varies. For example, U571G, which shows no measurable function, displays a larger 70S to 50S ratio than G570A-C866U U571A-A865U, which has 39% function. These profiles show that some mutations inhibit the long-term formation of 70S tight-couples, but it is unclear if the mutations disrupt association-competent 30S subunits. It is possible that the 571-865 base pair

needs to be a dynamic interaction that must be able to break and reform, with the 571 base involved in a second interaction. This hypothesis would explain why the U571A-A865U mutation is more active than the U571G-A865C and U571C-A865G mutations because the guanosine-cytosine pair is too strong. This would also explain why preserving the wild-type uracil at position 571 allows the ribosome to maintain some function regardless of its pairing nucleotide at position 865. It seems that this nucleotide pair plays a key role in ribosome function.

4.7 MUTANT STRUCTURE-FUNCTION ANALYSIS

Genetic analysis of 571 pseudoknot mutants has revealed a clear relationship between the ability of the pseudoknot to form Watson-Crick base pairs and the function of the ribosome. Data also suggest the importance of sterics, and therefore we wanted to analyze the overall structure of the 571 pseudoknot. In addition, based on the crystal structure of the 30S published by Ramakrishnan in 2002 (figure 1.10) and secondary structure pictures (figure 1.9), it appears that if this pseudoknot is dynamic, alternate base pairing could be possible with adjacent nucleotides 572 or 864. We turned to homology modeling software to help us analyze the structure of representative mutations.

Homology models of single mutations at position 571 highlight the importance of sterics in this structure. When the wild-type nucleotide undergoes a transversion mutation to U571A (seen in figure 3.13) or U571G (figure 3.14), both the 571 and 865 position are displaced, inhibiting their ability to base pair. This is confirmed by the lack of function of these mutants in genetic assays. Transition mutation U571C (figure 3.15), however, shows little to no displacement of the nucleotides, which is consistent with the 60% activity this mutation retains.

We expected to see some distortion of nucleotide positioning in the homology model of single mutation A865C because these ribosomes are only $15\pm 1\%$ active. However, while the mutated base does appear to be tilted, the alteration is not as dramatic as the structures seen in ribosomes with mutations at position 571. This is consistent with our hypothesis that the individual base pairs of the pseudoknot are less important than the ability of these nucleotides to form alternate interactions. Compensatory mutation U571G-A865C (figure 3.19) shows little to no displacement and yet these ribosomes retain little function ($10\pm 1\%$). This suggests that loss of activity due to mutations at these positions is not related to defects in ribosome assembly. Double compensatory mutants G570U-C866A U571G-A865C ($64\pm 4\%$) (figure 3.17) and G570A-C865U U571G-A865C ($21\pm 1\%$) (figure 3.18) show little difference in the amount of nucleotide displacement, yet there is a noteworthy difference in their percent activity.

The first criterion that must be met for active mutants is that they be able to form Watson-Crick base pairs at the pseudoknot. However, as we see in these collective data, preserving a Watson-Crick bond does not necessarily preserve structure or function of the ribosome. Some mutations caused more bond disruptions than others, but did not correlate with loss of function. From this observation, the data is consistent with our hypothesis that an alternate structure formation is necessary to keep the ribosome active, and to do this, particular bases are needed at either position 571 or 865. Also, if a mutation at position 570 or 866 disrupts the bond formation at 571 and 865, loss of function is observed. Low functioning or dead mutants may be due to a defect in association because although there appears to be minimal distortions in the homology models, sucrose gradients show a decrease in complete 70S subunit formation. Thus, minor changes in structure surrounding the pseudoknot may disrupt critical intersubunit bridges.

4.8 PSEUDOKNOT BASE CONSERVATION

The strong correlation between the bases at positions 571 and 865 and the function of their ribosomes prompted our investigation of the pseudoknot's base conservation. The Gutell lab has compiled information about RNA structure and evolution that has been determined using comparative sequence analysis.¹²⁸ Among the data they have compiled were nucleotide frequencies of the four bases involved in the 571 pseudoknot. A modified version of the conservation data can be seen in table 4.1. The base pair frequencies at position 570-866 are highly conserved among individual phylogenetic domains, but overall, all possible Watson-Crick base pairs are equally represented with the exception of the A570-U866 base pair. This is not surprising because many non-wild-type base pair combinations that yield active ribosomes were observed as long as a Watson-Crick pair was conserved between positions 571-865. Dissimilarly, U571-A865 is universally conserved throughout all life. In this case, it is curious that we saw functional ribosomes with any pair other than U571-A865. We found other canonical base pairs at this position that gave us functional ribosomes which disagrees with the base conservation data. The importance of this pair merits future research.

4.9 FUTURE DIRECTIONS

It has long been known that protein synthesis is an inherently dynamic process. Though we cannot see all of the nucleotide interactions in the crystal structures of static ribosomes, we know other conformations, and therefore bonds, must exist. Our data suggest this pseudoknot is dynamic and forms alternate interactions during translation. The tertiary structure of the pseudoknot seen in figure 4.1 shows nucleotides 572 and 864 are in close enough proximity to be potential alternate binding partners. Our preliminary data does not suggest that U572 interacts in a theoretical alternate conformation with A865. However, if A864 and U571 mutants are

complimentary when mutated and they recover some function to the ribosome, this would suggest that U571 moves between pairing with A865 and A864 during wild-type conformational changes essential for ribosome function.

Analysis of the crystal structure of this region suggests that the unpaired bases 864 and 572 are close enough to the pseudoknot that they might be interacting with a dynamic bond. To test this, we have begun to create point mutations at these two residues and combined them with select single mutations at 571 or 865 to be assayed for function. Our preliminary data indicate that specific interactions between 572 and 865 are not required for protein synthesis, but that canonical pairing between 571 and 864 is important for ribosome function.

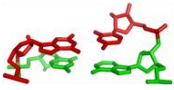
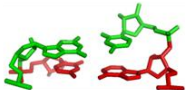
16S rRNA Model Base Pair Frequencies for Helical Element 570												
Base Pair (570:866)					# of Sequences Analyzed		Base Pair (571:865)					# of Sequences Analyzed
	% of event occurrence							% of event occurrence				
	GC	CG	UA	AU			GC	CG	UA	AU		
Bacteria	94.0	--	5.5	0.1	4558	Bacteria	--	--	99.7	--	4553	
Archaea	--	83.1	18.7	--	219	Archaea	--	--	100.0	--	220	
Eukarya	--	--	99.9	--	1013	Eukarya	--	--	99.6	--	1015	
Mitochondria	85.7	2.4	5.7	1.5	880	Mitochondria	--	2.3	93.0	0.7	881	

Table 4.1: 16S rRNA Base Pair Frequencies for Helical Element 570
Data taken from Gutell lab,¹²⁸ see text for details.

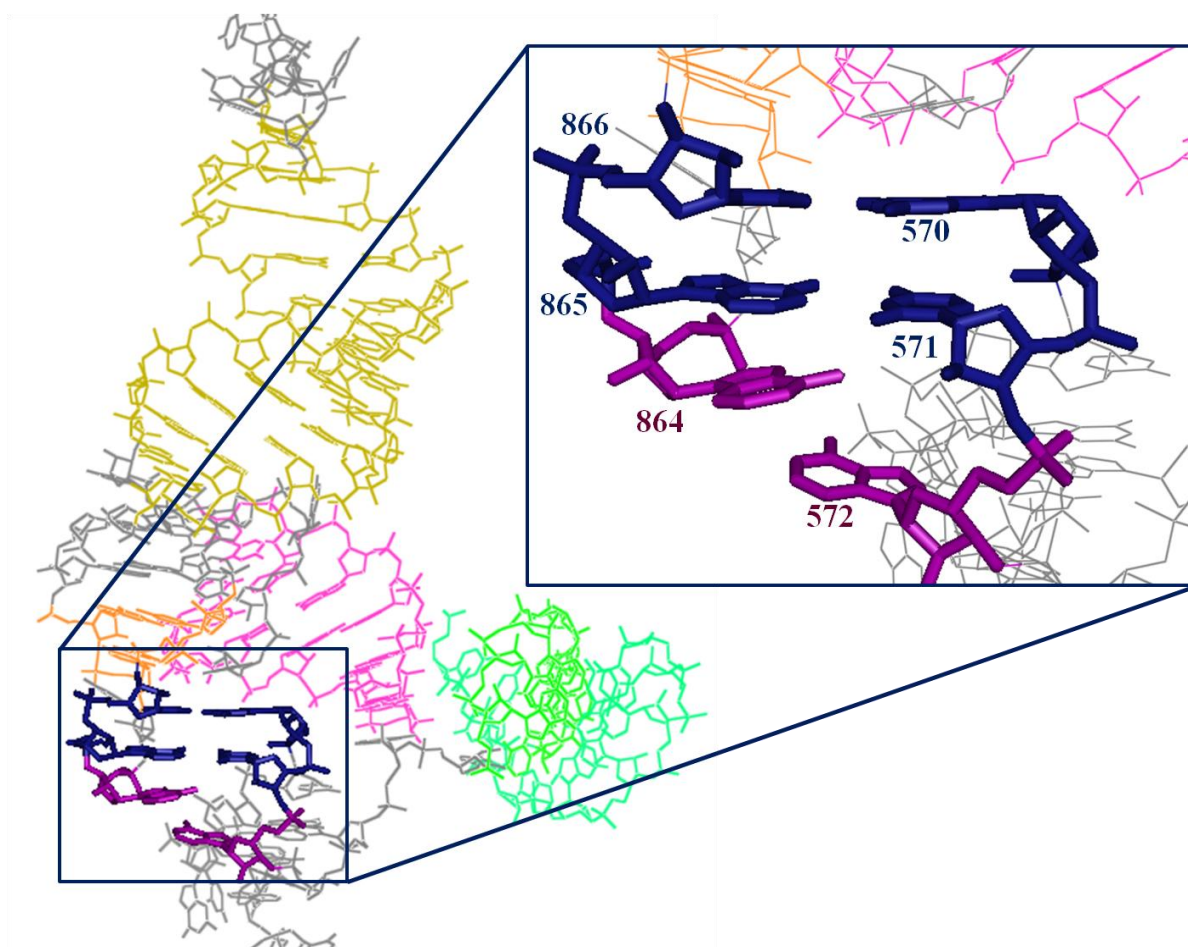


Figure 4.1: Potential Alternate Binding Partners

We begin to theorize potential alternate binding partners for the dynamic pseudoknot. We imagine bases A864 or A872 may be involved in the conformational switch. Image modified from PDB 2i2p.

REFERENCES

1. Carl Woese, *The Genetic Code* (New York: Harper and Row, 1967).
2. Kruger, K, Grabowski, PJ, Zaug, AJ, Sands, J, Gottschling, DE, and Cech, TR (1982).
Self-splicing RNA: autoexcision and autocyclization of the ribosomal RNA intervening
sequence of Tetrahymena. *Cell*, 31(1):147-57.
3. Yang JH, Perreault JP, Labuda D, Usman N, Cedergren R. (1990).“Mixed DNA/RNA
polymers are cleaved by the hammerhead ribozyme” *Biochemistry*. Dec
25;29(51):11156-60.
4. Wu HN, Lin YJ, Lin FP, Makino S, Chang MF, Lai MM. (1989) Human hepatitis delta
virus RNA subfragments contain an autocleavage activity.*Proc Natl Acad Sci U S A*.
Mar;86(6):1831-5.
5. Garriga G, Lambowitz AM. RNA splicing in neurospora mitochondria: self-splicing of a
mitochondrial intron *in vitro*.*Cell*. 1984 Dec;39(3 Pt 2):631-41.
6. Marvin MC, Engelke DR. Broadening the mission of an RNA enzyme. *J Cell Biochem*.
2009 Oct 20.
7. Bärwald KR, Reid RE, Gutte B. Formation and enzymic properties of dimeric RNase P.
FEBS Lett. 1975 Dec 15;60(2):423-6.
8. Taft RJ, Pang KC, Mercer TR, Dinger M, Mattick JS. Non-coding RNAs: regulators of
disease. *J Pathol*. 2009 Oct 30.
9. Gillespie J, Mayne M, Jiang M. RNA folding on the 3D triangular lattice. *BMC
Bioinformatics*. 2009 Nov 5;10(1):369.
10. Schmeing TM, Voorhees RM, Kelley AC, Gao YG, Murphy FV 4th, Weir JR,
Ramakrishnan V The crystal structure of the ribosome bound to EF-Tu and aminoacyl-
tRNA. *Science*. 2009 Oct 30;326(5953):688-94. Epub 2009 Oct 15

11. Scott M. Stagg†, a, Jason A. Mears†, a and Stephen C. Harvey. A Structural Model for the Assembly of the 30 S Subunit of the Ribosome. *Journal of Molecular Biology*. Volume 328, Issue 1, 18 April 2003, Pages 49-61
12. Wilson, D.N., Blaha,G., Connell, S.R., Ivanov, P.V., Jenke, H., Stelzl, U., Teraoka, Y., and Nierhaus, K.H. (2002) Protein synthesis at atomic resolution: mechanics of translation in the light of highly resolved structures for the ribosome, *Curr Protein Pept Sci* 3, 1-53.
13. Wilson, D.N., and Nierhuas K.H. (2003) The ribosome through the looking glass, *Angew Chem Int Ed Engl* 42, 3464-3486.
14. Schuwirth, B.S., Borovinskaya, M.A., Hau, C.W, Shang, W., Vila-Sanjurjo, A., Holton, J.M., and Cate, J.H. (2005) Structures of the bacterial ribosome at 3.5Å resolution, *Science* 310, 827-834.
15. Shine, J. and Dalgarno, L. The 3'-terminal sequence of Escherichia coli 16S ribosomal RNA: complementarity to nonsense triplets and ribosome binding sites. *Proc Natl Acad Sci USA* 71, 1342-1346 (1974).
16. M. Nomura, S. Mizushima, M. Ozaki, P. Traub and C.V. Lowry, Structure and function of ribosomes and their molecular components, *Cold Spring Harb. Symp. Quant. Biol.* 34 (1969), pp. 49–61
17. Cox RA. 2003. Correlation of the rate of protein synthesis and the third power of the RNA : protein ratio in Escherichia coli and Mycobacterium tuberculosis. *Microbiology* (Reading, England) 149:729-737.
18. Ban N, Nissen P, Hansen J, Moore PB, Steitz TA. 2000. The complete atomic structure of the large ribosomal subunit at 2.4 Å resolution. *Science* 289:905–920.

19. U Stelzl and K H Nierhaus. A short fragment of 23S rRNA containing the binding sites for two ribosomal proteins, L24 and L4, is a key element for rRNA folding during early assembly. 2001 *RNA* 7: 598-609
20. Laurie Betts and Linda L. Spremulli, Analysis of the Role of the Shine-Dalgarno Sequence and mRNA. *J Biol Chem.* 1994 Oct 21;269(42):26456-63.
21. Secondary Structure on the Efficiency of Translational Initiation in the *Euglena gracilis* Chloroplast atpH mRNA. *J Biol Chem.* 1994 Vol. 269, No. 42, Issue of October 21. pp. 2645&26463,
22. Calogero RA, Pon CL, Canonaco MA, Gualerzi CO. 1988. Selection of the mRNA translation initiation region by *Escherichia coli* ribosomes. *Proc Natl Acad Sci USA* 85:6427–6431.
23. Adilakshmi T, Bellur DL, Woodson SA. Concurrent nucleation of 16S folding and induced fit in 30S ribosome assembly. *Nature.* 2008 Oct 30;455(7217):1268-72.
24. Nomura, Masayasu. Assembly of Bacterial Ribosomes. *In vitro* reconstitution systems facilitate study of ribosome structure, function, and assembly. *Science* 179, 864 (1973).
25. Valsan Mandiyan, Santa J. Tumminia, Joseph S. Wall, James F. Hainfeld, and Miloslav Boublik. Assembly of the *Escherichia coli* 30S ribosomal subunit reveals protein-dependent folding of the 16S rRNA domains. *Proc. Natl. Acad. Sci, USA.* Vol 88, pp. 8174-8178, Sept 1991
26. P. Traub and M. Nomura, Structure and function of *E. coli* ribosomes. V. Reconstitution of functionally active 30S ribosomal particles from RNA and proteins, *Proc Natl Acad Sci U S A* **59** (1968), pp. 777–784

27. G.M. Culver, Assembly of the 30S ribosomal subunit, *Biopolymers* **68** (2003), pp. 234–249
28. P. Traub and M. Nomura, Structure and function of *Escherichia coli* ribosomes. VI. Mechanism of assembly of 30 s ribosomes studied *in vitro*, *J Mol Biol* **40** (1969), pp. 391–413.
29. Paul, B. J., Ross, W., Gaal, T., and Gourse, R. L. (2004). rRNA transcription in *Escherichia coli*. *Annu Rev Genet* **38**, 749-770.
30. Yusupov, M. M., Yusupova, G. Z., Baucom, A., Lieberman, K., Earnest, T. N., Cate, J. H., and Noller, H. F. (2001). Crystal structure of the ribosome at 5.5 Å resolution. *Science* **292**, 883-896.
31. Brodersen, D. E., Clemons, W. M., Jr., Carter, A. P., Morgan-Warren, R. J., Wimberly, B. T., and Ramakrishnan, V. (2000). The structural basis for the action of the antibiotics tetracycline, pactamycin, and hygromycin B on the 30S ribosomal subunit. *Cell* **103**, 1143-1154.
32. Rohl R, Nierhaus KH. 1982. Assembly map of the large subunit (50S) of *Escherichia coli* ribosomes. *Proceedings of the National Academy USA* **79**:729-733.
33. Wilson, K.S. & Noller, H.F. (1998). Molecular movement inside the translational engine. *Cell* **92**(3), 337-349.
34. Brodersen, D. E., Clemons, W. M., Jr., Carter, A. P., Wimberly, B. T., and Ramakrishnan, V. (2002). Crystal structure of the 30 S ribosomal subunit from *Thermus thermophilus*: structure of the proteins and their interactions with 16 S RNA. *J Mol Biol* **316**, 725-768.

35. Priya Ramaswamy and Sarah A. Woodson* (2005). S16 throws a conformational switch during assembly of 30S 5' domain. *Nature Structural & Molecular Biology* **16**, 438 – 445.
36. Woese, C. R., Winker, S., and Gutell, R. R. (1990). Architecture of ribosomal RNA: constraints on the sequence of “tetra-loops”. *Proc Natl Acad Sci U S A* **87**, 8467-8471.
37. Eric Westhof and Pascal Auffinger. RNA Tertiary Structure. *Encyclopedia of Analytical Chemistry*. R.A. Meyers (Ed.) pp. 5222–5232. Ó John Wiley & Sons Ltd, Chichester, 2000
38. Megan W. T. Talkington, Gary Siuzdak & James R. Williamson (2005). An assembly landscape for the 30S ribosomal subunit. *Nature articles*, Vol 438|1 December 2005|doi:10.1038/nature04261.
39. Lee, K., Holland-Staley, C.A. & Cunningham, P.R. (1996). Genetic analysis of the Shine-Dalgarno interaction: selection of alternative functional mRNA-rRNA combinations. *RNA* **2**, 1270-85.
40. Tama, F., Valle, M., Frank, J., and Brooks, C.L., III (2003). Dynamic reorganization of the functionally active ribosome explored by normal mode analysis and cryo-electron microscopy. *Proc. Natl. Acad. Sci. U. S. A.* **100**, 9319–9323.
41. Staple DW, Butcher SE (2005). Pseudoknots: RNA structures with diverse functions. *PLoS Biol* **3**(6): e213.
42. Rietveld K, Van Poelgeest R, Pleij CW, Van Boom JH, Bosch L (1982). The tRNA-like structure at the 3' terminus of turnip yellow mosaic virus RNA. Differences and similarities with canonical tRNA. *Nucleic Acids Res* **10**: 1929–1946.

43. Gegenheimer, P., and Apirion, D. (1981). Processing of prokaryotic ribonucleic acid. *Microbiol Rev* 45, 502-541.
44. Schuwirth BS, Borovinskaya MA, Hau CW, Zhang W, Vila-Sanjurjo A, Holton JM, Cate JH. (2005). Structures of the bacterial ribosome at 3.5 Å resolution. *Science* 310:827-834
45. White S. A., Nilges M., Huang A., Brunger A. T., Moore P. B. (1992). An NMR analysis of helix I from the 5S RNA of *Escherichia coli*, *Biochemistry* 31, 1610-1621
46. Hilbers, C.W., Michiels, P.J.A. and Heus, H.A. (1998). New developments in structure determination of pseudoknots. *Biopolymers*, 48, 137–153
47. Kyungsook Han and Yanga Byun (2003). Pseudo Viewer2: visualization of RNA pseudoknots of any type. *Nucleic Acids Research*, Vol.31, No. 13 3432-3440
48. Brierley, Ian, Gilbert, Robert J.C., and Pennell, Simon. (2008). RNA pseudoknots and the regulation of protein synthesis. *Biochemical Society Transactions* Vol. 36, part 4.
49. Kim, N., Shiffeldrim, N., Gan, H. H. & Schlick, T. (2004). Candidates for novel RNA topologies. *J. Mol. Biol.* **341**, 1129–1144
50. Theimer CA, Blois CA, Feigon J (2005). Structure of the human telomerase RNA pseudoknot reveals conserved tertiary interactions essential for function. *Mol Cell* 17: 671–682.
51. Ke A, Zhou K, Ding F, Cate JH, Doudna JA (2004). A conformational switch controls hepatitis delta virus ribozyme catalysis. *Nature* 429: 201–205.
52. Rastogi T, Beattie TL, Olive JE, Collins RA (1996). A long-range pseudoknot is required for activity of the *Neurospora* VS ribozyme. *EMBO J* 15: 2820–2825.
53. Adams PL, Stahley MR, Kosek AB, Wang J, Strobel SA (2004). Crystal structure of a self-splicing group I intron with both exons. *Nature* 430: 45–50.

54. Shen LX, Tinoco I Jr (1995). The structure of an RNA pseudoknot that causes efficient frameshifting in mouse mammary tumor virus. *J Mol Biol* 247: 963–978.
55. Nixon PL, Rangan A, Kim YG, Rich A, Hoffman DW, et al. (2002). Solution structure of a luteoviral P1-P2 frameshifting mRNA pseudoknot. *J Mol Biol* 322: 621–633.
56. Michiels PJ, Versleijen AA, Verlaan PW, Pleij CW, Hilbers CW, et al. (2001). Solution structure of the pseudoknot of SRV-1 RNA, involved in ribosomal frameshifting. *J Mol Biol* 310: 1109–1123.
57. Egli M, Minasov G, Su L, Rich A (2002). Metal ions and flexibility in a viral RNA pseudoknot at atomic resolution. *Proc Natl Acad Sci U S A* 99: 4302–4307.
58. Adams PL, Stahley MR, Gill ML, Kosek AB, Wang J, et al. (2004). Crystal structure of a group I intron splicing intermediate. *RNA* 10: 1867–1887.
59. Chen, Jiunn-Liang and Greider, Carol W. (2005). Functional analysis of the pseudoknot structure in human telomerase RNA. *Proc Natl Acad Sci USA* 102: 8080-8085.
60. C.A. Theimer, C.A. Blois, and J. Feigon (2005). Structure of the human telomerase RNA pseudoknot reveals conserved tertiary interactions essential for function, *Mol. Cell* 17, 671-682
61. Vulliamy T, Marrone A, Dokal I, Mason PJ. (2002). Association between aplastic anaemia and mutations in telomerase RNA. *The Lancet* 359:2168-2170
62. Vullimay T, Marrone A, Sxydlo R, Walne A, Mason PJ, Dokal I. (2004). Disease anticipation is associated with progressive telomere shortening in families with TERC. *Nat Genet.* 5:447-449

63. Marrone A et al. (2007). Functional characterization of novel telomerase RNA (TERC) mutations in patients with diverse clinical and pathological presentations. *Haematologica* 8:1013-1020.
64. Du, H et al. (2009) TERC and TERT gene mutations in patients with bone marrow failure and the significance of telomere length measurements. *Blood* 113(2):309-16.
65. Brierley I, Pennell S and Gilbert R (2007) Viral RNA pseudoknots: versatile motifs in gene expression and replication. *Nature Reviews Microbiology* 5,598-610.
66. Serganov A, Keiper S, Malinina L, Tereshko V, Skripkin E, et al. (2005) Structural basis for Diels-Alder ribozyme-catalyzed carbon-carbon bond formation. *Nat Struct Mol Biol* 12: 218–224
67. Thill G, Vasseur M, Tanner NK (1993) Structural and sequence elements required for the self-cleaving activity of the hepatitis delta virus ribozyme. *Biochemistry* 32: 4254–4262.
68. Marzi, S., Myasnikov, A.G., Serganov, A., Ehresmann, C., Romby, P., Yusupov, M. and Klaholz, B.P. (2007) Structured mRNAs regulate translation initiation by binding to the platform of the ribosome. *Cell* **130**, 1019–1031
69. Hansen, T.M., Reihani, S.N., Oddershede, L.B. and Sorensen, M.A. (2007) Correlation between mechanical strength of messenger RNA pseudoknots and ribosomal frameshifting. *Proc. Natl. Acad. Sci. U.S.A.* **104**, 5830–5835
70. Roth A, Breaker RR. (2009) The structural and functional diversity of metabolite-binding riboswitches. *Annu Rev Biochem.* 78:305-34.
71. Gilbert, S.D., Rambo, R.P., Van Tyne, D. and Batey, R.T. (2008) Structure of the SAM-II riboswitch bound to *S*-adenosylmethionine. *Nat. Struct. Mol. Biol.* **15**, 177–182

72. Powers T. & Noller H.F. (1991) A functional pseudoknot in 16S ribosomal RNA. *EMBO J.* 10:2203-2214.
73. Vila A, Viril-Farley J, Tappich W.E. (1994) Pseudoknot in the central domain of small subunit ribosomal RNA is essential for translation. *Proc. Natl. Acad. Sci. USA* 91:11148-11152.
74. "The Nobel Prize in Chemistry 1989". Nobelprize.org. 14 Mar 2011
http://nobelprize.org/nobel_prizes/chemistry/laureates/1989
75. Altman, S; Baer, M F; Bartkiewicz, M; Gold, H; Guerrier-Takada, C; Kirsebom, LA; Lumelsky, N; Peck, K (1989). Catalysis by the RNA subunit of RNase P--a minireview. *Gene* 82 (1): 63-4
76. Song JJ, Smith SK, Hannon GJ, Joshua-Tor L. 2004. **Crystal structure of Argonaute and its implications for RISC slicer activity.** *Science*, **305**:1434-1437
77. R. K. Montange and R. T. Batey (2008). Riboswitches: emerging themes in RNA structure and function, *Annu Rev Biophys* 37, 117-133.
78. Wyatt HD, West SC, Beattie TL. 2010 May 11. InTERTpreting telomerase structure and function. *Nucleic Acids Res.* Sep;38(17):5609-22.
79. Johnson IM. 2010 Jan . RNA as a drug target: recent patents on the catalytic activity of trans-splicing ribozymes derived from group I intron RNA. *Recent Pat DNA Gene Seq.*;4(1):17-28.
80. Hershey JWB. 1983. Protein Synthesis. In: Neidhardt FC, others, eds. *Escherichia coli and Salmonella typhimurium: Cellular and Molecular Biology*. Washington D.C.: *American Society of Microbiology*. pp 613-647.

81. Subramanian AR, Davis BD. 1970. Activity of initiation factor 3 in dissociating *Escherichia coli* ribosomes. *Nature* 228:1273-1275.
82. Grunberg-Manago M, Dessen P, Pantaloni D, Godefroy-Colburn T, Wolfe AD, Dondon J. 1975. Light-scattering studies showing the effect of initiation factors on the reversible dissociation of *Escherichia coli* ribosomes. *J Mol Biol* 94:461-478
83. Caserta E, Tomsic J, Spurio R, La Teana A, Pon CL, Gualerzi CO. 2006. Translation initiation factor IF2 interacts with the 30 S ribosomal subunit via two separate binding sites. *J Mol Biol* 362:787-799
84. Nissen P, Hansen J, Ban N, Moore PB, Steitz TA. 2006. The structural basis of ribosome activity in peptide bond synthesis. *Science (New York, NY)* 289:920-930).
85. Noller HF, Hoffarth V, Zimniak L. 1992. Unusual resistance of peptidyl transferase to protein extraction procedures. *Science (New York, NY)* 256:1416-1419)
86. Horan LH, Noller HF. 2007. Intersubunit movement is required for ribosomal translocation. *Proc Natl Acad Sci U S A* 104(12):4881-5.
87. Gao H. et al. 2003. Study of the structural dynamics of the *E. coli* 70 S ribosome using real-space refinement. *Cell* 113:789–801
88. Nierhaus KH. 1990. The allosteric three-site model for the ribosomal elongation cycle: features and future. *Biochemistry* 29:4997-5008.
89. Rodnina MV, Pape T, Fricke R, Kuhn L, Wintermeyer W. 1996. Initial binding of the elongation factor Tu.GTP.aminoacyl-tRNA complex preceding codon recognition on the ribosome. *The Journal of biological chemistry* 271:646-652.

90. Ogle JM, Brodersen DE, Clemons WM, Jr., Tarry MJ, Carter AP, Ramakrishnan V. 2001. Recognition of cognate transfer RNA by the 30S ribosomal subunit. *Science* 292:897-902
91. Ogle JM, Murphy FV, Tarry MJ, Ramakrishnan V. 2002. Selection of tRNA by the ribosome requires a transition from an open to a closed form. *Cell* 111:721-732.
92. Rodnina MV, Wintermeyer W. 2001. Ribosome fidelity: tRNA discrimination, proofreading and induced fit. *Trends in biochemical sciences* 26:124-130.
93. Spirin, A.S 1985. Ribosomal translocation: Facts and models. *Prog. Nucleic Acid Res. Mol. Biol.* 32:75-114
94. Moazed, D., Noller, H.F. 1989b. Intermediate states in the movement of transfer RNA in the ribosome. *Nature* 342: 142-148
95. Spiegel, Clint P., Ermolenko, Dmitri N., Noller, Harry F. 2007. Elongation factor G stabilizes the hybrid-state conformation of the 70S ribosome. *RNA*. 13: 1473-1482
96. Zhang, W., Dunkie, J.A., Cate, J.H. 2009. Structures of the ribosome in intermediate states of ratcheting. *Science*. 326(5953):677-678
97. Sanger, F., Nicklen, S. & Coulson, A.R. 1977. DNA sequencing with chain-terminating inhibitors. *Proc Natl Acad Sci U S A* 74, 5463-5467
98. Lee K, Varma S, SantaLucia J, Jr., Cunningham PR. 1997. *In vivo* determination of RNA structure-function relationships: analysis of the 790 loop in ribosomal RNA. *Journal of molecular biology* 269:732-743
99. Lee K, Holland-Staley CA, Cunningham PR. 2001. Genetic approaches to studying protein synthesis: effects of mutations at Psi516 and A535 in Escherichia coli 16S rRNA. *The Journal of nutrition* 131:2994S-3004S

100. Shine J, Dalgarno L. 1974. The 3'-terminal sequence of *Escherichia coli* 16S ribosomal RNA: complementarity to nonsense triplets and ribosome binding sites. *Proc Natl Acad Sci U S A* 71:1342-1346
101. Vila, A., Viril-Farley, J. and Tapprich, W.E. 1994. Pseudoknot in the Central Domain of Small Subunit Ribosomal RNA is Essential for Translation. *PNAS*. 91:11148-11152.
102. Marinus MG, Carraway M, Frey AZ, Brown L, Arraj JA. 1983. Insertion mutations in the *dam* gene of *Escherichia coli* K-12. *Mol Gen Genet* 192:288-289
103. Woodcock, D. M. et al. 1989. Quantitative evaluation of *Escherichia coli* host strains for tolerance to cytosine methylation in plasmid and phage recombinants *Nucl. Acids Res*, 17, 3469-3478.
104. Luria, S.E., and Burrous, J.W. 1957. Hybridization between *Escherichia coli* and *Shigella*, *J Bacteriol* 74, 461-476
105. Bertani, G. 1951. Studies on lysogenesis. I. The mode of phage liberation by lysogenic *Escherichia coli*, *J Bacteriol* 62, 293-300.
106. Dower, W.J., Miller, J.F. & Ragsdale, C.W. 1988. High efficiency transformation of *E.coli* by high voltage electroporation. *Nucleic Acids Res* 16, 6124-6145
107. Chang, A.C. & Choen, S.N. 1978. Construction and characterization of amplifiable multicopy DNA cloning vehicles derived from the P15A cryptic miniplasmid. *J Bacteriol* 134, 1141-1156.
108. Chung, C.T. & Miller, R.H. 1988. A rapid and convenient method for the preparation and storage of competent bacterial cells. *Nucleic Acids Res* 16, 3580.
109. Hanahan, D. 1983. Studies on transformation of *Escherichia coli* with plasmids. *J Mol Biol* 166, 557-580.

110. Krzyzosiak, W. J., Denman, R., Cunningham, P. R., and Ofengand, J. (1988) An efficiently mutagenizable recombinant plasmid for *in vitro* transcription of the *Escherichia coli* 16S RNA gene, *Anal Biochem* 175, 373-385.
111. Vogelstein, B. and Gillespie, D. 1984. Preparative and analytical purification of DNA from agarose. *Proc. Natl. Acad. Sci.* 76: 616-619.
112. Birnbiom, H.C., and Doly, J. 1979. A rapid alkaline extraction procedure for screening recombinant plasmid DNA. *Nucleic Acids Research.* 67:1513-1523.
113. Dugaiczky, A., Boyer, H.W., and Goodman, H.M. 1975. Ligation of EcoRI endonuclease generated DNA fragments into linear and circular structures *J. Mol. Biol.* 96:174-184.
114. Focus. 1979. Vol.2 No.3
115. Chung CT, Miller RH. 1988. A rapid and convenient method for the preparation and storage of competent bacterial cells. *Nucleic Acids Res* 16:3580.
116. McAllister, William T., and Carter, Anthony D. 1980. Regulation of promoter selection by the bacteriophage T7 RNA polymerase *in vitro*. *Nucleic Acids Research.* Vol. 8, No. 20 4821-4838.
117. Jelenc, P.C. 1980 Rapid purification of highly active ribosomes from *Escherichia coli*. *Analytical Biochemistry.* 105(2):369-74
118. G Spedding, Ribosomes and Protein Synthesis: A Practical Approach (*Oxford University Press*; USA, 1990).
119. Vila, A., Viril-Farley, J. and Tapprich, W.E. 1994. Pseudoknot in the central domain of small subunit ribosomal RNA is essential for translation. *Proc. Natl. Acad. Sci USA* 91; 11148-11152.

120. Leontis NB, Stombaugh J, Westhof E. 2002. The non-Watson-Crick base pairs and their associated isostericity matrices. *Nucleic Acids Res* 30:3497-3531.
121. Terribilini, Michael et al. 2007. RNABindR: a server for analyzing and predicting RNA-binding sites in proteins. *Nucleic Acids Res* Vol 35, W578-W584.
122. van Batenburg, F.H., Gulyaev, A.P., and Pleij, C.W. 2001. PseudoBase: structural information on RNA pseudoknots. *Nucleic Acids Res.* 29(1):194-5.
123. Nikolaev, N., Silengo, L., and Schlessinger, D. (1973). Synthesis of a large precursor to ribosomal RNA in a mutant of *Escherichia coli*. *Proc Natl Acad Sci USA* 70, 3361-3365.
124. Caskey, C. T., Forrester, W. C., Tate, W., and Ward, C. D. (1984). Cloning of the *Escherichia coli* release factor 2 gene. *J Bacteriol* 158, 365-368.
125. Weiss, R. B., Murphy, J. P., and Gallant, J. A. (1984). Genetic screen for cloned release factor genes. *J Bacteriol* 158, 362-364.
126. Freistroffer, D. V., Pavlov, M. Y., MacDougall, J., Buckingham, R. H., and Ehrenberg, M. (1997). Release factor RF3 in *E. coli* accelerates the dissociation of release factors RF1 and RF2 from the ribosome in a GTP-dependent manner, *The EMBO journal* 16, 4126-4133.
127. Trobro S, Aqvist J. 2007. A model for how ribosomal release factors induce peptidyl-tRNA cleavage in termination of protein synthesis. *Molecular cell* 27:758-766
128. Ferre-D'Amare AR, Zhou K, Doudna JA . 1998. Crystal structure of a hepatitis delta virus ribozyme. *Nature* 395: 567–574
129. Serganov A, Keiper S, Malinina L, Tereshko V, Skripkin E, et al. 2005. Structural basis for Diels-Alder ribozyme-catalyzed carbon-carbon bond formation. *Nat Struct Mol Biol* 12: 218–224.

130. Zhang A, Zheng C, Hou M, Lindvall C, Li KJ, Erlandsson F, Björkholm M, Gruber A, Blennow E, Xu D (April 2003). "Deletion of the telomerase reverse transcriptase gene and haploinsufficiency of telomere maintenance in Cri du chat syndrome". *Am. J. Hum. Genet.* **72** (4): 940–8.
131. Marciniak RA, Johnson FB, Guarente L. 2000. Dyskeratosis congenita, telomeres and human ageing. *Trends Genet* 16: 193–195.
132. Gilbert, W. and Müller-Hill, B. 1966. Isolation of the lac repressor. *Proc Natl Acad Sci USA* 56(6): 1891-8.
133. Shimomura, O., Johnson, F. H., and Saiga, Y. 1962. Extraction, purification and properties of aequorin, a bioluminescent protein from the luminous hydromedusan, *Aequorea*. *Cell. Comp. Physiol.* 59: 223-239.
134. Prasher, D., Eckenrode, V., Ward, W., Prendergast, F. and Cormier, M., 1992. Primary structure of the *Aequorea victoria* green-fluorescent protein. *Gene*. **111**: 229-33.
135. Morse, DE; Mosteller RD; Yanofsky C. 1969. Dynamics of synthesis, translation, and degradation of trp operon messenger RNA in *E. coli*. *Cold Spring Harb Symp Quant Biol.* **34**: 725–40.
136. Burns, D.K. and Crowl, R.M. 1987. An immunological assay for chloramphenicol acetyltransferase. *Analytical Biochemistry* 162(2): 399-404.
137. Stark, B. C., Kole, R., Bowman, E. J., and Altman, S. 1978. Ribonuclease P: an Enzyme with an Essential RNA Component. *Proc. Natl. Acad. Sci. U. S. A.* 75, 3717–3721
138. Frank, J., Penczek, P., Grassucci, R.A., Heagle, A., Spahn, C.M.T. & Agrawal, R.K. (2000). Cryo-electron microscopy of the translational apparatus: experimental evidence for the paths of mRNA, tRNA, and the polypeptide chain. In *The Ribosome: Structure,*

- Function, Antibiotics, and Cellular Interactions*. (Garrett, R.A., Douthwaite, S.R., Liljas, A., Matheson, A.T., Moore, P.B. & Noller, H.F., eds) ASM Press, Washington, DC.
139. Müller, F. & Brimacombe, R. (1997). A new model for the three dimensional folding of *Escherichia coli* 16S ribosomal RNA. I. Fitting the RNA to a 3D electron microscopic map at 20 Å. *J. Mol.Biol.* **271**, 524-544.
140. Weixlbaumer, A et al. (2008). Insights into Translational Termination from the Structure of RF2 Bound to the Ribosome. *Science*. Vol. 322 no. 5903 pp. 953-956.
141. Khaitovich P, Mankin AS, Green R, Lancaster L, Noller HF. (1999). Characterization of functionally active subribosomal particles from *Thermus aquaticus*. *Proc Natl Acad Sci USA*. 96(1):85-90.
142. Studier SM, Joseph S. (2007). Binding of mRNA to the bacterial translation initiation complex. *Methods Enzymol*; 430:31-44.
143. Robert T. Batey, Robert P. Rambo, and Jennifer A. Doudna. (1999). Tertiary Motifs in RNA Structure and Folding. *Angew. Chem. Int. Ed.* 38, 2326 – 2343.
144. Wilson, D. N., Blaha, G., Connell, S. R., Ivanov, P. V., Jenke, H., Stelzl, U., Teraoka, Y., and Nierhaus, K. H. (2002). Protein synthesis at atomic resolution: mechanistics of translation in the light of highly resolved structures for the ribosome. *Curr Protein Pept Sci* 3, 1-53.
145. M. A. Tanner, T. R. Cech. Joining the two domains of a group I ribozyme to form the catalytic core. *Science* 1997, 275, 847 ± 849.
146. Woese, CR., Winker, S., and Gutell, RR. (1990). Architecture of ribosomal RNA: Constraints on the sequence of “tetra-loops”. *Proc. Natl. Acad. Sci. USA* 87; 8467-8471.

147. Tamura, M. and Holbrook, S.R., (2002). Sequence and Structural Conservation in RNA. Ribose Zippers. *J. Mol. Biol.* 320, 455–474.
148. Moore, P.B. (1999). Structural Motifs in RNA. *Annu. Rev. Biochem.* 68:287–300.
149. Berk V., Zhang W., Pai R.D., Cate J.H. (2006) Structural basis for mRNA and tRNA positioning on the ribosome. *Proc Natl Acad Sci USA.* 103(52)19931.
150. Bolivar, F (1977). Construction and characterization of new cloning vehicles. II. A multipurpose cloning system. *Gene* (0378-1119), 2 (2), p. 95.
151. Chang A.C., Cohen S.N. (1978). Construction and characterization of amplifiable multicopy DNA cloning vehicles derived from the P15A cryptic miniplasmid. *J Bacteriol.* 134(3): 1141-56.
152. Smith B.R., Schleif R. (1978). Nucleotide sequence of the L-arabinose regulatory region of *Escherichia coli* K12. *J Biol Chem.* 253(19):6931-3.
153. Elrich H.A., Gelfand D., Sinsky J.J. (1991). Recent advances in the polymerase chain reaction. *Science.* 252(5013):1643-51.
154. Sanger, F., Nicklen, S., Coulson, A.R. (1977). DNA sequencing with chain-terminating inhibitors. *Proc. Natl. Acad. Sci. U.S.A.* 74; 5463-5467
155. Chung CT, Niemela SL, and Miller RH. (1989). One-step preparation of competent *Escherichia coli*: Transformation and storage of bacterial cells in the same solution. *Proc. Natl. Acad. Sci. USA.* 86; 2172-2175.
156. Vilcek J, Havell EA. (1973). Stabilization of interferon messenger RNA activity by treatment of cells with metabolic inhibitors and lowering of the incubation temperature. *Proc. Natl. Acad. Sci. USA.* 70(12):3909-13.

157. Turner, D. (1996). Thermodynamics of Base Pairing. *Current Opinion in Structural Biology*. 6(3); 299–304.
158. Poland D., Scheraga H.A.(1966). Occurrence of a phase transition in nucleic acid models. *J. Chem. Phys.* 45:1464-1469.
159. Rouzina I., Bloomfield V.A. (1999). Heat capacity effects on the melting of DNA. 1. General aspects. *Biophys. J.* 77:3242-3251.
160. Kamenetskii, M.F. (1987). How the double helix breathes. *Nature*. 328:17-18.
161. Ginoza, W. and Zimm, B.H. (1961). Mechanisms of inactivation of deoxyribonucleic acids by heat. *Proc. Natl. Acad. Sci. USA*. 47(5): 639-652.
162. Frank, J. (2000). The ribosome- a macromolecular machine par excellence. *Chem Biol*. Jun;7(6):R133-41.
163. Ramaswamy P, Woodson S. (2009). S16 throws a conformational switch during assembly of 30S 5' domain. *Nat Struct Mol Biol*. April: 16(4): 438-445.
164. Agalarov S.C., Williamson J.R. (2000). A hierarchy of RNA subdomains in assembly of the central domain of the 30S ribosomal subunit. *RNA*. Mar;6(3):402-408.
165. Orr, J. W., Hagerman, P. J. & Williamson, J. R. (1998). Protein and Mg²⁺-induced conformational changes in the S15 binding site of 16 S ribosomal RNA. *J. Mol.Biol.* 275, 453–464.
166. Hermann, T. and Patel, D. J. (1999). Stitching Together RNA Tertiary Architectures. *J. Mol. Biol.* 294, 829±849
167. Chen, G. et al. (2009). Triplex structures in an RNA pseudoknot enhance mechanical stability and increase efficiency of -1 ribosomal frameshifting. *PNAS* 106(31) 12706-12711.

ABSTRACT**INVESTIGATION OF A 16S RNA CENTRAL DOMAIN PSEUDOKNOT**

by

JENNA JASINSKI-BOLAK**December 2012****Advisor:** Dr. Philip R. Cunningham**Major:** Biological Sciences**Degree:** Master of Science

X-ray crystallography of the prokaryotic 30S ribosomal subunit revealed a myriad of complex RNA-RNA, RNA-protein, and protein-protein interactions. Among these are several phylogenetically conserved RNA pseudoknots. Pseudoknots are structurally and functionally diverse RNA secondary structures. They are generally formed by two short complimentary sequences separated by many bases of single stranded regions or loops. These relatively simple folds are often yield complex structures that are key components of functionally important conformational changes in RNA structure. One such pseudoknot is located in the central domain of the 16S rRNA.

The central domain pseudoknot is formed by Watson-Crick base pairing between G570-C866 and U571-A865. Previous studies by other groups show that formation of this pseudoknot is critical for ribosome function. To examine the role this pseudoknot in ribosome function, we constructed and assayed all 255 possible mutations at these four residues. Our data show that disruption of base pairing between positions 570-866 reduces ribosome function by approximately 50% and that mutations that disrupt pairing between 571-865 completely block protein synthesis.

Ribosomal proteins S8, S11 and S5 have binding sites near the central pseudoknot. To

determine if mutations in the pseudoknot affect the binding of these proteins, the genes for S8, S11 and S5 were cloned and coexpressed with representative mutations at each of the sites in the pseudoknot. No complementation was observed in any of the mutants tested, indicating that loss of function in the mutants is not due to reduction in binding of ribosomal proteins.

To determine the influence of thermodynamics on the activity of the mutants, each mutant was assayed at 25°C, 30°C, 37°C, and 40°C. Mutants with no measurable protein synthesis activity at 37° were unaffected by changes in incubation temperatures. Mutants with partial activity, however, were slightly more active at 40°C but were strongly inhibited by incubation temperatures below 37°C. These data suggest that the central pseudoknot is dynamic and may facilitate the switch between two active conformations of rRNA. Mutations in the pseudoknot may therefore create thermodynamic minima that favor one conformation over the other. Homology modeling and ribosome profiles suggest that the mutations may affect ribosome association or one of the partial reactions during the protein synthesis process itself.

AUTOBIOGRAPHICAL STATEMENT**JENNA JASINSKI-BOLAK****Advisor:** Dr. Philip R. Cunningham**Thesis Title:** INVESTIGATION OF A 16S RNA CENTRAL DOMAIN PSEUDOKNOT**Education:**

Master of Science, Biological Sciences
Wayne State University, Detroit, MI Dec 2012

Bachelor of Science, Biological Sciences
Wayne State University, Detroit, MI Aug 2007

Research Experience:

Undergraduate research, Cunningham Lab
Wayne State University, Detroit, MI April 2006-Aug 2007

Graduate thesis research, Cunningham lab
Wayne State University, Detroit, MI Sept 2007-Feb 2010

Research Interest:

Structure-Function relationship in functional RNA's
 Mutations that disrupt function in ribosomes
 Thermodynamics
 Base conservation

Activities:

- RNA Club
- Intramural volleyball
- Rustbelt RNA meeting
- Graduate Student Union
- Biological Sciences Graduate Research Day
- Wayne State University Graduate Research Day
- Children's Miracle Network
- Wayne State Climbing Club